

Mechanics of
Vehicles
By Jaroslav J. Taborek

1957

EDC Library Ref. No. 1110

DISCLAIMER

These materials are available in the public domain and are not copyrighted. Engineering Dynamics Corporation (EDC) copies and distributes these materials to provide a source of information to the accident investigation community. EDC makes no claims as to their accuracy and assumes no liability for the contents or use thereof.

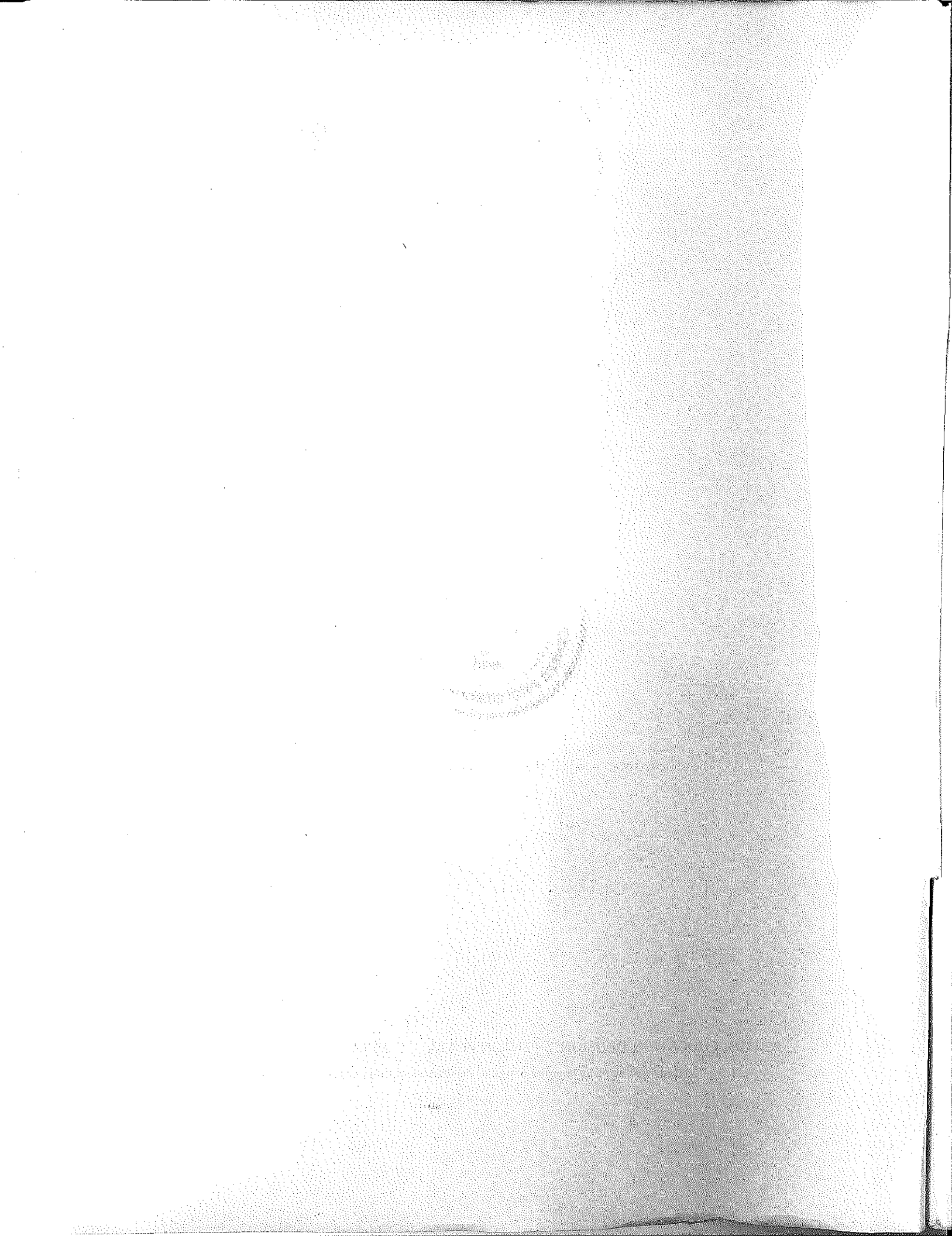
MECHANICS OF VEHICLES

By Jaroslav J. Taborek

The articles listed overleaf are from **MACHINE DESIGN Magazine**.

PENTON EDUCATION DIVISION PENTON PLAZA CLEVELAND, OHIO 44114

Copyright 1957 by Penton Publishing Co., Cleveland, Ohio 44114



CONTENTS

Part		Page
1	Motion of Wheels	4
2	Cornering and Directional Control	10
3	Steering Forces and Stability	16
4	Stability on a Curve	25
5	Motion-Resisting Forces	30
6	Resistance Forces	35
7	Center of Gravity	42
8	Longitudinal Stability	47
9	Limits of Vehicle Performance	54
10	Performance Limits (continued)	59
11	Dynamics of Braking	64
12	Braking Performance Limits	70
13	Powerplant Characteristics	78
14	Performance Prediction	84

Mechanics of Vehicles-1

By Jaroslav J. Taborek*

Development Engineer
Towmotor Corp.
Cleveland

Family resemblances among "automotive" vehicles are often quite subtle. Wheels—and the fact that the vehicles are self-propelled—seem to form the sole common denominator of off-the-highway earthmovers, automobiles and fork-lift trucks, to name a few well-known members of the breed.

From the designer's viewpoint, however, vehicle differences usually prove to be matters of functional emphasis, not engineering principle. Whatever the vehicle purpose, study of forces and motions guides layout of best steering, braking and drive systems.

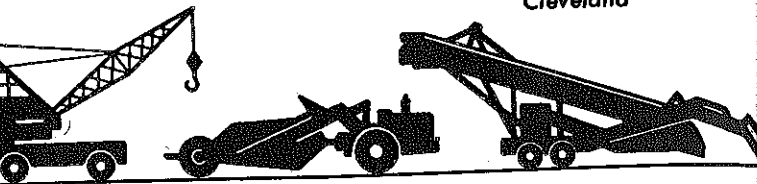
Mechanics of vehicle motion are outlined and correlated in this series. Terminology, for the most part, will be familiar to the engineer-owner of a passenger car. Caster, camber and toe-in, for example, are practically everyday words for describing wheel orientation with the ground.

Motion of wheels . . . control and stability . . . static and dynamic forces . . . accelerated and decelerated motion . . . performance prediction . . . these subjects form the backbone of the presentation. Emphasis throughout will be on principle rather than on specific design problems.

TRACTIVE forces for primitive transport vehicles—the oxcart is an ancient example—were externally applied. For such towed vehicles, the fundamental purpose of the wheel served admirably: while providing ground support for the body structure, it replaced high-friction sliding with the much easier rolling motion.

The self-propelled vehicle, on the other hand, demands certain additional characteristics from the rolling wheel: it is required to transform torque originating within the vehicle to a propelling thrust while, at the same time, providing high frictional resistance to side forces. This last characteristic—resistance to side thrust—permits effective directional control of the vehicle from within its structure.

Survey of vehicle mechanics begins in this ar-



ticle with a look at physical laws governing progression of the rigid rolling wheel. From this simple case, the analysis is extended to the more complex behavior of the flexible or rubber-tired wheel.

Rigid Wheels

Although the primary function of the wheel is to reduce friction, the existence of rolling motion depends, paradoxically, on the presence of high values of static friction. By experience, motion of a wheel takes two forms:

1. Sliding, as for any other pushed or pulled body.
2. Rolling, defined as the progressive motion of a cylindrical body in which the instantaneous contact point has no motion relative to the ground. In rolling, translatory speed of the

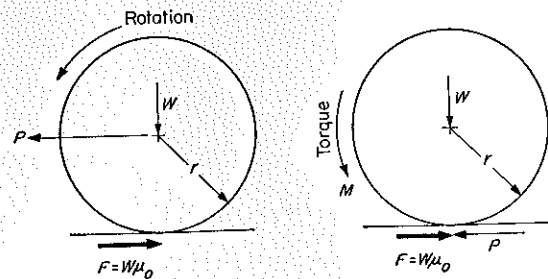
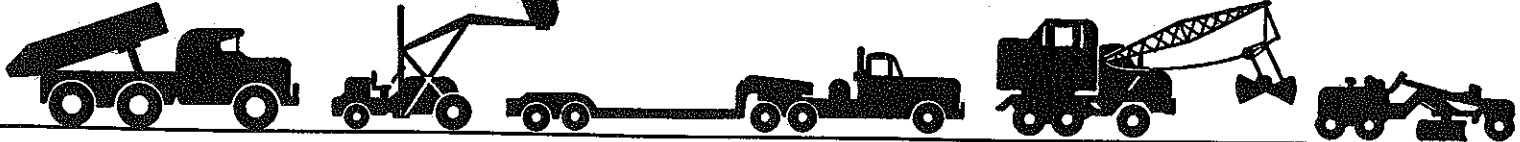


Fig. 1—Tractive force on a rolling wheel can be an external towing force (left) or result from an internally developed torque (right). Rolling continues as long as the tractive force remains within limits of the static-friction force.

*Now Research and Development Engineer, Phillips Petroleum Co., Bartlesville, Okla.

Motion of Wheels

- rolling resistance
- wheel slip
- braking stability
- coefficient of adhesion



wheel center equals the circumferential or tangential speed of the wheel rim.

The question remains: under what physical conditions can each type of motion be expected? Rolling of a wheel depends ultimately upon the existence of a static frictional force acting at the ground contact point so as to prevent the wheel from sliding. If the frictional force is too low to balance the tractive force, rolling cannot be maintained and the wheel starts to slide.

Static Friction: Coulomb's friction law offers a mathematical explanation for the rolling process and permits calculation of the limiting conditions. In equation form, the relationship is

$$F = W\mu \quad (1)$$

The coefficient of friction μ can assume two different forms: μ_s , the coefficient of sliding friction, and μ_o , the coefficient of static friction. From equi-

Nomenclature

B	Braking force, lb
E	Energy, ft-lb
F	Frictional force, lb
f	Coefficient of rolling resistance
f_o	Coefficient of rolling friction, in.
g	Acceleration of gravity, ft per sec ²
M	Torque or moment, lb-ft
m	Mass, lb-sec ² per ft
P	Propelling or tractive force, lb
R_r	Rolling resistance, lb
r	Rolling radius, ft
s	Wheel slip, per cent
v	Velocity, ft per sec
W	Weight, lb
μ	Coefficient of friction
μ_o	Coefficient of static friction
μ_s	Coefficient of sliding friction
ω	Angular velocity, rad per sec

librium of forces, Fig. 1, and according to Equation 1, the condition for rolling motion is

$$P_{\max} \leq W\mu_o \quad (2)$$

As this equation shows, rolling motion of a wheel exists as long as the tractive force P remains smaller than the static-friction force.

Principal distinction between rolling and sliding of a wheel lies in its effective utilization of frictional ground forces. Coefficients of static friction, having higher values than coefficients of sliding friction, permit greater forces to be transmitted by a rolling wheel than by a sliding one. This is especially important during braking. The rolling wheel can also maintain its direction of travel, while a sliding wheel is directionally unstable.

The propelling force can assume two different forms:

1. External force, either pulling or pushing, acting at the wheel center.
2. Internal force, originating within the vehicle itself and translated as torque to the driving wheels. The frictional reaction of the ground is then the actual driving force.

In rolling motion it is unimportant whether the force acts on the wheel center or on its periphery. The internal traction force of a self-propelled vehicle is, however, directly limited by the available ground friction, and torque in excess of this limit is ineffective as propelling agent. Obviously, the ultimate limit on vehicle performance is set by the capacity of the wheels to create the necessary frictional connection with the ground.

Equation 2 can be rewritten to give the maximum internal torque that can be transferred to the ground by a wheel:

$$M_{\max} = rW\mu_o \quad (3)$$

Rolling Resistance: For sliding motion, the fric-

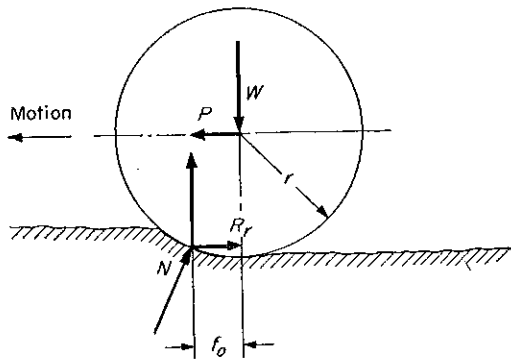


Fig. 2—Rigid wheel rolling on plastic ground. Coefficient of rolling resistance f_o has the dimension of length.

tional force $W\mu_s$ is the motion-resisting force to be overcome by traction. Static friction $W\mu_0$ is for the rolling wheel only a *limiting* force and otherwise does not participate in the actual rolling motion. The force opposing the rolling progression of a wheel is called rolling resistance.

A wheel of weight W pulled at its pivot point by a tractive force P is shown in Fig. 2. In accordance with general physical deductions on rolling resistance, the wheel, considered rigid, forms a deformation in the ground. Acting at the pressure center of the ground contact area is force N . This force can be resolved into a vertical component, forming equilibrium with wheel weight W , and a horizontal component, representing the rolling resistance R_r . Considering the height of the ground deformation negligible compared to the rolling radius r , the equilibrium equation around the action point of the ground force is

$$P = R_r = \frac{Wf_o}{r} \quad (4)$$

Here, the proportionality factor f_o is the coefficient of rolling friction. Its value is determined by the nature of the contacting materials. Dimension of the factor is a length, which has a certain physical significance as the lever arm represented by the hypothetical horizontal distance between the point of application of the ground reaction force and the vertical axis through the wheel center (Fig. 2). Accurate measurements of f_o are difficult to make, and generally accepted data are scarce.

Elastic Wheels

Behavior of an elastic wheel, such as the rubber tire, will not exactly follow the general laws of friction and rolling that have been developed for the rigid wheel. The important difference is in the type of ground contact. On a rigid wheel, ground contact is ideally a line; on a rubber tire, it becomes a relatively large area, Fig. 3.

Rolling Resistance: Determination of rolling re-

sistance for rubber-tired vehicles, because of wheel elasticity, requires variation in the approach developed for the rigid wheel. For the elastic wheel, Equation 4 can be written

(5)

$$R_r = Wf$$

where rolling resistance R_r is simply a function of the radial weight W and of a dimensionless factor f , which is the coefficient of rolling resistance. This coefficient is itself a complicated function of the rolling radius, as well as of the materials and elastic qualities of wheel and ground.

Wheel Slip: Tests show that static friction of an elastic wheel reaches maximum, not for the theoretically required state of pure rolling, but for partial sliding. The symbol s denoting slip is introduced as a means of defining the proportion (in per cent), of sliding to rolling:

$$s = \left(\frac{v - r\omega}{v} \right) \times 100 \quad (6)$$

where v is translatory and $r\omega$ is peripheral wheel speed.

Sliding can assume two different forms: (1) where a locked wheel is pulled over the ground (as in braking), and the translatory speed is greater than the speed of rotation ($v > r\omega$); or (2) where the wheel is turning without equivalent translatory progression (as in accelerating on slippery ground) and $r\omega > v$.

Rolling radius r is usually assumed to be the loaded radius of the tire at static nominal load. This approximation is accurate enough for performance calculations. However, the actual rolling radius will be larger due to centrifugal force effects, especially at high speeds and on low-pressure tires.

Tire Deformation: Observation of the rolling of a rubber tire on rigid ground shows that contraction of the tire surface must take place because the chord of the projected tire-contact area is

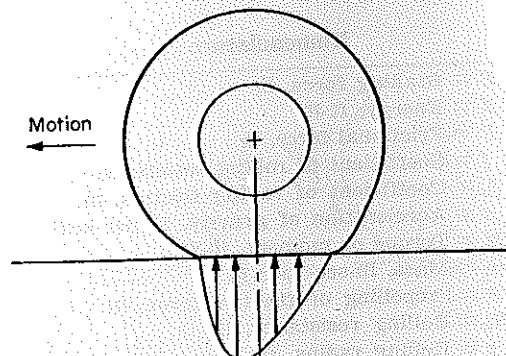


Fig. 3—Elastic wheel (rubber tire) rolling on rigid ground. Pressure distribution in the tire footprint is asymmetric. Contraction of the tire periphery gives the effect of tire slip.

obviously shorter than the arc of the undeflected tire, Fig. 3. Pressure distribution in the tire footprint is shifted in the travel direction, and a pronounced surface elevation of compressed tire particles is formed behind the ground contact area. The contracted part of the tire surface will expand again after it passes the ground-contact area through the action of its elastic forces. This expansion is, in fact, a sliding motion, resulting in retardation of the translatory speed against the speed of rolling and may be called the deformation slip. Every torque transfer through a tire will therefore result in a certain slip and vice versa. Contrary to the behavior of the rigid wheel, where the highest static friction is reached with zero slip, the maximum transferable force through a pneumatic tire is reached somewhere between 10 and 20 per cent slip. According to some experimental data, 20 per cent is the limit of deformation slip, since the coefficient of friction μ_o reaches maximum at this point. Further increase of slip results in an unstable condition, with μ values falling rapidly to pure sliding value μ_s . To emphasize the particular behavior of the elastic wheel, the coefficient of friction for rubber tires has been more appropriately called *coefficient of road adhesion*.

Resultant Friction Forces: Mechanics of frictional forces on a rubber tire can be illustrated by an example. The right side of Fig. 4 is a schematic top view of a tire transferring a braking force B in the rolling direction and a side force S , perpendicular to the rolling direction. These conditions may exist, for example, in a car being decelerated on a curve. Limits of frictional forces are proportional to available μ values and are represented as circles to indicate that the tire has no preference regarding the direction of the frictional force it is transferring.

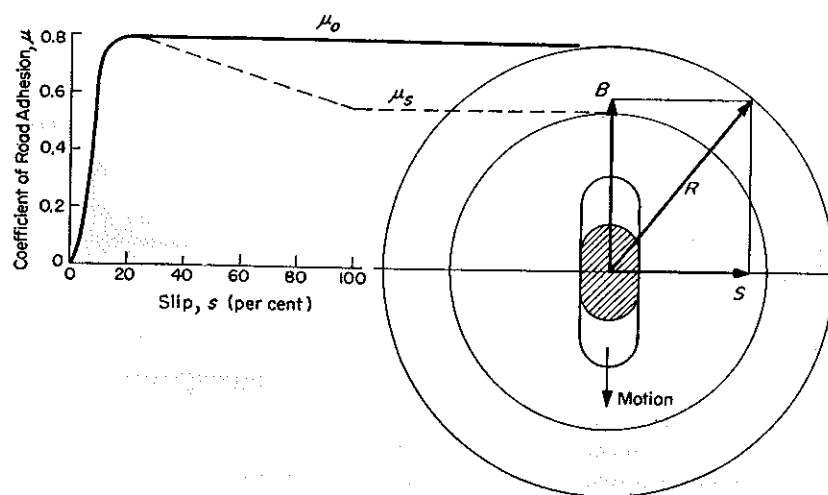
Forces B and S form a vector resultant R . As long as R stays inside the circle μ_o , rolling will exist. Should either B or S increase to the point where R cannot be contained by μ_o , the friction will fall very rapidly to μ_s values and the wheel will start to slide. Side force S , which then cannot be maintained, disappears entirely; B loses its previous direction of rolling and is opposed only to the instantaneous motion.

These considerations are significant in the braking of a vehicle. Locked wheels result in the utilization of lower μ_s values and the complete loss of rolling resistance as a decelerating force. Furthermore, and this is even more important, the locked wheel loses its ability to absorb side thrust and becomes directionally unstable.

Stability in Braking: Side thrust can be created by centrifugal force, road side elevation, asymmetrical weight distribution in the vehicle or by uneven distribution of braking forces. If, on a car equipped with four-wheel brakes, the wheels on one axle become locked, Fig. 5, these wheels lose their side thrust absorbing capacity, and all the reaction is taken by the other axle. This action results in the following stability conditions:

1. For locked rear wheels, Fig. 5a, inertia force mb of the moving vehicle, acts as a pushing force leaning on the front wheels. Any deviation from symmetric weight distribution will create a self-increasing turning moment around the front-axle center. The condition of locked rear wheels must, therefore, be avoided by proper brake-force distribution.
2. If front wheels are locked, Fig. 5b, a turning moment around the rear-axle center is produced. This is a self-stabilizing effect, since

Fig. 4—Coefficient of road adhesion as a function of tire slip. Maximum ordinate value—static coefficient μ_o —is reached between 10 and 20 per cent slip. Higher angles result in an unstable condition, with tire action rapidly changing to pure slip and frictional coefficient μ_s .



View of tire footprint shows resultant R of braking force B and side force S . Circles represent forces transferable by rolling and sliding and are proportional in diameter to μ_o and μ_s . Resultant R must not exceed μ_o if rolling is to continue.

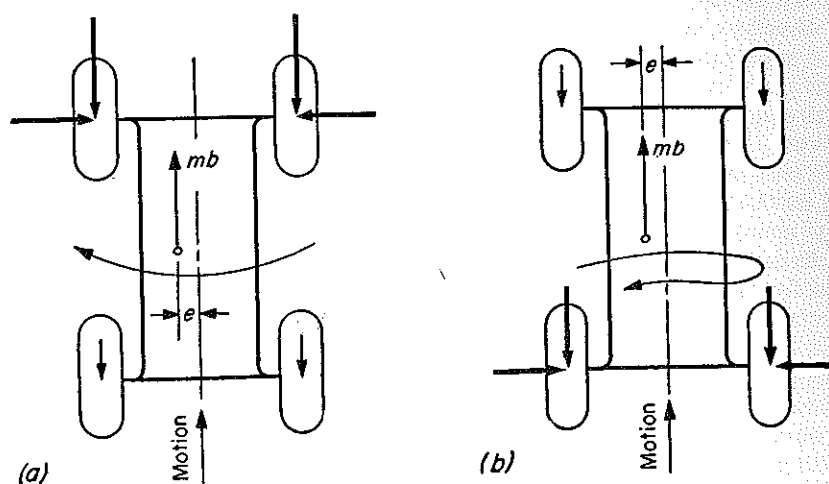


Fig. 5—Direction stability of a vehicle with four-wheel brakes. In *a*, rear wheels are locked, resulting in disappearance of the side-force reaction on the rear axle. Inertia force of the vehicle acts as a pushing force, and any asymmetrical weight distribution (distance *e*) creates a self-increasing turning or skidding moment. In *b*, front wheels are locked. Inertia force acts as a pulling force with self-stabilizing effect.

the inertia force is acting as a pulling force.

Coefficient of Road Adhesion: Measurement of the coefficient of road adhesion, Table 1, is difficult and has shown great variation because of the many variables that are difficult to control and define. Nevertheless, theoretical analysis of the physical processes involved leads to better understanding of the general problem of vehicle traction.

Following are the principal factors that affect the road-adhesion coefficient:

GROUND-SURFACE MATERIAL: Asphalt, concrete and stone pavement are the usual running surfaces for highway vehicles, and their respective μ values under dry conditions are very similar. Off-the-road vehicles, however, will operate on surfaces ranging from earthen roads to deep mud and snow of varying consistency, and the undefined structure of these materials will permit μ determination only as an approximate average value.

GROUND SURFACE CONDITION: State of lubrication of the surface, usually caused by rain, is the principal factor to be considered. Widely varying μ values in the literature for wet highways are explained by the tendency of some materials, especially stone pavement and certain kinds of asphalt, to form when *slightly* wet an exceedingly slippery layer of dust and dispersed oil particles. This layer is usually washed away by heavier rain, and a new condition may be created where μ values again approach those for the dry surface.

TIRE DESIGN: The elasticity of the tire, determined mainly by the inflation pressure and the tread pattern, are the most important factors. Influence of these tire characteristics on traction is complex, and a generally accepted solution is unlikely. Certain trends, however, are apparent. Fine lamination of the tire surface delivers superior traction on a hard, smooth surface like asphalt, while for deep, soft ground (snow and mud) wide, deep diagonal ribs give the best performance. Differences in tractive performance between existing competitive products, despite advertising claims, are rather minute. Dependable technical data for comparison purposes are practically nonexistent.

Of major importance is the fact that traction is usually paid for by an increase in rolling resistance and by inferior wearing properties. The practical solution is a compromise between these irreconcilable demands.

DRIVING SPEED: A definite decline of μ with increasing speed has been established. However, no specific agreement on numerical values is likely due to the intricacy of high-speed measurements under the disturbing influences of tire vibration, road shock and uplift forces.

Table 1—Average Coefficients of Road Adhesion

Surface		μ_0	μ_s
Asphalt or Concrete	(dry)	0.8–0.9	0.75
Concrete	(wet)	0.8	0.7
Asphalt	(wet)	0.5–0.7	0.45–0.6
Gravel		0.6	0.55
Earthen Road	(dry)	0.68	0.65
	(wet)	0.55	0.4–0.5
Snow	(hard packed)	0.2	0.15
Ice or Sleet		0.1	0.07

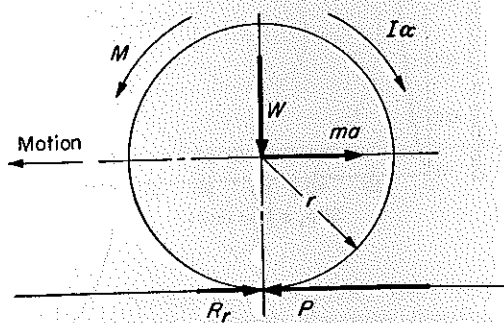


Fig. 6—Dynamics of rolling motion.

TIRE SLIP: From the function of μ versus slip (Fig. 4), two representative values are usually given, maximum friction μ_o and pure slip μ_s .

Selection of Road Adhesion Coefficient: The variety of factors influencing frictional forces, and the impossibility of accurately standardizing them usually means that only average μ values for representative conditions can be considered. Quality and condition of the surface are the important variables, while the influence of speed and tire design is normally neglected.

Choice of μ values for calculation of maximum transferable brake or traction force should be made with sufficient margin for the inevitable side forces, since the tire must transfer the vector resultant of both traction and side forces. As a safety factor, values for sliding friction μ_s are used, rather than the larger μ_o values.

Further simplification is often necessary since vehicles will operate on varying surface types. Only the general surface category (highway or off-the-road) is normally established. Accepted values of μ_s for highway vehicles are between 0.6 and 0.7.

For checking strength of transmission parts and brake systems, the opposite approach is indicated, and the highest possible μ_o values are assumed. Good practice calls for the choice of $\mu = 1.0$, a value which has frequently been observed under favorable conditions.

Dynamics of rolling motion: If torque M of varying magnitude is applied to a wheel with weight W and polar moment of inertia I , Fig. 6, the resulting motion may have characteristics outlined in the following sections.

ACCELERATION: For calculation of the tractive force necessary to accelerate the wheel, use is made of the energy theorem: change in the kinetic energy of a moving body equals work performed by forces acting on the body in the drive direction. The relation is

$$dE = (P - R_r) ds \quad (7)$$

where dE is change in the energy and ds is the elementary distance. Energy of a moving wheel consists of translatory and rotating components, or

$$E = \frac{mv^2}{2} + \frac{I\omega^2}{2} \quad (8.1)$$

Consequently, after differentiation

$$dE = mv dv + I\omega d\omega \quad (8.2)$$

Substituting this result in Equation 7 and rearranging, remembering that $v = \omega r$,

$$v dv \left(m + \frac{I}{r^2} \right) = (P - R_r) ds \quad (8.3)$$

Since $v = ds/dt$ and $a = dv/dt$, tractive force required to produce the acceleration is then

$$P = \frac{M}{r} = a \left(\frac{W}{g} + \frac{I}{r^2} \right) + R_r \quad (9)$$

After substitution of Equation 5 into Equation 9, it can be demonstrated that the maximum ac-

celeration that can be imposed on a rolling wheel is

$$a_{\max} = \frac{W(\mu_o - f)}{(W/g) + (I/r^2)} = \frac{g(\mu_o - f)}{1 + (k/r)^2} \quad (9.1)$$

The limiting condition for this case is $P = W\mu_o$.

MOTION AT CONSTANT SPEED: In this case, tractive force will balance only rolling resistance, and

$$P = \frac{M}{r} = Wf \quad (10)$$

LIMITS OF TRANSFERABLE FORCES: Increase of tractive force above the limit set by static friction will result in sliding motion of the wheel. Sliding friction then becomes the actual motion resisting force, or

$$P = W\mu_s \quad (11)$$

BRAKING: If a decelerating or braking moment is acting on the rolling wheel, it will be aided by the rolling resistance. The maximum braking force transferable is then

$$B_{\max} \leq W(\mu_o + f) \quad (12)$$

If the limits of the static friction are exceeded, the wheel starts to slide, rolling resistance as a decelerating force disappears and the maximum braking force becomes

$$B = W\mu_s \quad (13)$$

In the next part of this series, tire action in cornering, wheel-ground orientation and the mechanics of directional control will be examined.

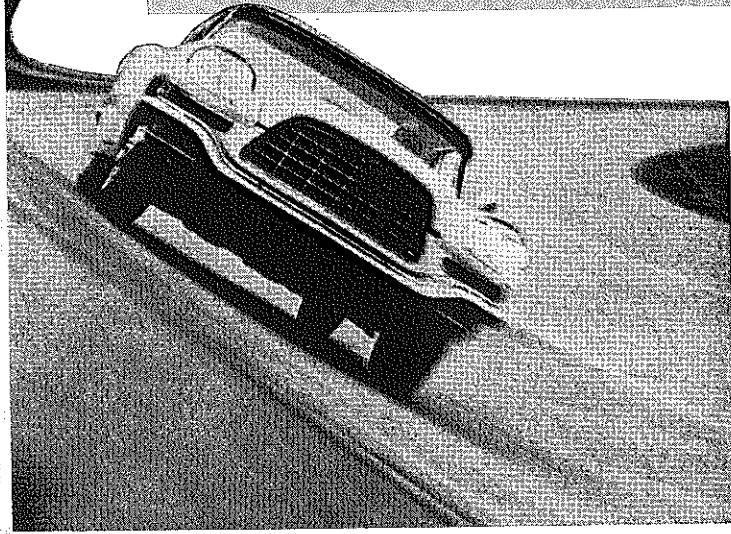
ACKNOWLEDGEMENT

The author expresses his appreciation to R. D. Evans, Manager Tire Design Research Dept., Goodyear Tire & Rubber Co. for providing certain experimental data and reference material used in this series. Thanks are also extended to G. G. Cooper, Design Engineer, Massey-Harris-Ferguson Co. for his valuable suggestions and corrections.

REFERENCES

The following references are applicable principally to Part 1:

1. T. R. Agg—*Bulletin 88*, Iowa State College Eng. Exp. Station, 1928.
2. J. Bradley and R. F. Allen—"Factors Affecting the Behavior of Rubber-Tired Wheels on Road Surfaces," *Proc. of the Inst. of Auto Eng.*, Vol. XXV.
3. P. Zanke—"Wechselwirkung zwischen Reifen und Fahrbahn beim Bremsen" (Interaction Between Tire and Ground During Braking), *ATZ*, 1939.
4. H. Klaue—"Bremswerkuntersuchungen an Kraftfahrzeugen" (Analysis of the Braking Process on Automotive Vehicles), Deutsche Kraftfahrtforschung Heft 13, VDI-Verlag.
5. Bauer Schuster—"Der Kraftschluss zwischen Reifen und Fahrbahn" (The Force Connection Between Tire and Ground), Deutsche Kraftfahrtforschung Heft 72, VDI-Verlag 1940.
6. Kent's *Mechanical Engineers' Handbook (Power Volume)*, John Wiley & Sons Inc., New York, 1953.
7. R. Bussien—*Automobiltechnisches Handbuch*, Cram, Berlin, 1952.
8. P. M. Heldt—*The Automotive Chassis (Without Powerplant)*, Chilton Co., 1952.
9. W. Kamm—*Das Kraftfahrzeug* (The Automotive Vehicle), Springer, Berlin, 1938.
10. R. Dean-Averns—*Automobile Chassis Design*, Iliffe, London, 1952.
11. H. Goldbeck—*Die Fahrmechanik des Kraftfahrzeuges* (Mechanics of Automotive Vehicles), Franckh'sche Verlag, Stuttgart, 1949.
12. H. Buerger—*Das Kraftwagen-Fahrgestell* (Automobile Chassis), Franckh'sche Verlag, Stuttgart, 1952.
13. Hütte—*des Ingenieurs Taschenbuch*, Teil V. A.



DIRECTIONALLY stable maneuvering of self-propelled vehicles presupposes the ability of tires to support side forces developed by centrifugal effects, side winds and road-bank elevations. Research in the mechanics of tire cornering is of relatively recent date, and advanced development is still in process. The unusual complexity of the subject permits treatment here of only basic principles. Detailed considerations are presented in references given at the end of the article.

Tire Action in Cornering

Rigid wheels give sufficient stability to a low-speed vehicle steered by outside forces. The horse and carriage is an example. An automotive vehicle steered from within, on the other hand, maintains directional stability at high speeds only by utilizing the much higher side-thrust capacity of a rubber tire.

Cornering Forces: Rolling motion of a wheel is obviously possible only in its longitudinal plane. If by action of external side forces, the travel direction of a wheel is forced to deviate from true rolling direction, the rubber tire counteracts with a frictional-reaction or cornering force, Fig. 7. Condition for its existence is an area ground contact, which contrasts with the linear contact of a rigid wheel. The tire cornering force originates in the elastic forces of rubber-tire particles which,

By Jaroslav J. Taborek*

Development Engineer
Towmotor Corp.
Cleveland

as they pass the ground-contact area, are forced to travel sideways in addition to their rolling progression. Conversely, the tire will develop a cornering force only if its path of travel deviates from the true direction of rolling. Cornering force is, in fact, proportional to the angle of deviation or slip angle.

Necessary consequence of this phenomenon is that the course of a vehicle negotiating a curve must differ from the theoretical path of rolling by the value of slip angle required to create the necessary cornering force. The relation between slip angle and cornering force gives rise to the practice where front or steering wheels are turned in toward the center of the vehicle at a small angle called the toe-in angle. For straight-ahead driving, toe-in angle is actually slip angle. This angle enables the steered wheels to absorb side thrusts and road shocks without deviating from a straight course. If the same deflecting forces act on a wheel without toe-in, the tire must create its slip angle with consequent directional change.

It is of fundamental importance that the hypothetical action point of the cornering force fall (in relation to the travel direction) behind the projected wheel center. The cornering force then exerts on the tire a horizontal torque which tends

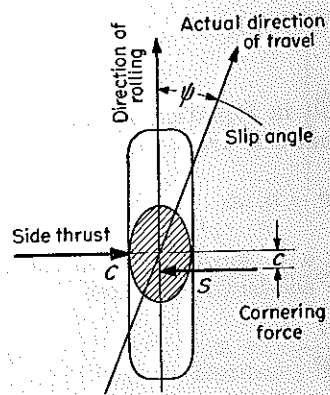


Fig. 7—To balance side thrust C , the rubber tire develops a cornering force S when its direction of travel deviates from the true rolling plane by slip angle Ψ .

*Now Research and Development Engineer, Phillips Petroleum Co., Bartlesville, Okla.

and Directional Control

- cornering forces
- self-aligning torque
- wheel-ground orientation
- static-steering torque

to decrease the existing slip angle and therefore realigns the directions of rolling and actual travel. This particular effect of cornering force is known as the *self-aligning torque*.

Factors Influencing Cornering Force: From the physical origin of cornering forces, factors influencing its magnitude can be deduced. Tire behavior in cornering is usually represented by characteristic curves like those shown in Figs. 8 through 12. These curves are presented to emphasize character of the functions rather than actual numerical values.

Principal factors affecting the cornering force are presented in following sections.

SLIP ANGLE: Cornering force is proportional to slip angle, Fig. 8. The function is practically linear up to about 5 deg slip; it then flattens out and reaches maximum value where the tire starts to skid. To aid comparison of cornering behavior of different tires, the factor *cornering power*, defined

as cornering force per deg slip angle, has been introduced. The cornering power of an average passenger-car tire is about 150 lb per deg slip angle.

RADIAL LOAD: Cornering force, since it is basically frictional in character, is proportional to the radial weight acting on the wheel. Tire deformation and changes in contact-area pressure distribution cause the function to deviate from the theoretical straight line. Maximum value falls near the nominal load point, Fig. 9.

For better comparison purposes, the combined factor, *cornering coefficient*, was created, defined as cornering power per unit vertical load. This factor is used as a true measure of the interrelation between load and cornering ability. The form of the curve indicates that relative cornering capacity declines with higher loads or, in other words, the more load a tire carries, the less effective it is in supporting side forces, Fig. 10.

CAMBER ANGLE: A cambered wheel—one with

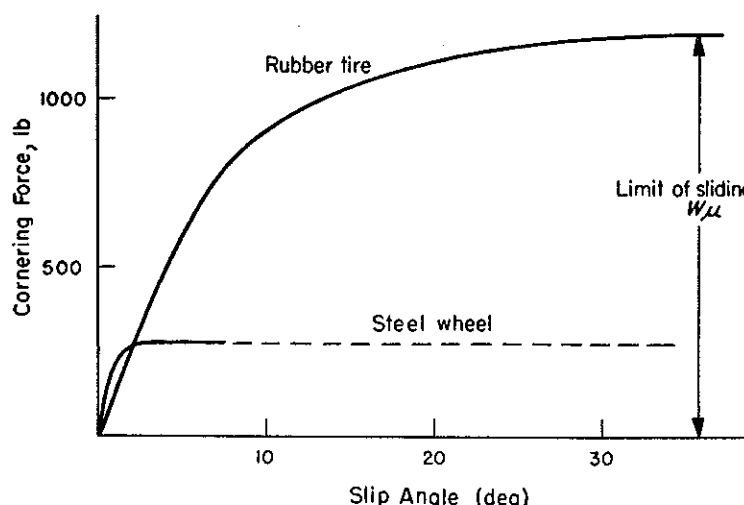


Fig. 8—Cornering force as a function of slip angle for typical rubber-tired and steel wheels. Force reaches maximum value W_{μ} where skidding begins.

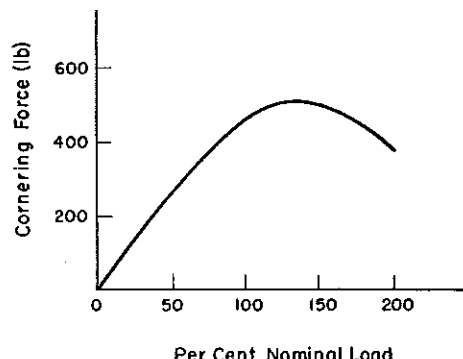


Fig. 9—Cornering force as a function of radial load (3-deg slip angle). Tire deformation and changes in footprint pressure distribution cause function to deviate from the theoretical straight line.

its plane of rotation angled away from the perpendicular—would follow a circular rolling path if not restricted. Direction of travel of a cambered wheel on a vehicle therefore deviates from its natural rolling path, creating a slip angle and, consequently, a cornering force. Value of this force is, for the usual camber angles of about 1 deg, relatively small. It subtracts or adds to the cornering force due to the centrifugal effect, depending on whether the camber inclination is toward or away from the inside of the curve.

INFLATION PRESSURE: Increase in side-wall stiffness accompanying higher inflation pressures results in an increase in cornering power. Higher inflation pressures are therefore often used to achieve better cornering effects, Fig. 11.

TIRE SIZE: Small tires have relatively higher cornering ability than large tires (per pound of load capacity). This accounts in part for the preference for small dual tires rather than single large ones.

SPEED: Cornering force has been found independent of speed.

Self-Aligning Torque: An important factor in steering behavior is self-aligning torque. Usually represented as a function of the slip angle, this factor shows a maximum around 5 deg slip angle, followed by a steady decline. For very high slip angles it reaches negative values.

The relation between cornering force and self-aligning torque is illustrated in Fig. 12. After the self-aligning torque has reached a positive maximum, it reverses and reaches a new high in the negative direction. Cornering force steadily increases with slip angle until the skidding limit W_μ is attained, Fig. 13. The average driver will

Nomenclature

- A = Area, sq in.
- b = Nominal tire width, in.
- C = Centrifugal force (side thrust), lb
- c = Action arm of cornering force, in.
- e = King-pin offset (projected distance on the ground), in.
- h = Effective moment arm of steered wheel, in.
- I_o = Polar moment of inertia of tire footprint, in.⁴
- k = Polar radius of gyration of tire footprint area, in.
- M_{ik} = Moment around king pin due to king pin inclination, lb-in.
- M_k = Moment around king pin required to turn one stationary wheel, lb-in.
- M_s = Static steering moment around footprint center, lb-in.
- S = Cornering force or side thrust, lb
- S_i, S_o = Side forces (subscripts i and o refer to inside and outside wheels, respectively), lb
- W = Weight or load, lb
- α = Steering angle, deg
- θ = King pin inclination, deg
- γ = Slip angle, deg
- μ_s = Coefficient of sliding friction
- μ_u = Effective coefficient of friction of a steered tire

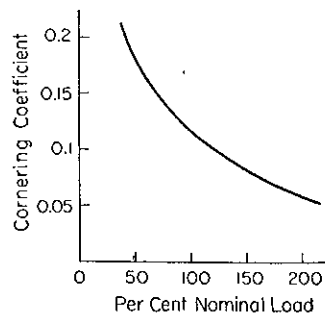


Fig. 10—Cornering coefficient (cornering power per unit radial load) as a function of radial load. Curve shows that the ability of a tire to support side thrust decreases as the load it carries increases.

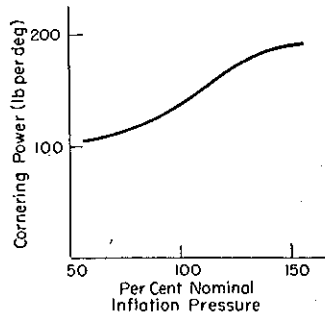


Fig. 11—Cornering power as a function of inflation pressure.

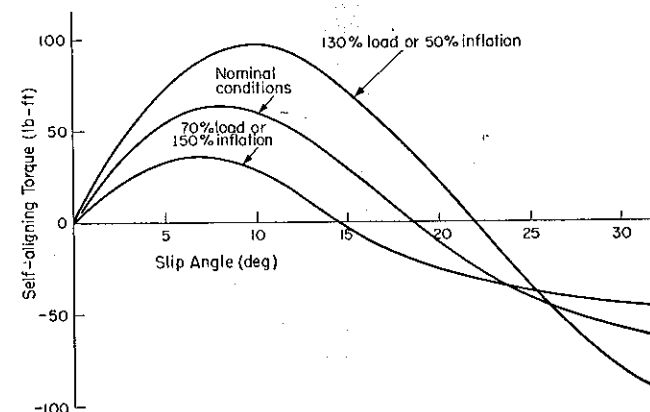


Fig. 12—Self-aligning torque as a function of slip angle. At high slip angles, self-aligning torque becomes negative, acting in a steer-angle increasing direction. Radial load and inflation pressure, because they determine footprint area, have an effect on self-aligning torque.

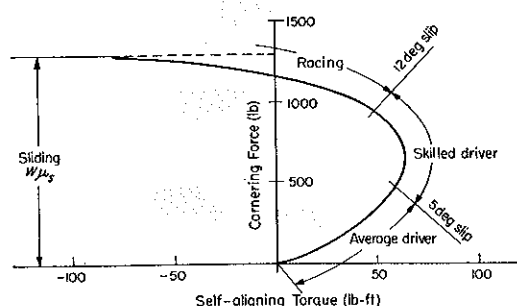


Fig. 13—Relationship between cornering force and self-aligning torque. Average driver can handle car at slip angles to 5 deg, skilled drivers to 12 deg; in racing, slip angles become high enough to give steer-angle increasing torques.

manage the car with slip angles up to 5 deg, skilled drivers up to 12 deg. If driving conditions require still higher cornering forces, extremely high slip angles must be used, and the field of negative self-aligning torque is entered. This effect often can be observed in auto racing, where the driver in a sharp turn steers against the track curvature.

Inflation pressure and radial tire load have an effect on self-aligning torque because of the way these variables change the footprint area. Higher loads and lower inflation pressures enlarge the area and the critical distance c (Fig. 7), consequently increasing the self-aligning torque.

Directional Control

Directional control is defined as the process of giving the vehicle a desired course. *Handling quality* is usually understood as the total of rather subjective impressions of the driver regarding behavior and response of the vehicle to directional commands.

Directional stability, on the other hand, is a dynamic property, implying the tendency of the vehicle to maintain a given course under the action of disturbing forces and its ability to create a new equilibrium condition after the disturbance has been removed. Despite the apparent importance of the problems of vehicle maneuverability, particularly at high speeds, systematic research in

this field has been undertaken only in the last decade or so.

Wheel-Ground Orientation: The steered wheel is suspended to pivot around the king pin. Angular position of both wheel and king pin is of basic importance with respect to steering behavior and steering forces. Simplified illustration of a steered wheel is shown in Fig. 14. Description of the functions of wheel and king pin angles is given in the following sections.

TOE-IN: The wheel angle with the longitudinal axis of the vehicle is toe-in angle. It forms with the drive direction an actual slip angle, creating, therefore, side-thrust capacity for absorbing side shocks from the road and eliminating steering-wheel flutter known as "shimmy." Too high toe-in angles result in excessive tire wear and high rolling resistance. Toe-in angle is measured as a linear deviation of the wheel rim, with usual values of about $\frac{1}{8}$ -in.

CAMBER: Angle of the wheel plane with the ground is described as camber. Opinions vary on its desirability and recommended magnitude. Its main purpose is to achieve axial bearing pressure and to decrease the king pin offset distance e . Camber on passenger cars is between $\frac{1}{2}$ and 1 deg. Too high camber angles promote excessive tire wear.

CASTER: King-pin angle in the longitudinal di-

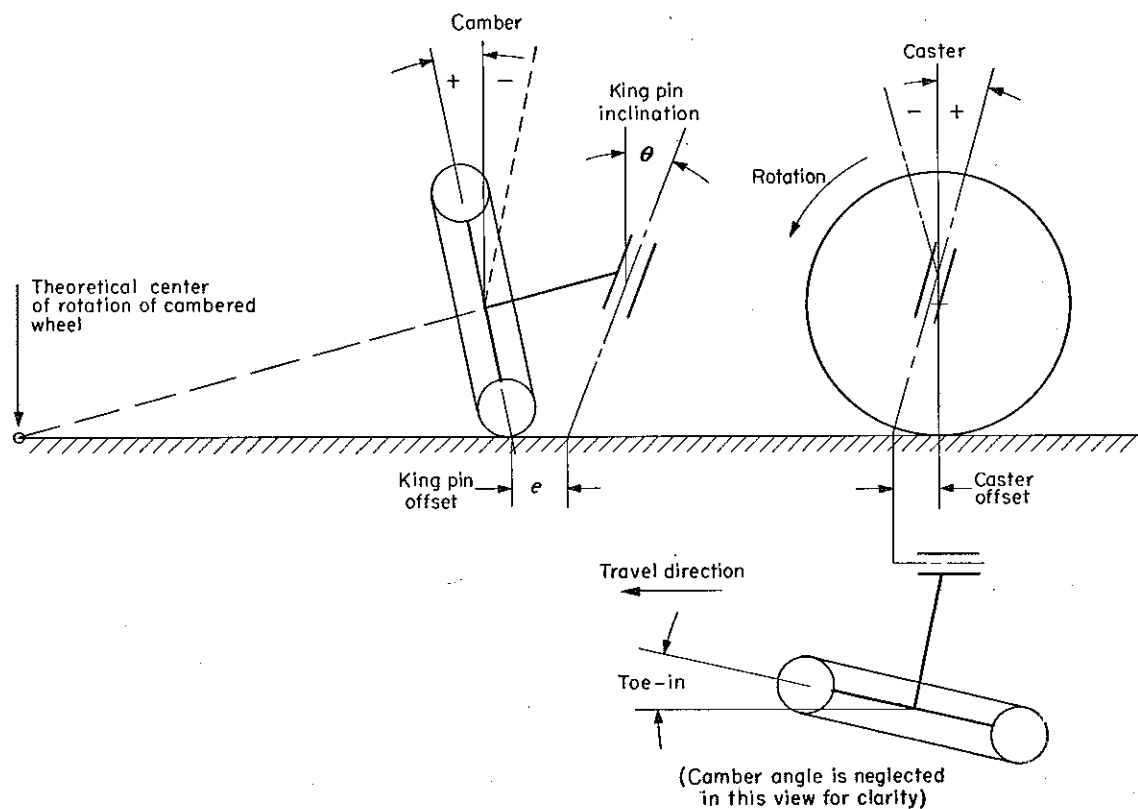


Fig. 14—Wheel orientation with the ground.

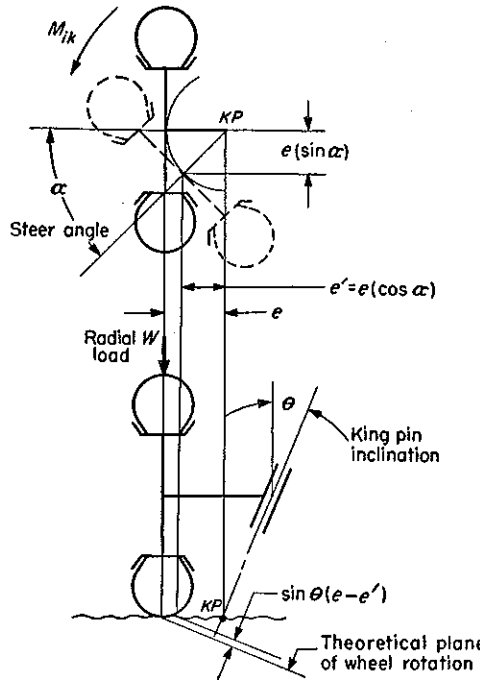


Fig. 15—Effect of king-pin inclination on steering. When wheel is turned around the inclined king pin, the axle is lifted, creating an unstable condition. Return to equilibrium is a self-aligning effect.

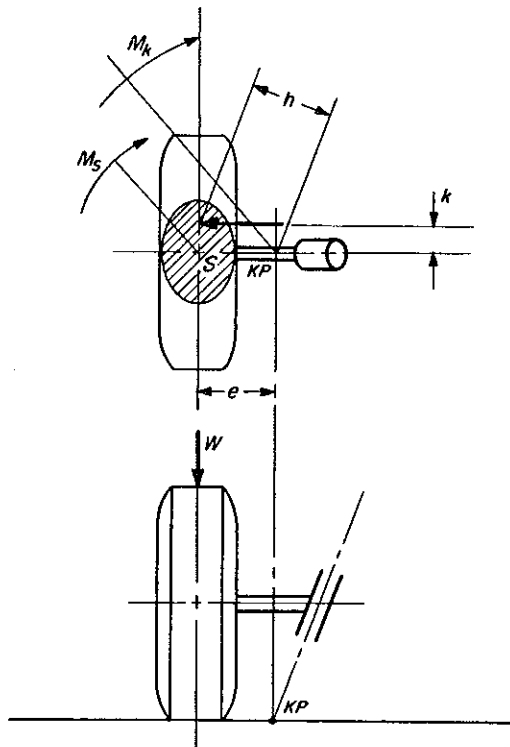


Fig. 16—Actual turning center of a steered wheel is the intersection of the king-pin axis with the ground. Steering motion of the wheel around this point combines wheel sliding and rotation.

rection is caster. It is positive if the ground intersection point relative to the travel direction is ahead of the projected tire center. Caster is used for the self-aligning effect it produces. Usual values are between 3 and 5 deg positive. On rear-axle steered vehicles, negative caster is applied.

KING-PIN INCLINATION: King pin angle θ , perpendicular to the direction of rolling, is king-pin inclination. This angle is used mainly to decrease king pin offset e and to achieve the self-aligning effect. When a wheel with an inclined king pin is turned, the whole axle must be lifted. The moment required to keep equilibrium at the steer angle α can be calculated from Fig. 15, as

$$M_{ik} = \frac{eW \sin \theta (1 - \cos \alpha)}{\sin \alpha} \quad (14)$$

The lifted axle represents, however, an unstable condition. When it tries to regain the low, stable position, a self-aligning torque is created. For the usual king pin inclination angles (about 6 deg) the self-aligning torque is relatively small.

Steering the Stationary Vehicle: The first problem in directional control is steering of the stationary vehicle. Fig. 16 shows the top view of a steered tire and king pin. Torque M_s required to turn the tire around its projected center S is the integral of the frictional forces of the footprint area. It can be calculated as

$$M_s = \mu_s W k \quad (15)$$

where μ_s is the coefficient of sliding friction, W

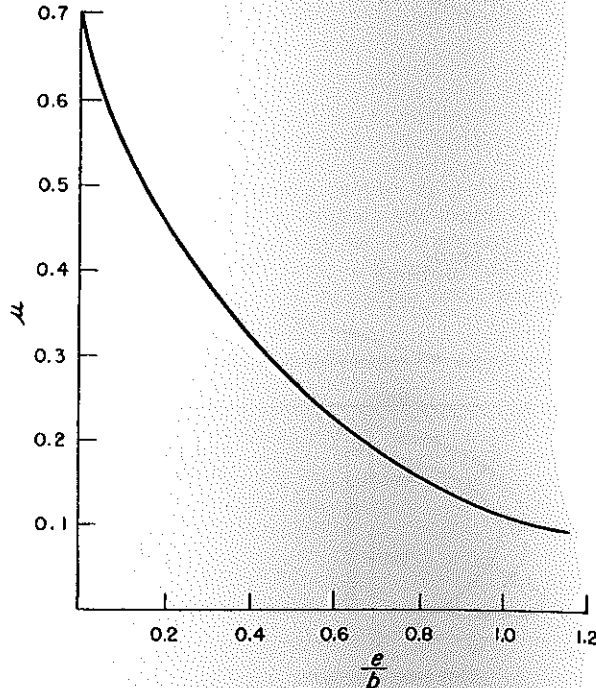


Fig. 17—Static-steering friction coefficient (stationary vehicle) as a function of ratio of king-pin offset to nominal tire width.

the radial load and k the polar radius of gyration of the footprint area.

Center of rotation, which is the hypothetical intersection of the king pin with the ground (point KP), is usually located at a distance e from the footprint center. Consequently, turning of the wheel around this point will not be pure sliding, but rather combined rolling and sliding. The rolling component will increase with larger e values. The effective torque arm becomes

$$h = \sqrt{e^2 + k^2} \quad (16.1)$$

and the torque necessary to turn the wheel is

$$M_k = \mu Wh \quad (16.2)$$

Here, the effective friction coefficient μ is a function of distance e and of tire size. Approximate values of μ on dry concrete ($\mu_s = 0.70$) are represented in Fig. 17 as a function of the factor e/b , where b is the nominal width of the tire.

Values of k can be calculated from the actual tire footprint, which in turn, is a function of inflation pressure and radial load. In rough approximation, the footprint area is a circle, and for nominal tire load conditions, the diameter of this equivalent circle can be assumed equal to the nominal tire width b . The value of k can be then calculated from

$$k^2 = \frac{I_o}{A} = \frac{b^2}{8} \quad (17)$$

where A is the area of the footprint, and I_o the polar moment of inertia of the area.

Static torque M_k is proportional to μ and e , while μ itself decreases with larger e values. This indicates that an optimum king pin distance e must exist for which M_k will be minimum. This calculation was performed for a 7.60×15 tire and is shown in Fig. 18 as M_k/W , a function of e . The curve declines rapidly at first, then flattens off and finally rises again slightly. The design optimum for e is near the region where the rapid rate of change of M_k/W flattens out. Higher e values give only negligible decline in static steering torque and, in addition, exaggerate the highly

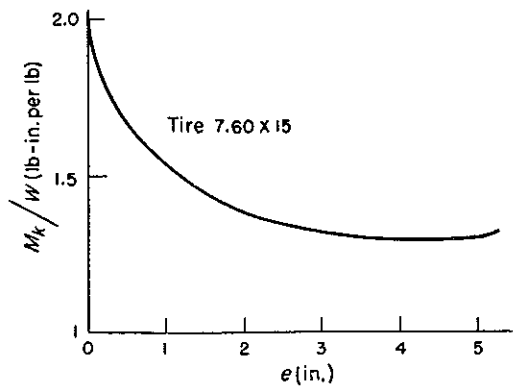


Fig. 18—Static-steering torque per unit radial load as a function of king-pin offset.

undesirable effects of road shocks. Actual design usually takes a compromise between the two requirements.

From the calculated torque M_k , the drag link force D necessary to produce this torque can be calculated from the geometrical relations of the steering linkages.

In the next part of this series, such calculations are illustrated for representative manual and power-steering linkage assemblies.

REFERENCES

14. R. D. Evans—"Properties of Tires Affecting Riding, Steering and Handling," *SAE Journal*, Feb., 1935.
15. K. A. Stonex—"Car Control Factors and Their Measurement," *SAE Transactions*, 1941.
16. A. W. Bull—"Tire Behavior in Steering," *SAE Journal*, Aug., 1939.
17. E. Schuboth—"Beitrag zur Systematik der Kraftfahrzeuglenkung" (Fundamental Research on Steering of Automotive Vehicles), *Automobiltechnische Zeitschrift, ATZ*, Nov., 1939.
18. V. E. Gough—"Cornering Characteristics of Tires," *Automobile Engineering*, London, April, 1954.
19. R. Flala—"Seitenkraefte am Rollenden Reifen" (Side Forces on Rolling Tires), *Zeitschrift des VDI*, Dusseldorf, 1954.

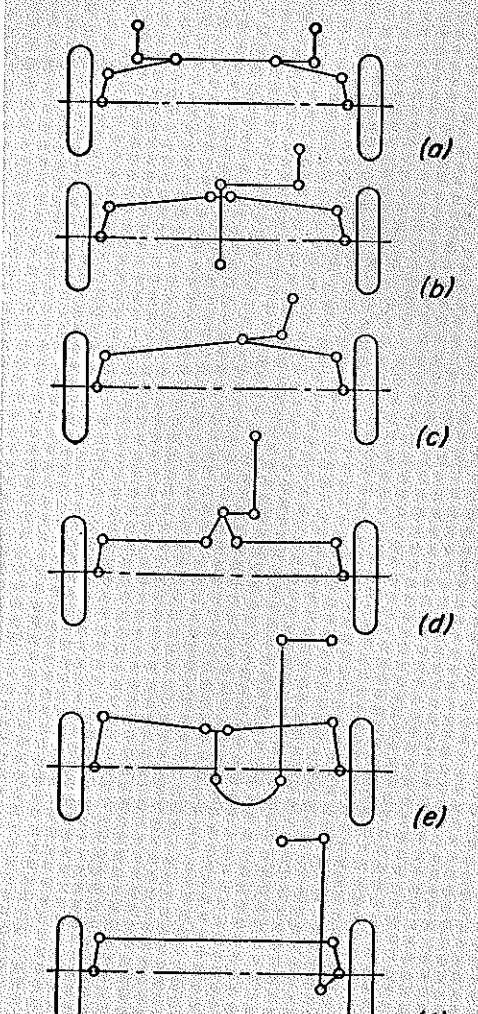


Fig. 19—Typical steering-linkage assemblies. Center-point linkage, *d*, and spindle-lever linkage, *f*, are most common forms in use.

Mechanics of Vehicles-3

By Jaroslav J. Taborek*

Development Engineer
Towmotor Corp.
Cleveland

VEHICLE steering geometry is characterized by a wide variety of linkage forms, Fig. 19.

Two problems are basic in the design of such assemblies: (1) steering or "cramp" angles must be made sufficiently high for vehicle maneuverability without exceeding practical limitations on linkage size, and (2) camber angles must remain substantially constant as the wheels pass over a bump. Most common of the systems shown are the *center-point linkage*, Fig. 19*d*, and the *spindle-lever linkage*, Fig. 19*f*.

*Now Research and Development Engineer, Phillips Petroleum Co., Bartlesville, Okla.

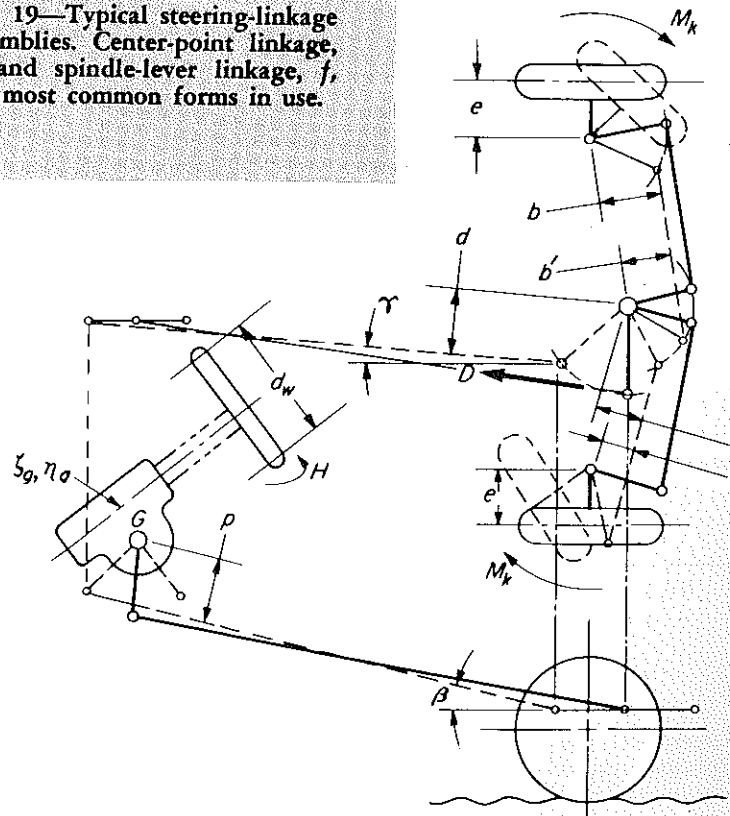


Fig. 20—Rear-axle steering with center-point linkage. Handforce *H* applied to steering wheel produces drag-link force *D*, which is force necessary to overcome steering-resisting moment *M_k* on the stationary vehicle.

Steering Forces and Stability

- steering geometry
- drag-link forces
- power steering
- ground forces and stability

Linkage Forces: Analysis of a typical center-point linkage, Fig. 20, shows drag-link force D to be

$$D = \frac{M_k}{d \cos \beta \cos \gamma} \left(\frac{a'}{a} + \frac{b'}{b} \right) \quad (18)$$

where drag-link angles β and γ are usually small enough to be neglected (less than 15 deg).

For center-point linkage, the steering linkage ratio ζ_s can, for simplification be expressed as

$$\zeta_s = \frac{a'}{a} + \frac{b'}{b} \quad (19)$$

Substituting this relationship in Equation 18, and assuming $\cos \beta = \cos \gamma \approx 1.0$,

$$D = \frac{M_k \zeta_s}{d} \quad (20)$$

which is a simplified expression for the drag-link force.

Summing moments at the gearbox output shaft G and using the results of Equation 20,

$$M_g = Dp = \frac{M_k p \zeta_s}{d} = \frac{H d_w \zeta_g \eta_g}{2} \quad (21)$$

Similar analysis for the spindle-lever linkage, Fig. 21, shows the drag-link force D to be

$$D = \frac{M_k}{d \cos \beta \cos \gamma} \left(1 + \frac{b}{a} \right) \quad (22)$$

Steering-gear linkage ratio ζ_s is

$$\zeta_s = 1 + \frac{b}{a} \quad (23)$$

which, when substituted into Equation 22, gives

$$D = \frac{M_k \zeta_s}{d} \quad (24)$$

Summing moments as before at the gearbox output shaft,

$$M_g = Dp = \frac{M_k p \zeta_s}{d} = \frac{H d_w \zeta_g \eta_g}{2} \quad (25)$$

which is identical to the relationship derived for the center-point linkage.

Nomenclature

A	= Area, sq in.
a, a'	= Steering-linkage lever arms, in.
B, B_i, B_o	= Decelerating forces (subscripts i and o refer to inside and outside wheels, respectively), lb
b_t	= Nominal tire width, in.
b, b'	= Steering-linkage lever arms, in.
C	= Centrifugal force as side thrust, lb
c	= Action arm of the cornering force, in.
D	= Drag link force, lb
d	= Steering lever arm, in.
d_p	= Hydraulic-cylinder diameter, in.
d_r	= Piston-rod diameter, in.
e	= King-pin offset (projected distance on the ground), in.
h	= Effective moment arm of steered wheel, in.
F	= Power-steering cylinder force, lb
H	= Manual steering effort (handforce) on the wheel, lb
I_o	= Polar moment of inertia of the tire footprint, in. ⁴
k	= Polar radius of gyration of the tire footprint area, in.
M_g	= Torque on the steering-gear output shaft, lb-in.
M_{ik}	= Moment around the king pin due to king pin inclination, lb-in.
M_k	= Moment around the king pin required to turn one stationary wheel, lb-in.
M_s	= Static steering moment around footprint center, lb-in.
P_p	= Pump power, hp
Q	= Flow rate, gpm
S	= Cornering force or side thrust, lb
S_i, S_o	= Side forces (subscripts i and o refer to inside and outside wheels, respectively), lb
S_v	= Force required to actuate valve, lb
t	= Steering time, sec
W	= Weight or load, lb
α	= Steering angle, deg
θ	= King pin inclination, deg
ζ_s	= Linkage reduction ratio
ζ_g	= Steering-gear reduction ratio
ψ	= Slip angle, deg
μ_s	= Coefficient of sliding friction
μ	= Effective coefficient of friction of a steered tire
η_g	= Steering gear efficiency

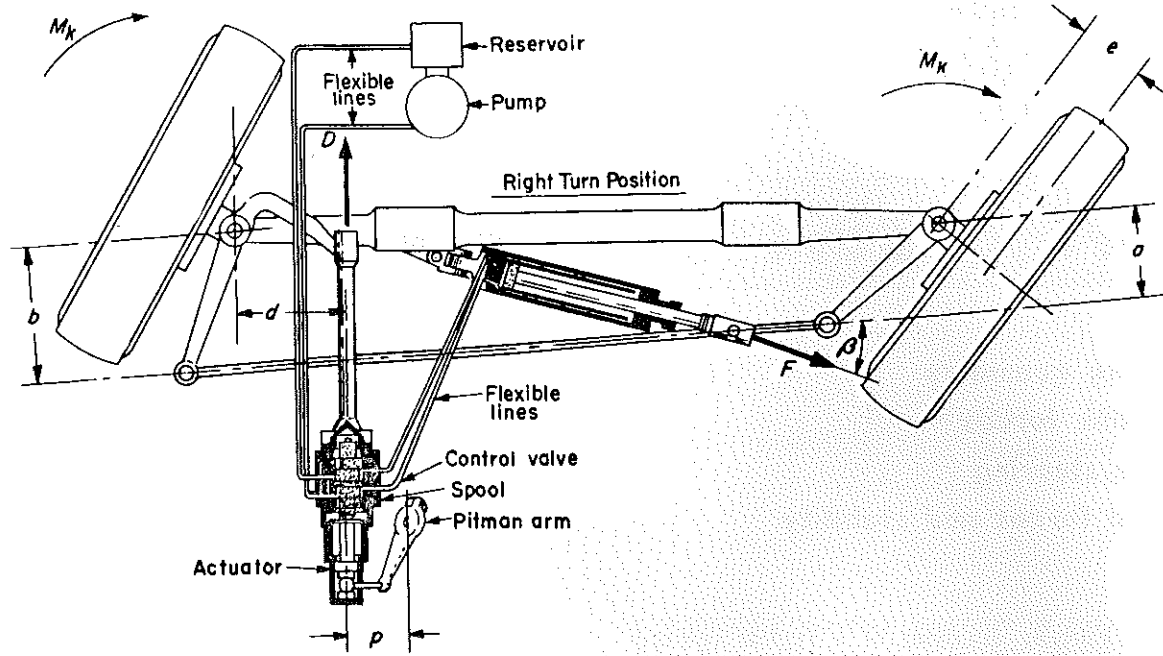


Fig. 21—Spindle-lever linkage with power-steering accessories (Bendix). If handforce applied to the steering wheel exceeds the force required to operate the control valve, the manual-steering force supports efforts of the power cylinder.

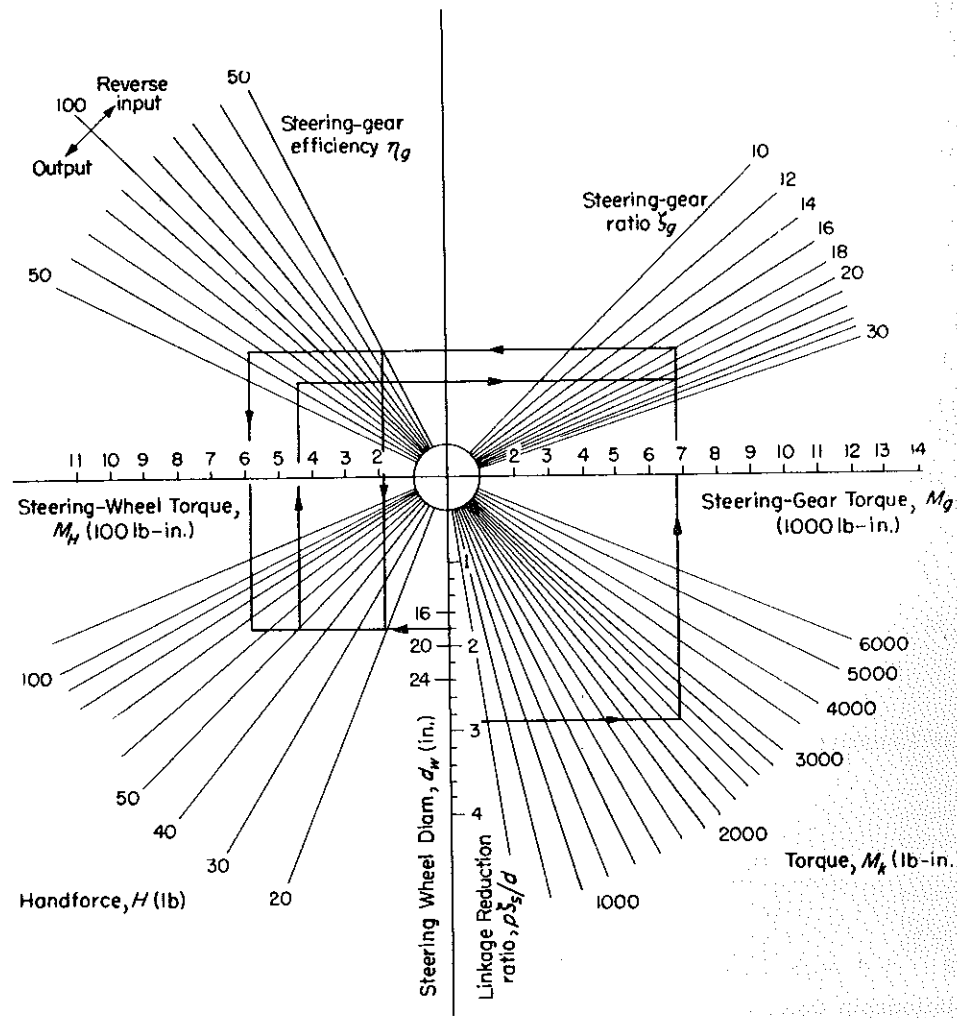


Fig. 22—Manual-steer-
ing calculation chart,
representing Equation
21.

Relationship among the principal steering-linkage design variables—that is, a plot of Equation 21—is given in Fig. 22. Use of the chart to determine steering-linkage parameters is illustrated by Example 1.

In an evaluation of steering linkages, a plot of steering-gear torque M_g as a function of steering angle is useful, Fig. 23. A good steering layout gives no more than 15 per cent variation in M_g between extreme wheel positions. Should torque variations fall outside this limit, steering-linkage elements can be altered in length and angular

position until the torque-angle curve is as desired.

Handforce required to steer a stationary vehicle is usually restricted to certain arbitrary design limits. Generally accepted values—assuming vehicle operation on smooth, dry concrete—are given in Table 2.

Power Steering: If the manual effort required for steering approaches or exceeds practical limits, power steering can be used. Essential elements of

Example 1—Steering Force Calculation

Problem: Calculate all essential elements of a steering system for a vehicle with 3400 lb weight on the steering axle. King-pin offset e is 2 in.; steering-wheel diameter d_w is 18 in.; the proposed steering gear has ratio 18:1 and 65 per cent efficiency. Reduction of the linkage reaches maximum for an extreme steering angle. At this point, the following data have been determined (Fig. 20): $a = 7.5$ in.; $b = 10$ in.; $d = 9$ in.; $p = 11$ in. Tire size is 7.60 x 15.

Manual-Steering Solution: Torque required to turn a stationary wheel around the king pin is calculated from Equation 16.2 (Part 2). Data necessary for use of the equation are determined from the conditions of the problem.

Square of radius of gyration k of the footprint area is given by Equation 17 (Part 2) as

$$k^2 = \frac{b_t^2}{8} = \frac{7.60^2}{8} = 7.2 \text{ sq in.}$$

The effective coefficient of friction μ , taken from Fig. 17 (Part 2) for a value of the ratio $e/B = 2.76 = 0.26$, has the value $\mu = 0.42$.

The effective torque arm is given by Equation 16.1 as

$$h = \sqrt{k^2 + e^2} = \sqrt{7.2 + 4} = 3.3 \text{ in.}$$

With one wheel carrying half the axle load, the moment around the king pin as given by Equation 16.2 is

$$M_k = \mu W h = (0.42)(1700)(3.3) = 2350 \text{ lb-in.}$$

From Equation 21 or from the chart in Fig. 22, steering-gear torque and required handforce on the steering wheel can be found. Steeraxle linkage reduction ratio is found from Equation 23 as

$$\xi_s = 1 + \frac{b}{a} = 1 + \frac{10}{7.5} = 2.33$$

The total reduction factor as used in the chart will be:

$$\frac{p \xi_s}{d} = \frac{(11)(2.33)}{9} = 2.9$$

For the given values, Fig. 22 gives the steering gear torque $M_g = 6800$ lb-in. and the handforce $H = 65$ lb.

From Fig. 22, it can be seen that the same

gear torque induced as shock from the steered wheels could be resisted by a handforce on the steering wheel of only 20 lb. In such a case, the reverse input efficiency of the gear (assumed to be 50 per cent) will consume part of the disturbing torque.

Should a handforce of 50 lb be desired as acceptable maximum, a gear with the ratio of 24:1 should be used.

To check for king pin inclination effect, assume $\theta = 6$ deg and the steerangle $\alpha = 40$ deg. From Equation 14 (Part 2),

$$\begin{aligned} M_{ik} &= eW \sin \theta \left(\frac{1 - \cos \alpha}{\sin \alpha} \right) \\ &= (2)(1700)(0.1) \left(\frac{1 - 0.76}{0.64} \right) \\ &= 12.8 \text{ lb-in.} \end{aligned}$$

which is a negligible torque.

Power Steering Solution: Steering handforce as calculated in the first part of this example may be excessive. Power steering can then be considered.

From Fig. 21, the moment equilibrium equation around the left king pin is

$$M_k + \frac{M_k b}{a} = d \left(\frac{Hd_w}{2p} \xi_s \eta_g - S_v \right) + b \eta_c F \cos \beta$$

This equation includes the steering supporting effect of handforce H , the reaction force of the actuating valve (in S) and the efficiency η_c of the hydraulic cylinder. The effect of these elements is partly compensating and can usually be neglected.

The simplified equation for the required cylinder force is then

$$F = \frac{M_k \xi_s}{b \cos \beta} = \frac{(2350)(2.33)}{(0.94)(10)} = 600 \text{ lb}$$

An available cylinder has a bore $d_p = 1.75$ in., a piston-rod diameter $d_r = 0.75$ in. and a net area A on the piston-rod side of 2.0 sq in.

From the chart in Fig. 26, it is seen that a pump will be required that can deliver hydraulic fluid at 400 psi at an approximate rate of 2.25 gpm. This performance should be achieved at a pump speed corresponding to engine idling speed. The expected steering time will be between 2.5 and 5 sec, which is satisfactory.

Table 2—Steering-Handforce Limits

Vehicle	Handforce, H (lb)
Passenger car	45
Trucks and industrial vehicles	80
Very heavy vehicles	100

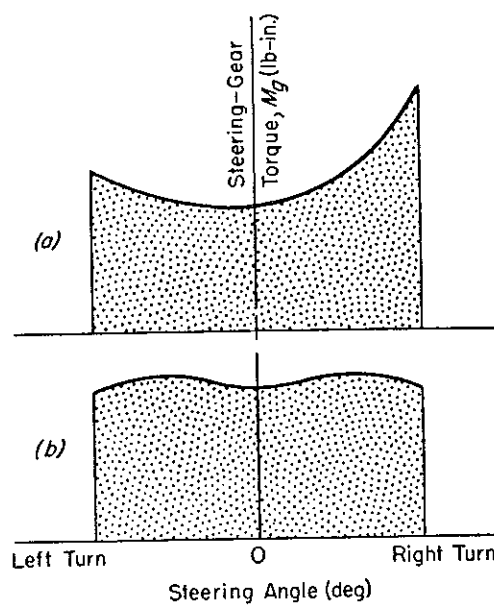


Fig. 23—Torque on gearbox output shaft as function of steering angle. An example of poor steering-gear design is shown at *a*; torque peaks on one side of straight-ahead position. Desirable torque distribution is shown at *b*. Shaded area under each curve represents work performed by steering gear and is unaffected by changes in linkage reduction, gear ratio or angular linkage travel.

the usual power-steering system, Figs. 21 and 24, are described in the following sections.

DOUBLE-ACTING HYDRAULIC CYLINDER: Integral with the steering gear, or mounted as a separate booster, Fig. 25, the hydraulic cylinder can act on any steering-linkage element. Effective work performed by the cylinder is in each case the product of force and displacement. Steering work is substantially constant for various combinations of cylinder diameter, stroke and fluid pressure. Quality of power steering will, to a large extent, depend on the proper balancing of these elements. Force required from the cylinder can be calculated from equilibrium of moments around an appropriate point (see Example 1).

ACTUATOR VALVE: Flow of hydraulic fluid under pressure is directed to the proper cylinder port by an actuator valve. The valve can be integral with the steering gear, integral with the cylinder, or separately mounted in the drag-link line. Wherever the valve is mounted, its action is the same: torque applied by hand to the steering wheel opens one valve port, supplying oil under pressure to one side of the cylinder. The other port simultaneously directs the return flow from the cylinder back to the reservoir. If the handforce acting on the steering wheel exceeds the force required to actuate the valve, it supports the effort of the hydraulic cylinder.

HYDRAULIC PUMP: Power source for a steering system is a hydraulic gear pump which supplies a definite volume of hydraulic fluid at the required pressure p_p . Power to drive the pump can be calculated from the general pump equation

$$P_p = \frac{Q p_p (144)}{\eta (550) (449)} \approx \frac{Q p_p}{(1770) \eta} \quad (26)$$

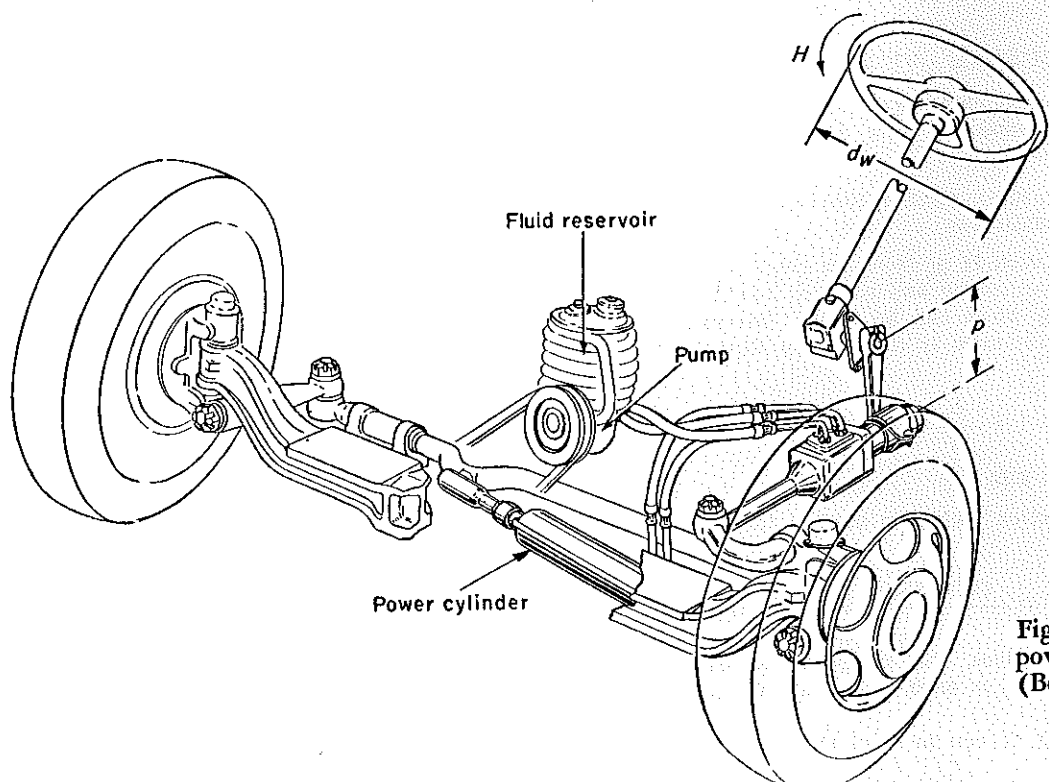


Fig. 24 — Typical power-steering system (Bendix).

where P_p = power required (hp), Q = volume output (gpm), p_f = pressure (psi) and η = total efficiency of the pump (usually 70 to 80 per cent). Characteristic curves supplied by pump manufacturers showing the relation between Q and p_f for different pump speeds are, in practical applications, often distorted by use of flow-control and relief valves. It is therefore advisable to find actual pump output by experiment.

Volume output of the pump will determine the time necessary to fill the hydraulic cylinder displacement. Speed of the cylinder piston should be high enough so that it cannot be overtaken by a handforce turning the steering wheel with an average speed of about 1.5 rev per sec. A good power steering design will achieve full turn of the wheels in $3\frac{1}{2}$ to $4\frac{1}{2}$ revolutions of the steering wheel, giving a total time available to fill the cylinder of from 2.3 to 3 sec.

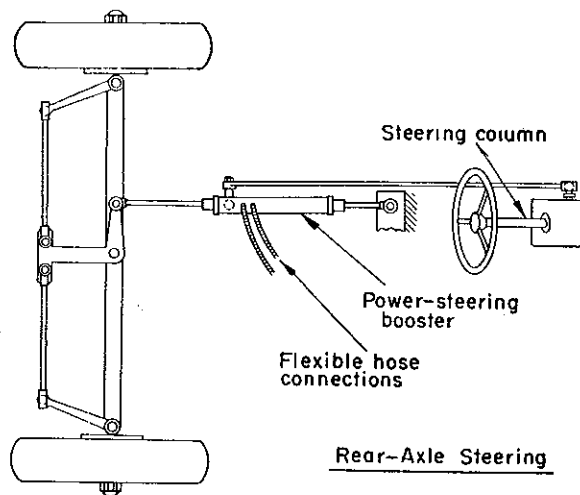
The following equations correlate the variables of a power steering system:

$$Q = \frac{60(As)}{231(t)} \quad (27)$$

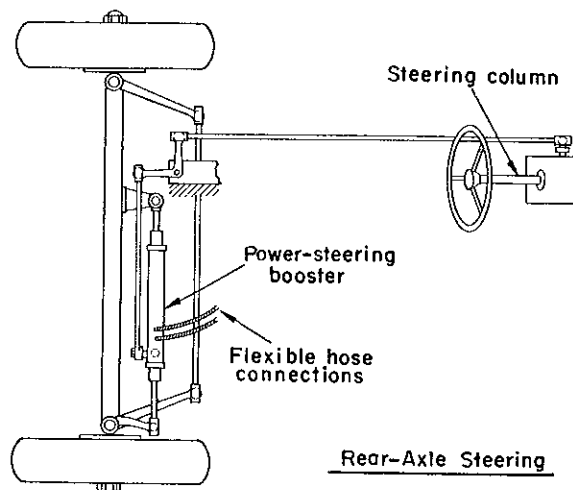
$$F = Ap = \frac{\rho \pi (d_p^2 - d_r^2)}{4} \quad (28)$$

where Q = rate of flow (gpm), A = effective cylinder area (sq in.), d_p and d_r are cylinder and piston-rod diameters (in.), s = piston stroke (in.), F = cylinder force (lb), and t = steering time for full turn (sec).

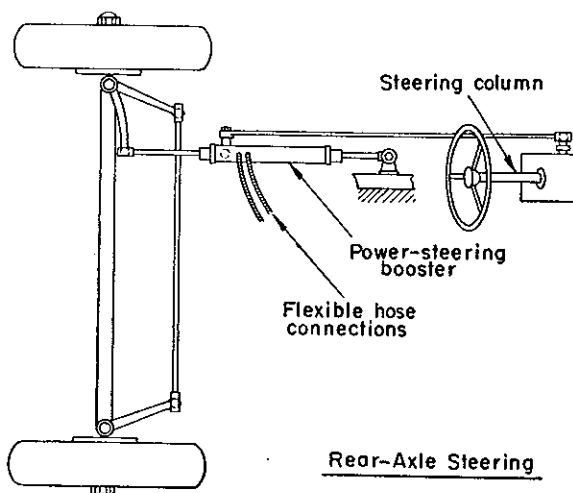
Relations between these interdependent variables are represented in a working chart, Fig. 26. Co-ordination among the design elements can be quickly established by use of this chart.



Rear-Axle Steering



Rear-Axle Steering



Rear-Axle Steering

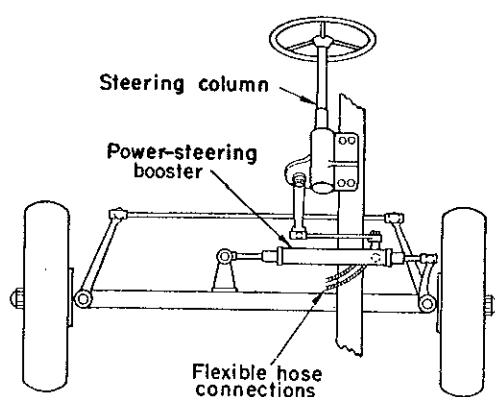


Fig. 25—Typical booster-type power-steering installations (Vickers). Generally, the advantage of the booster-type system is that the force reaction on the power cylinder is supported by the vehicle frame structure.

self-aligning tendency.

Forces and Stability: Forces that must be investigated are: (1) tractive forces, applicable when the steered wheels are also the drive wheels; (2) decelerating forces, including the always present rolling resistance and the braking force if applicable; (3) cornering forces (reaction of the

tire to side forces) acting perpendicular to the rolling direction.

Influence of these forces on steering is shown in Fig. 27. The three basic situations are discussed in the following sections.

STRAIGHT-AHEAD DRIVING: Tractive or decelerating forces, in this case, produce opposite but equal moments on left and right wheels, Fig. 27a.

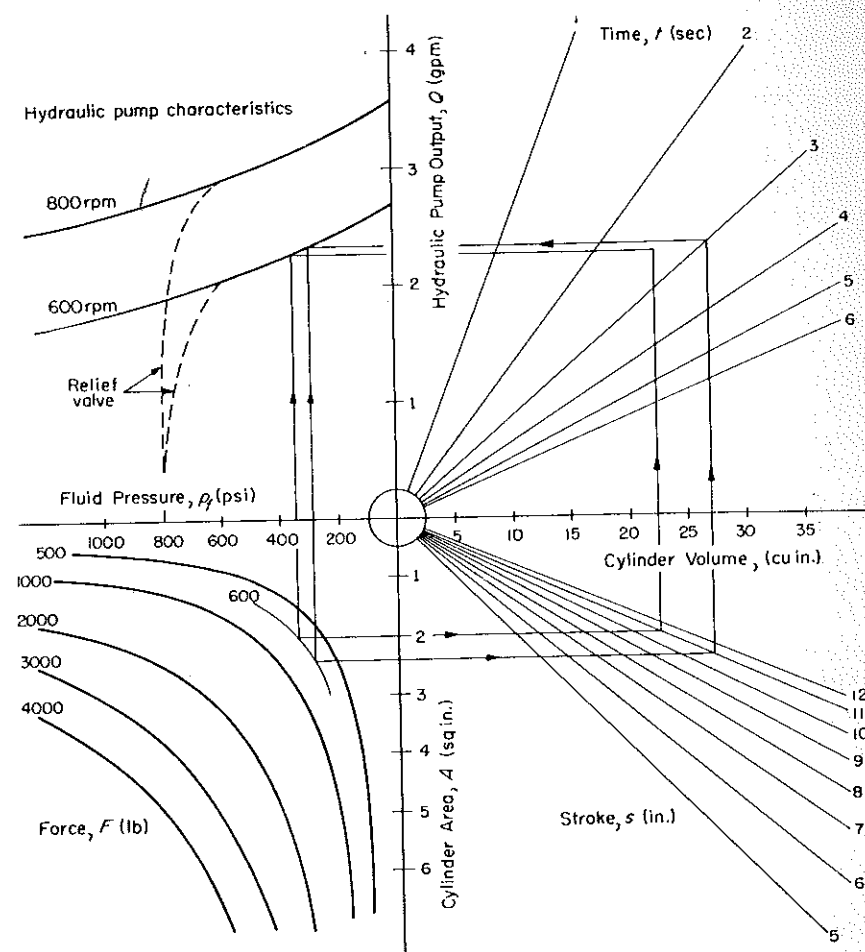
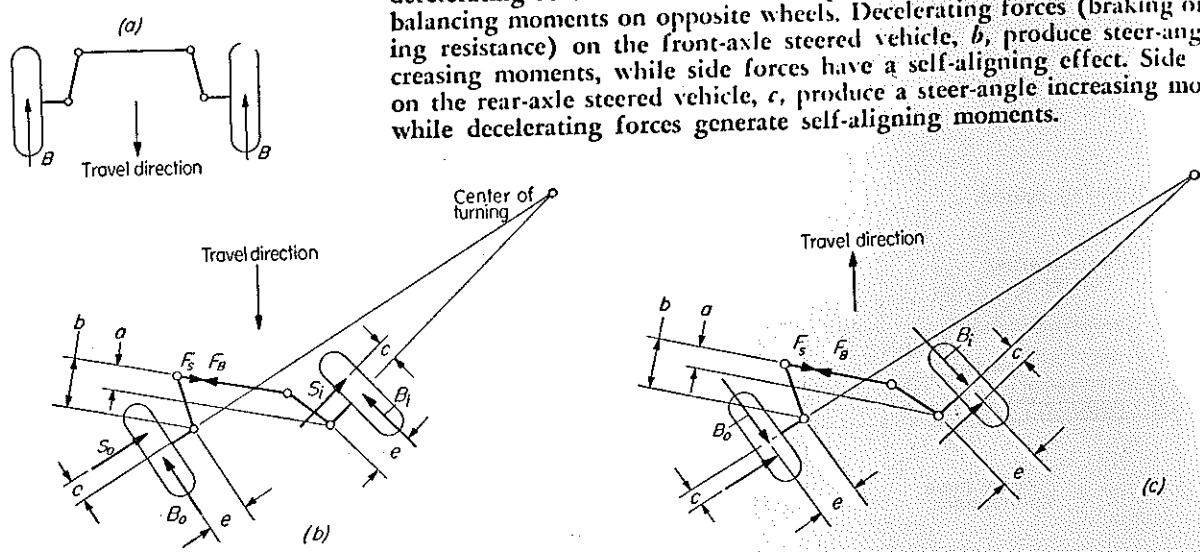


Fig. 26—Power-steering calculation chart, representing Equations 27 and 28. Pump characteristics are approximate and can be replaced by exact values if desired.

Fig. 27—Effect of ground-plane forces on steering stability. Tractive or decelerating forces on vehicle in straight-ahead motion, *a*, produce counterbalancing moments on opposite wheels. Decelerating forces (braking or rolling resistance) on the front-axle steered vehicle, *b*, produce steer-angle increasing moments, while side forces have a self-aligning effect. Side forces on the rear-axle steered vehicle, *c*, produce a steer-angle increasing moment, while decelerating forces generate self-aligning moments.



Torques therefore balance and have no effect on steering.

STEERING AND STABILITY

STEERED FRONT AXLE: A decelerating force B , Fig. 27b, creates the steer-angle increasing tie-rod force $B_i(e/a)$ on the wheel on the inside of the curve and a self-aligning tie-rod force $B_o(e/b)$ on the wheel on the outside of the curve. As lever arm a of the inside wheel is, because of tie-rod geometry, always smaller than arm b , the total effect of a decelerating force is steer-angle increasing. The tie-rod force is then

$$F_b = \frac{B_i e}{a} - \frac{B_o e}{b} \quad (29.1)$$

Tractive forces acting in the drive direction will produce a self-aligning torque. On front-wheel drive vehicles, therefore, less caster angle is normally used, since self-aligning effects derived from the tractive force are sufficient.

Cornering forces S of both wheels act in the self-aligning sense, producing in the tie rod the force

$$F_s = \frac{S_c c}{a} + \frac{S_o c}{b} \quad (29.2)$$

Value of the self-aligning torque depends on the length of moment arm c . Moment S_c is the self-aligning torque commonly called the caster effect. This action of the cornering force is important, since it overbalances the steer-angle increasing effect of rolling resistance.

STEERED REAR AXLE: On rear-axle steered vehicles (or front-axle steered vehicles driven backward) Fig. 27b, decelerating forces produce the self-aligning tie-rod force

$$F_b = \frac{B_i e}{a} - \frac{B_o e}{b} \quad (30)$$

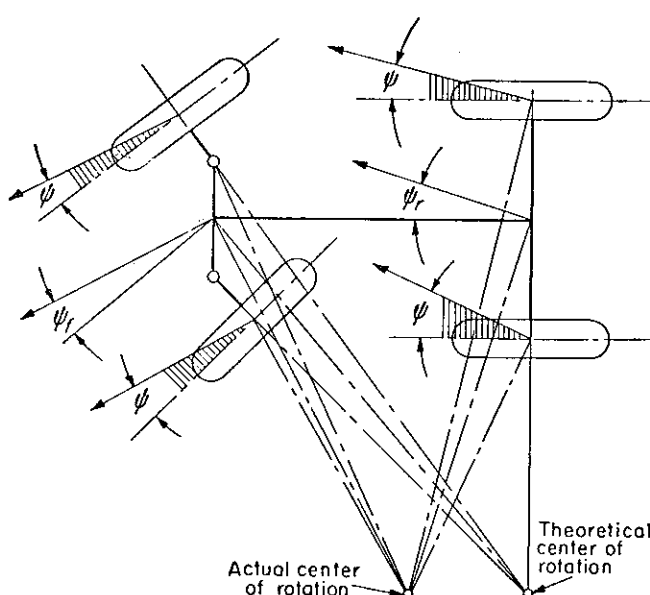


Fig. 28—Actual center of rotation of a vehicle negotiating a curve falls ahead of the theoretical center because of differences in slip angles of front and rear wheels.

The cornering force, however, creates a steer-angle increasing torque, resulting usually in inherent instability of the rear-axle steered vehicle. Negative caster angle may be applied in such cases, reversing the rotation sense of the cornering force around the king pin.

Slip-Angle Steering: It has been shown in a preceding section that any side force acting on a vehicle requires a counterbalancing cornering force of the same value. To produce the cornering force, the tire will run at a slip angle that is proportional to the force required.

Top view of a vehicle driving in a curve is shown in Fig. 28. The theoretical center of curvature, which for Ackerman steering is on the prolonged rear-axle axis, cannot be maintained if the wheels must run at a slip angle. To create the slip condition, the actual center of curvature is always ahead of the theoretical center.

If cornering powers of front and rear tires are different, or if weight distribution results in unequal side forces on front and rear axles, Fig. 29, equilibrium between side-thrust and cornering forces will be reached at unequal slip angles for front and rear tires. Such an effect can give rise

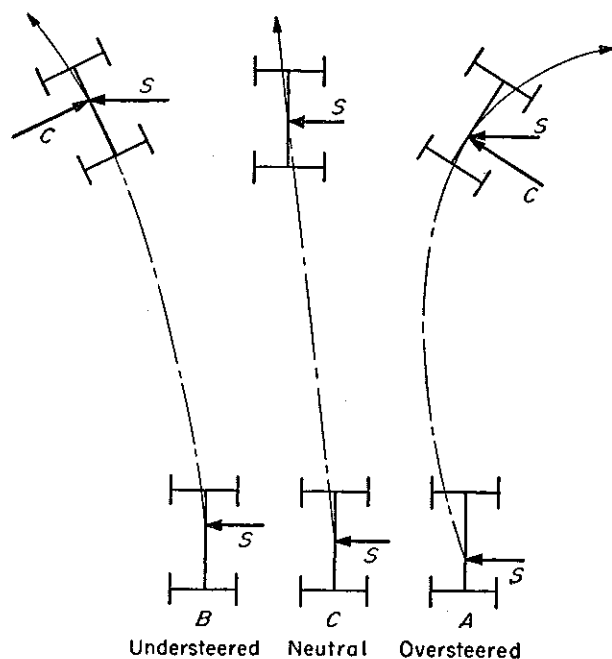


Fig. 29—Effect of slip angles on directional stability. Vehicles A , B and C are subjected to identical side forces S at different points along the vehicle centerlines. Rear-axle heavy vehicle A will "oversteer" and turn toward side force S because the slip angle on the rear axle is greater than the slip angle on the front axle. Centrifugal force created by the curvilinear motion adds to the force S . Front-axle heavy vehicle B "understeers," turning away from the disturbing force. Vehicle C with neutral steering characteristics follows a straight line.

to the following steering conditions:

OVERSTEERING: If the slip angle on the rear axle is greater than on the front axle, the rear end of the vehicle will drift away in the direction of the exciting force into a course of increasing curvature. Centrifugal forces created will add to the primary disturbing force. Oversteering is therefore a situation of inherent instability.

UNDERSTEERING: If the front-axle slip angle is greater, the course of the vehicle will have a self-straightening tendency, that is, away from the exciting force. The centrifugal force produced by the curved motion will subtract from the initial disturbance. This is a desirable condition of inherent stability.

It should be emphasized that slip-angle steering bears no relation to the actual steering of the vehicle. Conclusions reached would have the same validity for a towed trailer. Disturbing forces may be centrifugally caused, or result from any other side-thrust producing disturbance. With a side-wind force, the complexity of the problem is multiplied, since the aerodynamic properties of the body enter the picture.

The influence of slip-angle steering on the directional behavior of a vehicle is shown in Fig. 29.

The same side force S acts at different points on vehicles *A*, *B* and *C*. Vehicle *A* is rear-axle heavy and therefore oversteered; vehicle *B* is front-axle heavy and therefore understeered. Path of the oversteered vehicle is toward the center of the disturbance with increasing curvature, while curvature of the path of the understeered vehicle is decreasing. For comparison, the ideal line of a neutral steering path is shown. This represents a vehicle with identical slip angles on both axles. Should the disturbing force disappear, the oversteered vehicle continues in a path of increasing curvature due to continued centrifugal force, while the understeered vehicle straightens out by itself.

REFERENCES

20. C. W. Lincoln—"A Summary of Major Developments in the Steering Mechanisms of American Automobiles," *GM Engineering Journal*, March-April, 1955.
21. G. E. Lind Walker—"Directional Stability," *Automobile Engineer*, London, Aug. and Nov., 1950.
22. M. A. Julien—"Convergence des Theories Francaises et des Etudes et Realisation Anglo-Saxonnes Concernant la Stabilite de la Route" (Road Stability, Relation Between the French Theories and Anglo-Saxon Practice), *Societe des Ingeneurs de l'Automobile Journal*, Sept., 1948.
23. E. Sawatzki—"Die Luftkraefte und Luftkraftmomente am Kraftwagens" (Direction Stability of High Speed Automotive Vehicles), *Deutsche Kraftfahrorschung*, Heft No. 50, VDI-Verlag, Berlin, 1940.
24. L. Huber—"Die Fahrrichtungsstabilitaet das Schnellfahrenden Kraftwagens" (Direction Stability of High Speed Automotive Vehicles), *Deutsche Kraftfahrorschung*, Heft No. 44, VDI-Verlag, Berlin, 1940.
25. V. G. de Seze—"Stabilite de Route des Voitures a Traction Avant ou a Propulsion Arriere" (Directional Stability of Vehicles with Front and Rear Axle Drives), *Societe des Ingeneurs de l'Automobile Journal*, Oct., 1937.

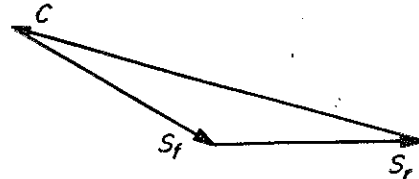
Mechanics of Vehicles-4

Stability on a Curve

- centrifugal forces
- force distribution
- sliding and tipping

By Jaroslav J. Taborek*

Development Engineer
Towmotor Corp.
Cleveland



DIRECTIONAL stability and the side-skidding characteristics of a vehicle negotiating a curve depend upon the balance of dynamic side forces. The nature of these forces, their distribution, and their effects on vehicle stability are examined in the following sections of this article.

Dynamic Side Forces

In curvilinear motion, centrifugal force C (acting ideally at the vehicle center of gravity) is held in equilibrium by the sum of the side-force reactions on all wheels, or

$$C = mr_c \omega^2 = \frac{Wv^2}{gr_c} = \sum S \quad (31)$$

Here, v is the translatory speed of a vehicle of mass m , ω is angular velocity, r_c is radius of curvature and $\sum S$ is the sum of the side-force reactions.

When a vehicle enters a curve, changing its motion from rectilinear to curvilinear, the side-force reactions impose a rate change of angular momentum I_a . For a vehicle with polar moment of inertia I (around the vertical axis), wheelbase L , road-adhesion coefficient μ and angular acceleration α , the relation between side forces and rate of change of angular momentum is

$$\sum S = \frac{I\alpha}{L} \leq W\mu \quad (32)$$

Obviously, the vehicle with small moment of inertia will exhibit fast directional response. Large inertia moments, while slowing down directional response, decrease sensitivity to secondary disturbances. Such a vehicle would tend to maintain

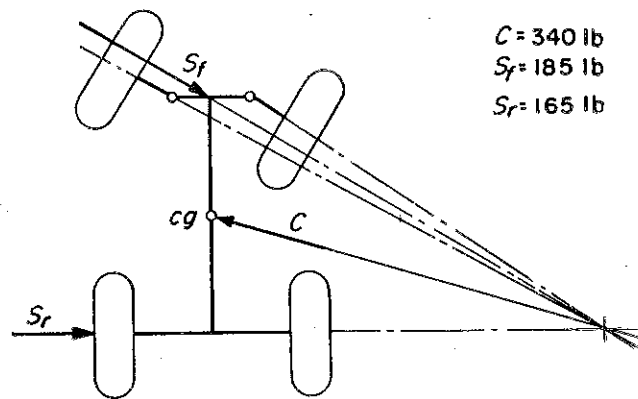


Fig. 30—Side-thrust distribution to front and rear wheels on a vehicle negotiating a curve. Only centrifugal force is assumed to act in this simplified case (rolling resistance is neglected).

its original direction of motion.

Weight distribution (fore and aft) is a determining factor for vehicle polar inertia. Heavy components are preferably located close to the center of gravity for minimum inertia moments. Intended use of the vehicle, since it dictates the necessary compromise between directional response and directional stability, decides the final solution to the weight-distribution problem.

Force Distribution: Equation 31 gave the side force required to balance the centrifugal force on the vehicle. Traction and braking forces acting on the steered wheels, as well as other motion-affecting forces acting ideally at the cg of the vehicle, all produce side-force components which may add to or subtract from the centrifugal force. The side-thrust reaction of the tires must balance the resultant of all these factors.

From a directional-stability standpoint, distribu-

*Now Research and Development Engineer, Phillips Petroleum Co., Bartlesville, Okla.

tion of side forces to the wheels is important. Limits of safe maneuverability are determined by the wheel which first starts to slide. Vectorial analysis by graphical techniques offers a method of determining side-force distribution. The method is demonstrated in sections that follow for a vehicle weighing 4000 lb (evenly distributed on front and rear axles) negotiating a curve of radius of $r_c = 20$ ft at a speed of 5 mph (7.33 ft per sec).

VEHICLE AT CONSTANT SPEED: In this example, rolling resistance of the vehicle is neglected and centrifugal force is assumed to be the only force acting. From Equation 31,

$$C = \frac{4000(7.33)^2}{(32.2)(20)} = 340 \text{ lb} \quad (33)$$

Centrifugal force C , acting through the vehicle center of gravity, is balanced by side thrusts of front and rear wheels, Fig. 30. Obviously, as the turning radius r_c increases, the vectorial sum

$$C = S_f + S_r$$

approaches the algebraic sum

$$C = S_f - S_r$$

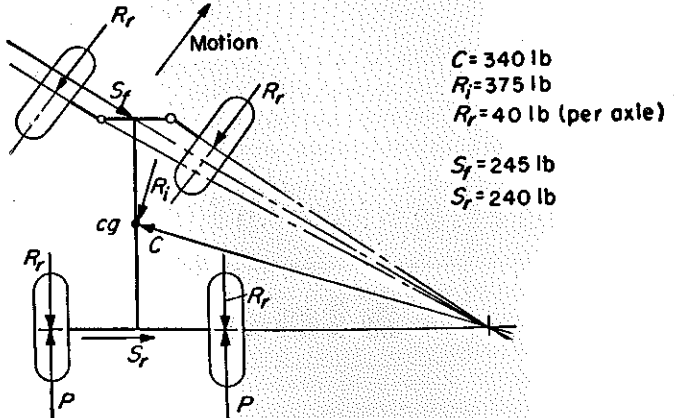
In this simple case, the difference in directions of the right and left-hand steered wheels is neglected, and a force on the center of the front axle is calculated. The error due to this simplification, especially for larger curve radii, is negligible. It is apparent that rear-wheel steering in this simplified case would produce an identical side-force distribution, since the drive direction does not appear in the calculations.

VEHICLE IN ACCELERATED MOTION: In this case, the following forces act on the vehicle: centrifugal force $C = 340$ lb (same as in simplified example); total rolling resistance $R_r = Wf = (4000)(0.02) = 80$ lb. Assuming an acceleration a of 3 fps², the inertia force is $R_i = (W/g)a = (4000/32)3 = 375$ lb.

Grade and air resistances are neglected here. The graphical method of calculation is demon-

Nomenclature

- C = Centrifugal force, lb
- H = Height of center of gravity, ft
- I = Polar moment of inertia of vehicle around vertical axis, ft-lb-sec²
- L = Wheelbase, ft
- m = Mass, lb-sec² per ft
- n = Distance determining tipping stability, ft
- P = Tractive force, lb
- R_i = Inertia resistance, lb
- R_r = Rolling resistance, lb
- r_c = Radius of curvature, ft
- S = Side-force reaction of wheels, lb
- V = Speed, mph
- v = Speed, ft per sec
- W = Vehicle weight, lb
- α = Angular acceleration, rad per sec²
- β = Superelevation angle, deg
- μ_s = Coefficient of sliding friction
- ϕ = Frictional angle, rad
- ω = Angular speed, rad per sec



$C = 340 \text{ lb}$
 $R_i = 375 \text{ lb}$
 $R_r = 40 \text{ lb} (\text{per axle})$

$S_f = 245 \text{ lb}$
 $S_r = 240 \text{ lb}$

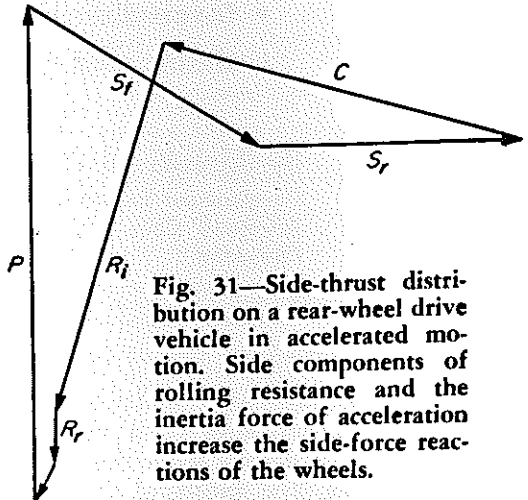
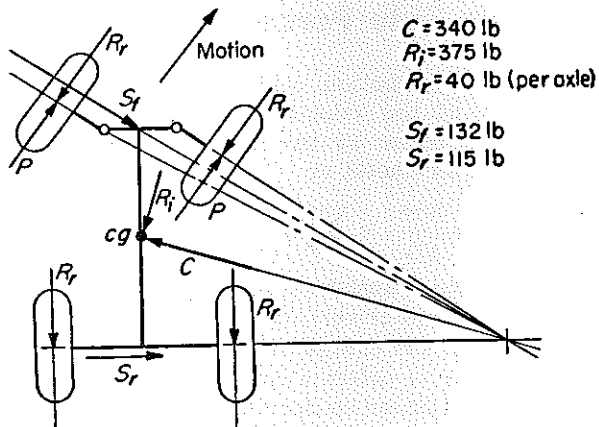


Fig. 31—Side-thrust distribution on a rear-wheel drive vehicle in accelerated motion. Side components of rolling resistance and the inertia force of acceleration increase the side-force reactions of the wheels.



$C = 340 \text{ lb}$
 $R_i = 375 \text{ lb}$
 $R_r = 40 \text{ lb} (\text{per axle})$

$S_f = 132 \text{ lb}$
 $S_r = 115 \text{ lb}$

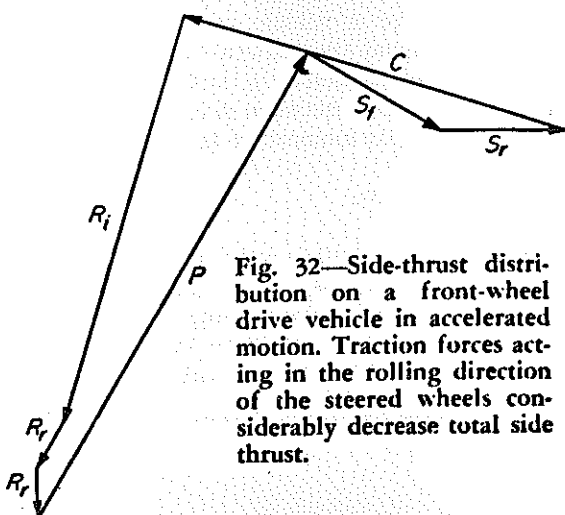


Fig. 32—Side-thrust distribution on a front-wheel drive vehicle in accelerated motion. Traction forces acting in the rolling direction of the steered wheels considerably decrease total side thrust.

strated for two representative cases: (1) rear-wheel drive with front-wheel steering, Fig. 31, (2) front-wheel drive with front-wheel steering, Fig. 32.

Comparing the resultant side forces S_x and S_y with the results of the simplified case (Fig. 30), it is observed that, on the rear-wheel drive car, forces acting at the cg and the rolling resistance of the front wheels all produce side components that increase the side-force reactions. On the front-wheel drive car, on the other hand, traction forces acting in the rolling direction of the steered wheels considerably decrease the side thrust. The rear-wheel drive car will, under the same driving conditions, impose higher side thrusts on the tires than

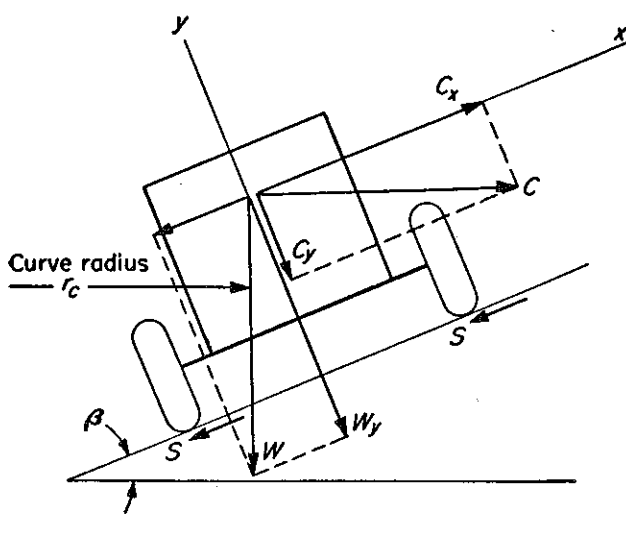


Fig. 33—Balance of forces on a vehicle negotiating a superelevated (banked) curve. Vehicle will slide to the outside of the curve if the resultant of forces acting in the x direction exceeds the maximum frictional side-force reaction.

will the front-wheel drive vehicle. This situation accounts for the well-known superior curve stability of the front-wheel drive, front-wheel steered car.

Other combinations, especially rear-axle steering, four-wheel drive and four-wheel steering may be investigated by the same graphical methods.

Sliding and Tipping Stability

Under some circumstances, the centrifugal force developed on a curve exceeds the maximum cornering capacity of the tires. The vehicle then either slides sideways or tips over. These conditions will be investigated for the general case of a vehicle negotiating a superelevated (banked) curve of radius r_c with constant speed v . Distribution of centrifugal force to the wheels is assumed to be in

proportion to the radial-load distribution.

Fig. 33 shows the situation schematically. The limit of the side reaction is determined by the frictional ground force and is therefore given by

$$\Sigma S_{\max} = \mu_s (C_y + W_y) \quad (34)$$

where $C_y = y$ component of centrifugal force, $W_y = y$ component of vehicle weight, and μ_s = coefficient of sliding friction.

To prevent the vehicle from sliding sideways, the resultant of forces acting in the x direction must not become larger than the maximum frictional side-force reaction, or

$$(\pm W_x \mp C_x) \leq \mu_s (C_y + W_y) \quad (35)$$

The relation between centrifugal force (and therefore driving speed) and the superelevation angle β can be obtained when forces in Equation 35 are expressed as functions of β . Conditions for skid-free curve driving can then be calculated.

Minimum Safe Speed: The vehicle must maintain a certain minimum speed to prevent it from sliding down the banked roadbed. The corresponding equilibrium equation developed from Equation 35 is

$$\mu_s (C \sin \beta + W \cos \beta) \geq C \cos \beta - W \sin \beta \quad (36)$$

After substitution of the value of centrifugal force C from Equation 31, minimum speed to prevent sliding becomes

$$v_{s,\min} = \left[\frac{gr_c(\tan \beta - \mu_s)}{(1 + \mu_s \tan \beta)} \right]^{1/2} \text{fps} \quad (37)$$

This equation can be further simplified by substituting for the friction coefficient μ_s the tangent of the frictional angle, where

$$\begin{aligned} \phi &= \tan^{-1} \mu_s \\ \mu_s &= \tan \phi \end{aligned} \quad (38)$$

For dry concrete, $\mu_s = 0.7$ and the frictional angle $\phi = 35$ deg. Substituting Equation 38 into Equation 37, converting v from feet per second to miles per hour, and letting $g = 32.2$ ft per sec²

$$\frac{g^{1/2}(3600)}{5280} = 3.9$$

and the minimum safe speed is

$$v_{s,\min} = 3.9[r_c \tan(\beta - \phi)]^{1/2} \text{ mph} \quad (39)$$

In verbal form, minimum speed is proportional to the tangent of the difference between the superelevation angle and the frictional angle.

An interesting application of this stability equation is seen at stunt-driving exhibitions, where a car is driven on a vertical circular wall. The minimum speed required for this stunt can be calculated by substituting $\beta = 90$ deg in Equation 39.

Further, the elevation angle under which the stationary vehicle would just start to slide can be found by substituting $v = 0$ in Equation 37. In this case, $\tan \beta = \mu_o$. Since the system is stationary, the coefficient of static friction applies.

With $\mu_s = 0.8$ for dry concrete, the stationary vehicle will start to slide at an elevation of 39 deg.

Maximum Safe Curve Speeds: Stability of a vehicle traveling at high speed on a superelevated curve presumes two conditions: (1) speed must not be high enough to cause the vehicle to slide up the slope of the superelevation, and (2) speed must not be high enough to tip the vehicle about the outside wheels. These conditions are examined in the following sections.

SLIDING: Equilibrium equation for the case where the vehicle tends to slide up the slope of the superelevation is

$$(C \sin \beta + W \cos \beta) \mu_s \geq C \cos \beta - W \sin \beta \quad (40)$$

where

$$C = \frac{mv^2}{r_c}$$

After simplification

$$v_{s,\max} = \left[\frac{gr_c(\tan \beta + \mu_s)}{(1 - \mu_s \tan \beta)} \right]^{1/2} \quad (41)$$

and, since the frictional angle is related to the friction coefficient by

$$\mu_s = \tan \phi$$

then

$$V_{s,\max} = 3.9[r_c \tan(\beta + \phi)]^{1/2} \text{ mph} \quad (42)$$

Maximum safe speed is therefore proportional to the tangent of the sum of the superelevation angle and the frictional angle. With speed increas-

ing to infinity ($v = \infty$) it can be found from Equation 40 that the superelevation need not exceed the value

$$\beta = \cot^{-1} \mu_s \quad (43)$$

For the hypothetical case of complete absence of friction, a superelevation angle can still be found that permits safe vehicle operation. In such a case, the resultant of all forces is exactly perpendicular to the road surface. Substituting $\mu_s = 0$ into Equation 40, the ideal superelevation angle becomes

$$\beta = \tan^{-1} \left(\frac{v^2}{gr_c} \right) \quad (44)$$

The existence of a frictional side-support force is nonessential in this case, and maximum and minimum speeds are equal.

Simplifying Equation 42 for the case of a level surface ($\beta = 0$),

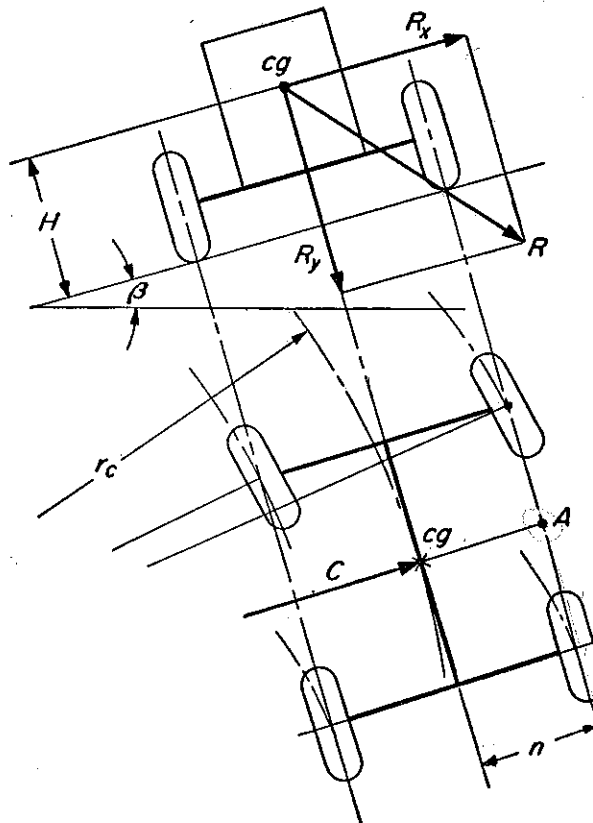
$$V_{s,\max} = 3.9(r_c \mu_s)^{1/2} \text{ mph} \quad (45)$$

TIPPING: When the resultant of horizontal and vertical forces passes through the line joining the points of contact of the outside wheels with the ground (point A, Fig. 34) tipping of the vehicle begins. Equilibrium of moments about point A can be written as

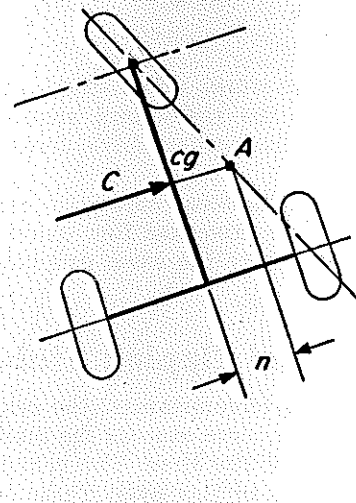
$$nR_y - HR_x = 0 \quad (46)$$

$$R_x = C \cos \beta - W \sin \beta$$

$$R_y = C \sin \beta + W \cos \beta$$



(a)



(b)

Fig. 34—Stability against tipping of three and four-wheeled vehicles on a superelevated curve is ensured if the resultant R passes inside of point A.

where n is the projected distance between A and the center of gravity, and R_x and R_y are the force components in the x and y directions. These components are given by

After substitution of these results in Equation 46, the critical speed of tipping becomes

$$v_{t,\max} = \left[\frac{gr_c(n + H \tan \beta)}{(H - n \tan \beta)} \right]^{1/2} \quad (47)$$

Simplifying again for the case of a level surface ($\beta = 0$),

$$v_{t,\max} = 3.9 \left(\frac{r_c n}{H} \right)^{1/2} \text{ mph} \quad (48)$$

Comparison of Equations 41 and 47 will reveal whether tipping or sliding will occur first as the speed of the vehicle increases. It is desirable that sliding occur first. This happens when speed that induces sliding is reached sooner than the critical tipping speed, that is, $v_{t,\max} > v_{s,\max}$. For a level surface, this results in the condition

$$\frac{n}{H} > \mu_s \quad (49)$$

In the preceding equations, the vehicle is assumed to be moving with constant speed, no tractive or braking forces are being simultaneously transferred, and the centrifugal force is distributed on the axles in the same proportion as the static level axle weights. Should this not be the case, the distribution of centrifugal side thrusts to the individual axles will have to be determined, and

the safety against sliding examined for each wheel separately. The wheel with reduced dynamic load (due to a hill, trailer pull, etc.) will start to slide first. Other conditions being equal, the driving or braking wheel with lower effective μ values will slide first. Further, for the coefficient of friction μ_s , only such values can be taken for the side forces that remain after vectorial subtraction of the portion already taken by tractive or decelerating forces. It is interesting to note also that all critical speeds are independent of vehicle weight.

With increasing vehicle speed, sliding usually starts before tipping on most passenger cars. On trucks, however, where H is large, the critical tipping speed may be reached sooner.

Tipping properties of four-wheeled vehicles with pivoted steering axles (e.g., lift trucks) are similar to those for a three-wheeled vehicle. In such a case, the central pivot point and not the wheels forms the effective front-end support against tipping.

REFERENCES

26. Timoshenko and Young—*Advanced Dynamics*, McGraw-Hill Book Co. Inc., New York, 1948.
27. R. Lindsay—*Physical Mechanics*, D. Van Nostrand Co. Inc., New York, 1950.
28. G. Goldbeck—“Die Begrenzung der Kurvengeschwindigkeit durch die Schleuder und Kippgefahr” (Speed Limits Imposed Through Skidding and Tipping on Curves), ZVDI Dusseldorf, 1939.
29. Dietz and Harling—“Die Fahrlage des Kraftfahrzeuges in der Kurve” (Dynamic Stability of Vehicles on Curves), Deutsche Kraftfahrforschung, Heft 44, VDI-Verlag, Berlin, 1940.

Mechanics of Vehicles—5

By Jaroslav J. Taborek*

Development Engineer
Towmotor Corp.
Cleveland

POWER is expended when a vehicle moves against a resisting force. In accelerated motion uphill, the forces or resistances that oppose the motion of a vehicle are: (1) Rolling resistance, (2) Grade resistance, (3) Air resistance, (4) Inertia resistance, and (5) Transmission resistance.

Here and in a following article, the magnitudes and characteristics of these motion-resisting forces are examined. Consideration of such forces will subsequently be shown to form an important part of vehicle performance prediction.

Force Characteristics

To move a vehicle at speed V (mph) against any resisting force R_x (lb), power N_x must be delivered to the driving axle. Magnitude of the power (hp) is given by

*Now Research and Development Engineer, Phillips Petroleum Co., Bartlesville, Okla.

$$N_x = \frac{R_x V}{375} \quad (50)$$

At any instant, the sum of all resisting forces ΣR_x is in equilibrium with the tractive force P , which is delivered as torque M_d to the driving wheels. Such a force balance is expressed as

$$\frac{M_d}{r} = P = \sum R_x \quad (51)$$

where r is the rolling radius of the driving wheels.

Rolling Resistance: In a sense, the most important of the resisting forces is rolling resistance. While other resistances act only under certain conditions of motion, rolling resistance is present from the instant the wheels begin to turn. Rolling resistance, in addition, has another undesirable property: a large part of the power expended in a rolling wheel is converted into heat within the tire itself. The consequent temperature rise reduces

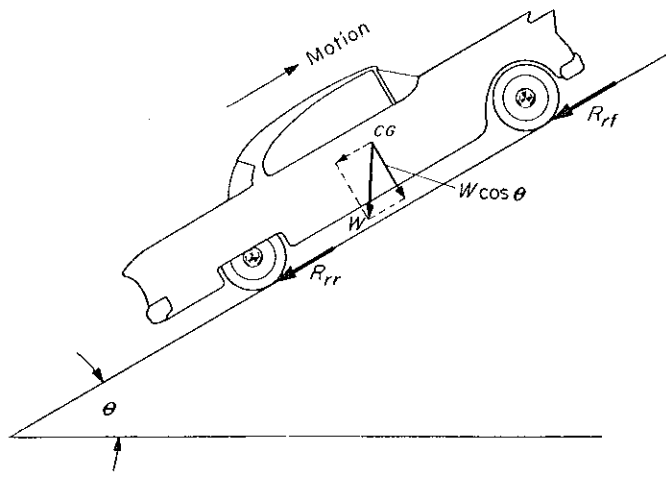
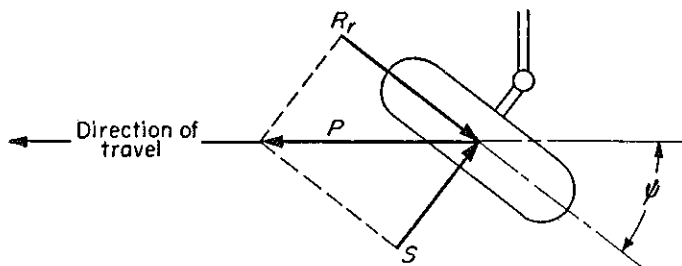


Fig. 35—Left—Rolling resistance of a vehicle is the sum of the rolling resistances of all wheels and is therefore independent of weight distribution. The weight used in rolling-resistance calculations is the normal (cosine) component of vehicle weight.

Fig. 36—Below—The rolling plane of the wheel is not parallel with the direction of travel. Tractive force P must overcome the vectorial resultant of rolling resistance R_r and side force S . Rolling is maintained as long as $f \tan \psi < \mu$.



Motion-Resisting Forces

- rolling resistance
- grade resistance

both the abrasive resistance and the flex fatigue of the tire material and becomes the limiting factor on tire performance.

Differing basically from resistance sources for rigid wheels (Part 1 of this series), the sources of rolling resistance on pneumatic tires are:

- (1) Work performed by flexing of the tire body as it passes the ground contact area.
- (2) Work performed by the wheel penetrating or compressing the ground.
- (3) Work performed by frictional motion due to tire slip.
- (4) Friction caused by air circulation inside the tire and the fan effect of the rotating wheel on the outside air.

The first two of these factors account for the greater part of rolling resistance; the remaining two have only secondary effect. Considering the vehicle as a whole, the total rolling resistance R_r is the sum of the resistances of all the wheels, or

$$R_r = R_{rf} + R_{rr} = fW \cos \theta \quad (52)$$

where R_{rf} and R_{rr} designate rolling resistances on front and rear wheels, $W \cos \theta$ is the normal-to-ground component of vehicle weight, and f is the coefficient of rolling resistance, Fig. 35.

For theoretically correct calculations, the dy-

Nomenclature

f	Coefficient of rolling friction
G	Measure of grade, per cent
N	Power, hp
P	Traction force on driving wheels, lb
R_g	Grade resistance, lb
R_r	Rolling resistance, lb
r	Rolling radius of tire, ft
S	Side force on tires, lb
V	Speed, mph
W	Vehicle weight, lb
θ	Horizontal incline of road, deg
μ	Friction coefficient
ψ	Slip angle, deg

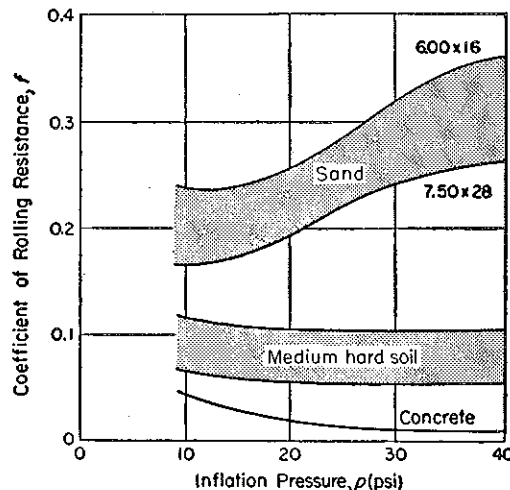


Fig. 37—Coefficient of rolling resistance as a function of inflation pressure. Values plotted assume reasonable vehicle speeds for each surface type.

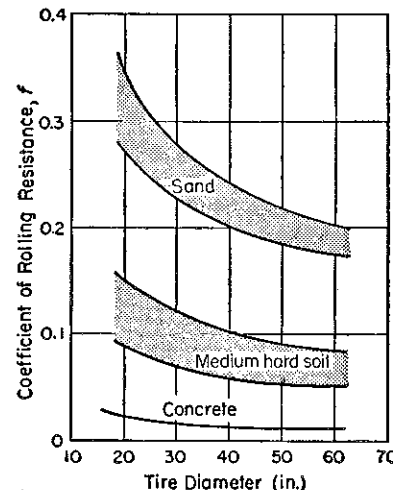


Fig. 38—Coefficient of rolling resistance as a function of tire diameter. Effect of tire diameter is negligible for hard surfaces (concrete) but decisive for soft ground or sand.

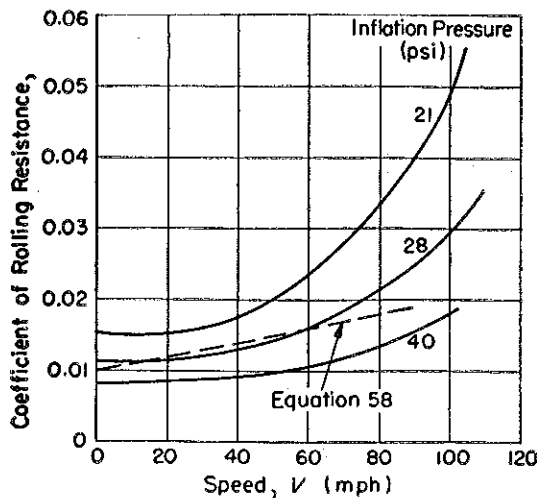


Fig. 39—Coefficient of rolling resistance as a function of speed. The effect of speed is more pronounced at lower inflation pressures. Curves for pressures of 21, 28 and 40 psi were calculated from Equation 57. An approximation for common passenger car speeds and inflation pressures is given by the plot of Equation 58.

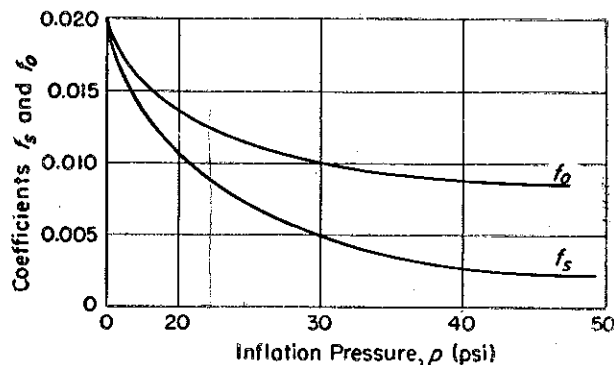


Fig. 40—Supplementary coefficients f_o and f_s for use in Equation 57.

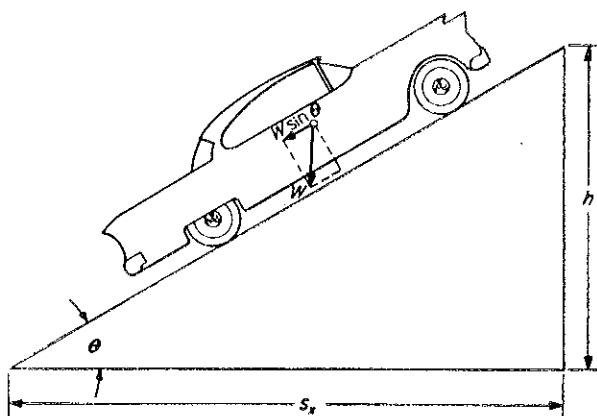


Fig. 41—Grade resistance of a vehicle is the downhill component of its weight. Grade is usually measured in per cent where $G (\%) = (100 h)/s_x = 100 \tan \theta$.

namic weight of the vehicle, including the effects of acceleration, trailer pull and the vertical component of air resistance, is used. For vehicle performance estimation, however, the changing magnitude of the dynamic weight complicates the calculations without offering significant improvements in accuracy. Furthermore, it is apparent from Equation 52 that a dynamic weight transfer toward one of the axles has no influence on the total rolling resistance.

For these reasons, static vehicle weight is usually taken as sufficiently accurate for computation of rolling resistance. As a further simplification, the effect of the horizontal grade angle θ is often neglected completely. Equation 52 then becomes

$$R_r = fW \cos \theta \approx fW \quad (53)$$

The error introduced by this simplification is only 5 per cent for the steepest existing grades (about 32 per cent).

All these considerations apply, in a strict sense, only for straight-line motion. For vehicles on curves, the direction of rolling deviates from the direction of actual travel, and the tractive force P must overcome the vectorial resultant of side force S and rolling resistance R_r , Fig. 36. In this case,

$$P = \frac{R_r}{\cos \psi} \quad (54)$$

where ψ is the slip angle, that is, the angle between the speed vector and the rolling plane of the wheel.

On a steered wheel, the side force S necessary to maintain equilibrium of forces must remain within the limits of sliding friction given by the radial load W and the friction coefficient μ , or

$$S = R_r \tan \psi \leq \mu W \quad (55)$$

These results, when combined with Equation 53, give the condition for rolling of the steered wheel as

$$f \tan \psi \leq \mu \quad (56)$$

For slippery ground ($\mu = 0.2$ and $f = 0.02$), Equation 56 gives $\psi_{max} = 84$ deg.

Factors Affecting Rolling Resistance: Coefficient of rolling resistance f is a dimensionless factor that expresses the effects of the complicated and interdependent physical properties of tire and ground. Establishment of standardized conditions for measurement of the effects of variables like the fine structure of the ground material, composition of the rubber, design elements of the tire, etc., proves difficult if not impossible. The following account of the most important of these factors will, nevertheless, contribute to a better understanding of the physical nature of rolling resistance.

GROUND-SURFACE STRUCTURE: Lowest f values are measured on hard, smooth, dry surfaces. A worn-out road almost doubles rolling resistance. On wet

surfaces, higher rolling resistances are observed, probably due to the cooling effect of the water and the correspondingly decreased flexibility of the rubber tire.

TIRE-GROUND ELASTICITY: The relative elasticity and hysteresis of both tire and ground are important factors that decisively influence rolling resistance. Three basic combinations are possible: (1) The tire is rigid as compared to soft, plastic ground, rolling resistance being due to penetration work only; (2) Both tire and ground are deformable, rolling resistance being due to both tire deformation and ground penetration work; and (3) The ground is rigid in relation to an elastic tire, rolling resistance being due entirely to tire deformation work.

TIRE INFLATION PRESSURE: To a large extent tire inflation pressure determines elasticity of the tire. It affects the value of f in a manner that depends on the elasticity of the ground, Fig. 37. For example, the following situations can be distinguished:

On plastic surfaces, like sand, high inflation pressures result in increased ground penetration work and therefore higher f values. Conversely, lower inflation pressures, while decreasing ground penetration, increase tire-flexure work. Obviously, an optimum pressure exists for a given surface.

On medium plastic surfaces, like grass sod, the effects of inflation pressure on tire and ground approximately balance, and f remains nearly independent of inflation pressure.

On hard surfaces, f decreases with higher inflation pressure, since flexing work of the tire body will be greatly reduced.

TIRE RADIUS: Basically, f is inversely proportional to rolling radius. The proportionality factor, however, is small on hard surfaces, becoming important on soft, plastic ground, Fig. 38.

DRIVING SPEED: Coefficient f is directly proportional to speed because of increased flexing work

and vibration in the tire body. Consequently, the influence of speed becomes more pronounced when speed is combined with lower inflation pressures, Fig. 39.

TRACTION FORCES: Wheels transferring tractive or braking forces show higher rolling resistance due to wheel slip and resulting frictional scrubbing.

RADIAL LOAD: Coefficient f is directly proportional to radial load due to the effect of load on tire deflection. This influence is, however, revealed only by exact measurement.

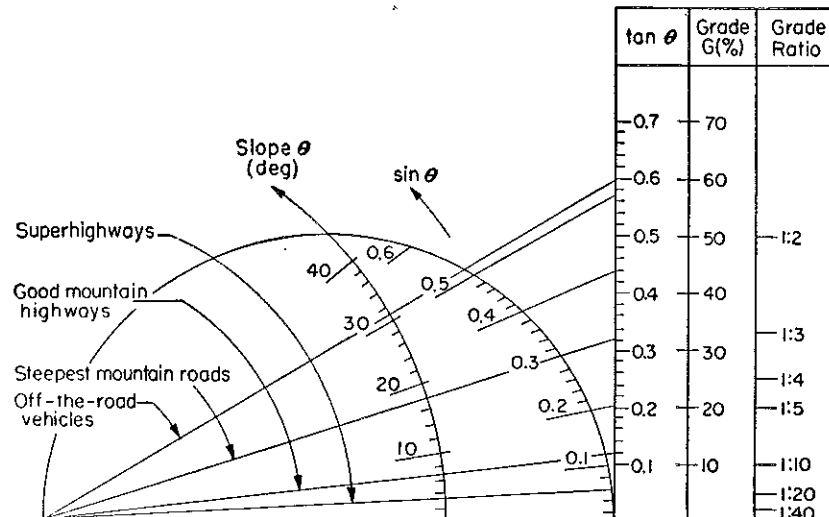
TEMPERATURE: Coefficient f decreases with increasing temperatures (ambient or internal) as a result of increased flexibility of the rubber.

TIRE MATERIAL AND DESIGN: Thickness of the tire base, usually expressed in plies, and thickness of the rubber tread determine the amount and stiffness of material to be deformed by rolling. Worn-out, smooth-tread tires show f values up to 20 per cent lower than new ones. Often for racing cars, the rubber tread is ground off to small fractions of an inch. Fine laminations, on the other hand, increase f as much as 25 per cent. The cord material in the tire carcass has only negligible effect; the rubber material and its compounding is of much greater importance. Synthetic rubber generally shows higher f values than natural rubber.

Determination of Rolling-Resistance Coefficient: The multiple and interrelated factors affecting f make it virtually impossible to devise a formula that takes all variables into account. Before a value of f is chosen for a particular application, the overall degree of accuracy required for the calculations should be established.

On test runs where other measurements are being performed, it may be essential that f be known as exactly as possible. Several equations for f have been developed for passenger-car tires rolling on

Fig. 42 — Comparison of grade designation methods. In calculations of vehicle performance, the correct sine value is often replaced by the more convenient tangent. Note that the error reaches about 5 per cent for the steepest roads normally encountered (32 per cent).



concrete surfaces. The variables in these equations are usually inflation pressure, speed and radial load. The accuracy of such a calculation is naturally limited by the influence of factors that are neglected. Laboratory measurements usually give f with steel as a ground surface. For concrete, a new value can be recalculated by use of established conversion factors.

For soft and plastic grounds it is very difficult to find accurate data of general validity. The structure of these materials is hardly definable and will change from place to place. Average values are usually accepted and seldom should there be need for any higher accuracy.

Relatively accurate values of f for concrete surfaces as function of inflation pressure and speed can be calculated from the following equation developed at the Institute of Technology in Stuttgart:

$$f = f_0 + 3.24 f_s \left(\frac{V}{100} \right)^{2.5} \quad (57)$$

Here, V is speed (mph), the factor f_0 represents the basic coefficient and f_s determines the speed effect. Both factors are taken from the diagram in Fig. 40. Equation 57 is also plotted with inflation pressure as a parameter in Fig. 40.

For many performance calculations, it is often sufficiently accurate to express f as a linear function of speed. For the most common range of inflation pressures (around 26 psi), the following equation gives average values of f for concrete surfaces:

$$f = 0.01 \left(1 + \frac{V}{100} \right) \approx .01 + V \quad (58)$$

The range of acceptable accuracy of this equation is up to about 80 mph. The advantage of this expression is that it can be substituted directly into

Table 3—Coefficient of Rolling Resistance*

Vehicle Type	Surface		
	Concrete	Medium	Hard
Passenger cars	0.015	0.08	0.30
Heavy trucks	0.012	0.06	0.25
Tractors	0.02	0.04	0.20

*Dimensions of f are lb per lb of vehicle weight.

other equations, therefore expressing rolling resistance as a function of speed.

In many cases, even the effects of speed can be ignored and average values of f , covering conditions for the particular application, can be used in performance calculations. Such values are sum-

marized in Table 3 for a variety of ground surfaces and vehicles.

The dimension of the coefficient of rolling resistance is pound per unit of vehicle weight. Vehicle weight is expressed either in units of pounds, 1000 pounds or tons. The author prefers to keep all forces and weights in the same units, avoiding unnecessary complication by the introduction of new units.

Grade Resistance: Grade resistance R_g is the component of vehicle weight acting downhill, Fig. 41. It is given by

$$R_g = W \sin \theta \quad (59)$$

In practice, it is customary to designate grade G (per cent) as the ratio of the climbed height to the projected horizontal distance, or

$$G = \frac{h(100)}{s_x} = 100 \tan \theta \quad (60)$$

Allowing for the approximation that for small angles $\sin \theta \approx \tan \theta$, the grade resistance equation becomes

$$R_g \approx W \tan \theta = \frac{WG}{100} \quad (61)$$

The error resulting from this simplification for the steepest known road grades (32 per cent or 18 deg) reaches an acceptable 5 per cent. For more exact calculations, or for still steeper grades, the simplification should not be used.

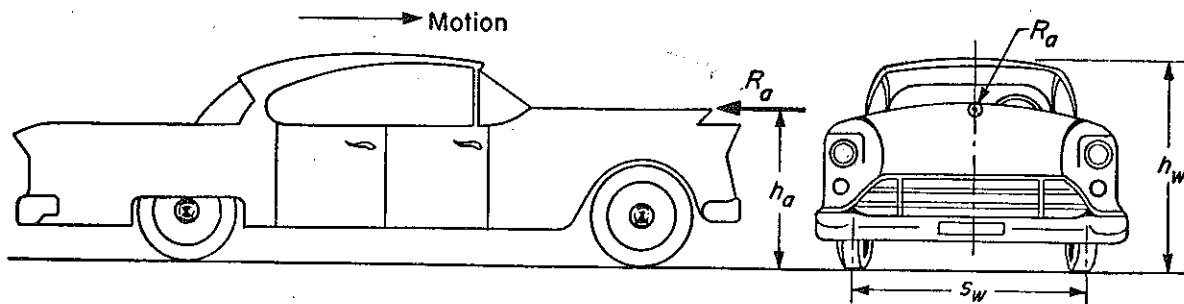
A comparison of grade designation methods is given in Fig. 42. Grades of modern super highways are kept below 6 per cent ($3\frac{1}{2}$ deg); in mountain areas, dual-highway up-hill slopes reach 7 per cent and downhill slopes are up to 8 per cent. Average mountain highways are kept under about 12 per cent (7 deg); the steepest known roads in high mountains reach slopes up to 32 per cent (18 deg) for short distances. Off-the-road and military vehicles are usually designed to negotiate slopes of 60 per cent (31 deg).

The highest grade that a vehicle can climb is called its gradability and is designated as G_{max} (per cent) or θ_{max} (deg).

BIBLIOGRAPHY

30. Billingsley, Evans, Hulswit, Roberts—"Rolling Resistance of Pneumatic Tires as a Factor in Car Economy," *SAE Transactions*, 1942.
31. McKibben—"Transportwheels for Agricultural Machines," *Agricultural Engineer*, Nov. 1939—Aug. 1940.
32. T. R. Agg—*Bulletin 88*, Iowa State College, Eng. Exp. Station, 1928.
33. Kamm, Schmidt—*Das Versuchs- und Messwesen auf dem Gebiete des Kraftfahrwesens* (Experimentation and Measuring on Automotive Vehicles), Springer Verlag, Berlin, 1939.
34. C. Schmidt—*Die Fahrwiderstände beim Kraftfahrzeug und die Mittel zu ihrer Verringerung* (Vehicle Motion Resisting Forces and Means for Their Reduction), AZT, Stuttgart, 1938.
35. L. C. Lundstrom—"Wind and Rolling Resistances," Part 4 of Symposium "Where Does All the Power Go?" *SAE Transactions*, 1957.

Fig. 43—The air-resistance force R_a is assumed to act at the centroid of the projected frontal area of the vehicle. As an approximation, the area can be taken as 0.9 (body height) (wheel tread), or 0.9 (h_w) (s_w).



Mechanics of Vehicles—6

Resistance Forces

- air resistance
- inertia resistance
- transmission resistance
- performance diagrams

By Jaroslav J. Taborek*

Development Engineer
Towmotor Corp.
Cleveland

ROLLING resistance and grade resistance—two of the forces that impede the motion of a vehicle—were discussed in the preceding article of this series. Both were shown to be proportional to vehicle weight. This article continues the examination of such motion-impeding forces, discussing air resistance, inertia resistance and transmission resistance and the relationship of such forces to vehicle performance.

Air Resistance: According to the laws of aerodynamics, a body moving through the air is resisted by a force R_a , where

$$R_a = \frac{c_a \rho A v_r^2}{2g} \quad (62)$$

In this expression, c_a is a dimensionless coefficient of air resistance (drag coefficient) with a value unique for each family of geometrically similar

body shapes. Remaining terms in the equation are ρ , the air density (lb per cu ft), A , the projected area of the body in the direction of travel (sq ft), and v_r , the velocity of the body relative to the air (ft per sec).

Because of the influence of air density, magnitude of the air-resistance force depends on the state of the air, i.e., the barometric pressure and temperature. The following relation relates density to pressure and temperature:

$$\rho = \frac{1440}{RT} = \frac{1.32 p'}{460 + t} \quad (63)$$

Symbols in this expression are defined in Nomenclature.

The influence of changes in air density must be taken into account in accurate performance calculation, since differences between density extremes may reach 20 per cent or higher. For example, at an altitude of 4000 ft, air density is only 83 per cent of the sea-level value.

*Now Research and Development Engineer, Phillips Petroleum Co., Bartlesville, Okla.

For many performance calculations, however, the density for "normal" or standard atmospheric conditions (60 F and 29.9 in. Hg) provides sufficient accuracy. In such cases, $\rho = 0.0763$ lb per cu ft is used as a constant value.

By substitution of the standard density, the equation for the air resistance can then be simplified to read

$$R_a = 0.12 c_a A \left(\frac{v_r}{10} \right)^2$$

$$= 0.26 c_a A \left(\frac{V_r}{10} \right)^2 \quad (64)$$

where V_r is the speed of the vehicle in mph and v_r in fps, both relative to the air.

The physical origin of air resistance on vehicles is derived from three sources:

1. Drag resistance, which is a function of the aerodynamic shape of the body with respect to all outside surfaces. Protruding objects like mirrors, exhaust mufflers, license plates, etc., can increase drag resistance considerably at higher

speeds. Of special importance is the shape of the rear part of the body, which determines the amount of turbulence in the wake of the vehicle.

2. Air friction on the outside surfaces or "skin" of the body. For the more or less standardized quality of surface finish on passenger cars, this portion amounts to about 10 per cent of the total air resistance.
3. Air flow through the car for purposes of cooling or ventilating. This influence can be resistance-increasing or resistance-decreasing, depending on the function, location and aerodynamic perfection of the channels.

These three factors are expressed in the coefficient of air resistance c_a , which has a value particular to each vehicle. It is found experimentally in scale model wind-tunnel tests and is confirmed by coasting tests performed on actual vehicles.

In some literature sources, the air-resistance coefficient is given as

$$C_a = \frac{c_a \rho}{2g} = 0.26 c_a \left(\frac{\text{lb-sec}^2}{\text{ft}^4} \right) \quad (65)$$

where the factor C_a includes the effect of the state of the air and is not a dimensionless number. Equation 64 can be rewritten to incorporate C_a , giving

$$R_a = C_a A \left(\frac{V_r}{10} \right)^2 \quad (66)$$

Average values of c_a and C_a at SAE standard air conditions for representative vehicles are given in Table 4.

While the coefficient of air resistance c_a is a function of the aerodynamic perfection of a body, the important criterion for comparison of vehicles is the product of the coefficient with the frontal area, i.e., $A(c_a)$. There are cases where, when the frontal area is enlarged, the total resistance is reduced

Nomenclature

A	Projected vehicle area in drive direction, sq ft
a	Acceleration, ft per sec ²
C_a	Coefficient of air resistance, lb-sec ² -ft ⁻⁴
c_a	Coefficient of air resistance, dimensionless
E	Kinetic energy, ft-lb
g	Acceleration of gravity, ft per sec ²
I	Moment of inertia, ft-lb-sec ²
I_w	Polar moment of inertia of wheels, ft-lb-sec ²
M	Torque, lb-ft
M_i	Torque required for accelerating rotating parts, lb-ft
m	Mass, lb-sec ² -ft ⁻¹
m_e	Equivalent mass, lb-sec ² -ft ⁻¹
m_t	Total effective mass of vehicle, lb-sec ² -ft ⁻¹
N	Power, hp
p	Pressure, lb per sq ft
p'	Barometric pressure, in. Hg
R	Gas constant (=53.3)
R_a	Air resistance, lb
R_g	Grade resistance, lb
R_i	Inertia resistance, lb
R_{it}	Inertia resistance of translatory mass, lb
R_r	Rolling resistance, lb
r	Rolling radius of tire, ft
s_m	Wheel tread, ft
T	Absolute temperature, deg Rankine
t	Temperature, deg F
V	Speed, mph
V_r	Speed relative to air, mph
v	Speed, ft per sec
v_r	Speed relative to air, ft per sec
W	Weight, lb
α	Angular acceleration, rad per sec ²
γ	Mass factor for rotating parts
ξ	Reduction ratio
η	Efficiency or efficiency factor
ρ	Density, lb per ft ³
ω	Angular velocity, rad per sec

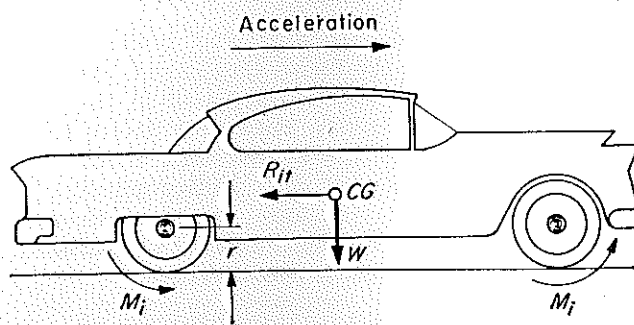


Fig. 44—Inertia force of the translating vehicle mass acts at the cg and is always directed against the acceleration vector. Translatory acceleration is necessarily accompanied by angular acceleration of the wheels and the drive-system components. As a means for simplifying performance calculations, the effects of rotational inertia of such parts can be represented by an equivalent translatory mass.

because of a resulting lower c_a value. This occurs, for example, when a protruding part is covered with a streamlined fairing.

The hypothetical point of action of the air-resistance force, Fig. 43, is the centroid of the projected area in the drive direction. Usual frontal areas (in sq ft) on present-day cars are: (1) Passenger cars (small), 14-20; (2) Passenger cars (standard), 22-30; (3) Buses and trucks, 60-80. Areas can also be estimated as 0.9 (*body height*) (*wheel tread*).

Combining Equation 64 with Equation 51 (Part 5), power N_u necessary to overcome air resistance is

$$N_u = \frac{0.0026 c_a A V_r^2 V}{375} \text{ (hp)} \quad (67)$$

where again V_r is the relative speed of the vehicle against the air and V is the ground speed of the vehicle, both in mph. For calm air $V_r = V$ and

$$N_u = \frac{0.0026 c_a A V^3}{375} = 0.07 c_a A \left(\frac{V}{10} \right)^3 \quad (68)$$

From this equation, it is seen that the power requirement is proportional to the third power of the speed.

Inertia Resistance: Every change of speed of a moving body is opposed by an inertia force which is proportional to the product of the mass of the body and the time rate of speed change. For vehicles considered herein, this force will be referred to as the inertia resistance R_i and will always be

directed against the vector of acceleration (or deceleration for decreasing speed). The point of action of this force is ideally located at the center of gravity of the vehicle mass, Fig. 44.

Considering first only the translatory mass of the vehicle, the inertia resistance R_{it} is given by

$$R_{it} = m \left(\frac{dv}{dt} \right) = \frac{Wa}{g} \quad (69)$$

where m is the mass of the vehicle and a is the translatory acceleration.

The state of translatory motion of a vehicle is inseparably coupled to the rotational speed of the wheels which, in turn, are positively connected to the rotating parts of the drive mechanism. Any change of translatory speed must, therefore, be accompanied by a simultaneous change in the rotational speed of all such parts.

For calculation of the torque M necessary to accomplish the change of the rotational speed, $d\omega$, use is made of the basic equation

$$M = I \left(\frac{d\omega}{dt} \right) = I\alpha \quad (70)$$

where M is torque, I is moment of inertia about the axis of rotation, and α is angular acceleration (see Nomenclature for dimensions).

With this equation applied to a vehicle with several groups of parts, each rotating at a different speed, the respective torques can be related to the drive-axle by

$$M_i = \sum M_\xi = \sum I\alpha_\xi \quad (71)$$

where M_i is the inertia resistance torque of all rotating parts reduced to the drive axle, and ξ is the reduction ratio between the drive axle and a particular part.

From the speed and acceleration relationships

$$\omega = \omega_d \xi \quad (72)$$

and

$$\alpha = \alpha_d \xi \quad (73)$$

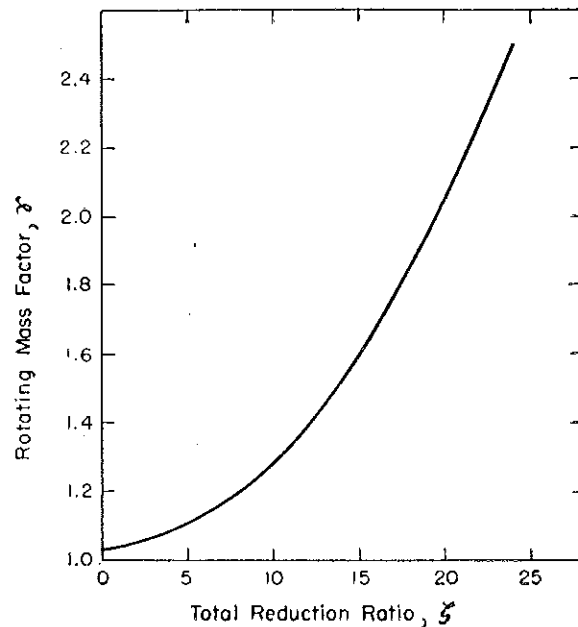


Fig. 45—Mass factor γ , representing the effect of the rotating parts on the inertia mass of the vehicle, is plotted here as a function of the total reduction ratio ξ between the drive axle and the engine.

Table 4—Air-Resistance Coefficients

Vehicle Type	c_a (dimensionless)	C_a^* (lb-sec ² -ft ⁻⁴)
Passenger car	0.4-0.5	0.104-0.13
Convertible	0.6-0.65	0.155-0.17
Racing car	0.25-0.3	0.078-0.065
Bus	0.6-0.7	0.155-0.182
Truck	0.8-1.0	0.208-0.260
Tractor-trailer	1.3	0.338
Motorcycle and rider	1.8	0.470
<i>Geometrical Bodies:</i>		
Sphere	0.47	0.122
Square plate	1.2	0.31
Streamlined body	0.1	0.026

* $C_a = 0.26 c_a$

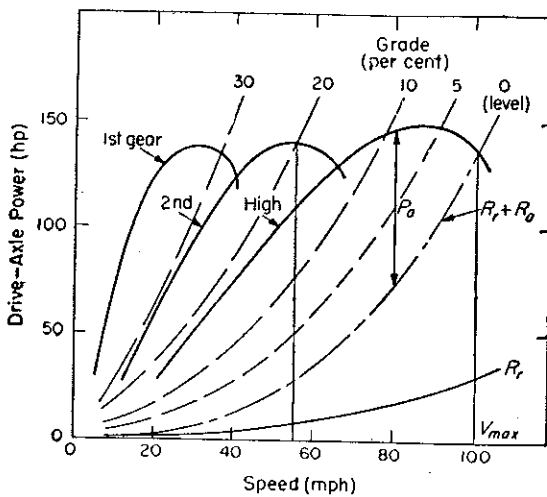


Fig. 46—Vehicle power diagram. Power required to overcome rolling, air and grade resistances is additively plotted against vehicle speed. Engine power delivered to the drive axle in first, second and high gears is also given. Curve summing rolling and air-resistance forces intersects high-gear power-available line at 100 mph, indicating maximum vehicle speed on level ground. In second gear, a 20 per cent grade can be negotiated at a speed of 55 mph. Difference between power required and power available is free or excess power for acceleration.

Equation 71 can then be written as

$$M_i = \alpha_d \sum I_s^2 \quad (74)$$

where the subscript *d* refers to the driving axle.

Equivalent Mass: To simplify calculation of the effects of rotating parts on total inertia resistance, use can be made of the fact that circumferential speed at the rolling radius of the tire is equal to the translatory speed of the vehicle (neglecting slip). An equivalent mass m_e can be determined which, hypothetically concentrated at the rolling radius r , will have the same effect on the inertia of translatory motion as the summation of inertia torques of individual rotating parts. The equivalent mass m_e can be calculated from

$$M_i = m_e r^2 \alpha_d = \alpha_d \sum I_s^2 \quad (75)$$

Solving for m_e ,

$$m_e = \frac{\sum I_s^2}{r^2} \quad (76)$$

Mass m_e can be added to the translatory mass m of the vehicle, giving the effective inertia mass of the vehicle, m' . It often proves convenient to express the effective mass m' in terms of the vehicle

mass m , or

$$m' = m + m_e = m\gamma \quad (77)$$

where γ is a dimensionless mass factor of the rotating parts that defines how much the effective mass exceeds the actual mass of the vehicle.

By use of the factor γ , Equation 69 can be rewritten to give the total inertia resistance of the vehicle, or

$$R_i = \gamma m a \quad (78)$$

Equation 78 can also be derived by an energy method. From the theorem that the change in kinetic energy of a body equals the work produced by external forces

$$dE = \left(P - \sum R_x \right) ds \quad (79)$$

where E is the kinetic energy of the moving vehicle, P is tractive force, and $\sum R_x$ is the summation of all resistance forces except R_i .

From the equilibrium of forces, the following relation applies:

$$R_i = P - \sum R_x \quad (80)$$

Further, the kinetic energy of the vehicle is

$$E = \frac{mv^2}{2} + \sum \frac{I\omega^2}{2} \quad (81)$$

Differentiating this equation,

$$dE = mv(dv) + \sum I\omega(d\omega) \quad (82)$$

Combining Equations 79 through 82,

$$R_i(ds) = mv(dv) + \sum I\omega(d\omega) \quad (83)$$

Separating R_i and substituting $ds/dt = v = r\omega_d$ and Equation 72,

$$R_i = \left(\frac{dv}{dt} \right) \left(m + \frac{\sum I_s^2}{r^2} \right) \quad (84)$$

Substituting further with the results of Equation 76, an equation identical to Equation 78 results.

For calculation of the value of γ , the rotating parts can be divided into two groups: (1) The vehicle wheels (both front and rear), and (2) Parts translating or rotating at engine speed, principally the flywheel, clutch, crankshaft and pistons (manual transmission parts, gears and shafts are usually neglected in a simplified calculation). The influence of parts rotating at engine speed gains in importance in the lower gear ranges, since the equivalent mass m_e is proportional to the square of the reduction ratio (Equation 76).

Numerical values of γ (Equations 77 and 78) have been calculated by several investigators. Reliable values are quite difficult to obtain because the inertia moment of most engine parts has to be measured experimentally. Average values of γ collected from the literature are given for capacity-loaded vehicles in Table 5.

An excellent method of calculation is presented in Reference 36 and is explained by the following

development:

Rearranging Equation 77,

$$\gamma = 1 + \frac{m_e}{m} = 1 + \left(\frac{\Sigma I_w}{mr^2} + \frac{\Sigma I \xi^2}{mr^2} \right) \quad (85)$$

where ΣI_w is the inertia moment of the wheels and I is the inertia of any part rotating at engine speed with speed ratio ξ with respect to the driving axle.

As a representative average from a number of calculations, γ can be expressed as function of the reduction ratio ξ , Fig. 45.

$$\gamma = 1 + (0.04 + 0.0025 \xi^2) \quad (86)$$

From this expression, factor γ corresponding to any given ratio can be calculated. The applicability of this calculation method for all road vehicles and for a relatively wide range of capacities is substantiated by the fact that the size of drive components, within the usual limits, is proportional to the vehicle capacity. Results of the equation are fairly accurate and are useful for preliminary performance calculations.

Transmission Resistance: Transmission resistance is not a resistance force in the same sense as the other motion-resisting forces. It represents, rather, the power consumed in the process of transmitting engine power to the driving wheels and is due mainly to the following elements:

1. Clutch, transmission, differential, universal joints and bearings. Power consumption in these components is function of both the quality of lubrication and the surface finish of the gears and is proportional to power transmitted.
2. Oil churning in the gear box. Power consumption in this respect is proportional to engine speed and is also a function of oil viscosity.

For vehicles in motion, the measure of transmission resistance is usually given as the efficiency η of the complete power train between the engine and the drive axle and is measured experimentally on a dynamometer. Preliminary design calculations are based on comparative data of existing similar applications. The breakdown of the overall efficiency factor into component subfactors delivers these average values: (1) Clutch efficiency, 0.99; (2) Gear shift transmission efficiency, in direct gear 0.98, in lower gears 0.95; (3) Differential efficiency, 0.95; (4) Joints and bearing efficiency, 0.99-0.98.

Efficiency of the whole power train is then the

³³J. L. Koffman—"Vehicle Performance (The Effect of Rotating Masses on Acceleration)", Automobile Engineer, London, Dec. 1955.

Table 5—Average Values of Mass Factor*

Vehicle Type	Gear			
	High	Second	First	Low
Passenger car (large) ...	1.09	1.14	1.30	...
Passenger car (small) ...	1.11	1.20	1.50	2.40
Truck	1.09	1.20	1.60	2.50

*Capacity-loaded vehicles.

product of the efficiency factors of all the components, resulting in the following average overall transmission efficiencies on present-day vehicles: (1) In direct gear, 0.90; (2) In lower gears, 0.85; (3) In transmissions with very high reduction, 0.75-0.80.

For calculations on vehicles coasting with the engine disconnected, torque M_t required on the drive axle to overcome transmission resistance is used. Its value can be found experimentally on dynamometers or by trailing tests. In equation form,

$$R_t = \frac{M_t}{r} \quad (87)$$

where R_t is the transmission resistance force.

Vehicle Performance: Calculation of the resistance forces supplies data essential to vehicle performance prediction. As a rule, performance is obtained by one of the following graphical methods.

POWER DIAGRAM: Power required to overcome rolling, air and grade resistance forces (Part 5)

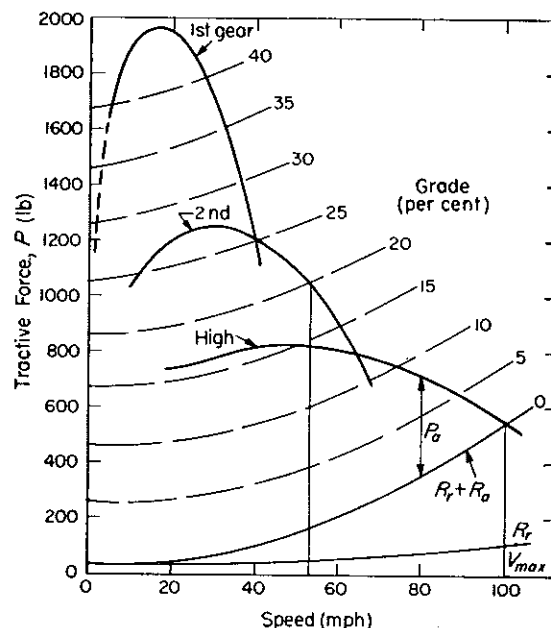


Fig. 47—Tractive-force diagram. Rolling, air and grade resistances are plotted additively against vehicle speed. Superimposed on the family of force-required curves is tractive force P available at the drive wheels in various gears. Maximum speed is given by the intersection of the $(R_r + R_a)$ curve with the high-gear tractive-force line. Speed at which a 20 per cent grade can be negotiated is 55 mph in second gear. Difference between the force-required and force-available curves is free or excess force for acceleration.

is graphically plotted against vehicle speed on the power diagram. On the same diagram engine power delivered to the drive axle at different gear reductions is plotted, Fig. 46. From the intersections of these power-required and power-available curves, the expected vehicle performance at any speed and grade can be determined directly or, conversely, the power necessary to reach a certain performance level can be established.

TRAACTIVE-FORCE DIAGRAM: In this method, rolling, air and grade-resistance forces are additively plotted in the given order against vehicle speed, Fig. 47. The tractive force available at the drive wheels in the different gear reductions is also superimposed on the diagram. Intersections of the two sets of curves give the graphical solution to the equation

$$\frac{M_e \eta \zeta}{r} = P = R_r + R_a + R_g \quad (88)$$

where M_e is engine torque (lb-ft) as function of speed, η is power transmission total efficiency, and ζ is the total reduction ratio between engine and drive axle.

Corresponding curve intersections indicate the tractive force (and therefore engine torque) required to balance the resistance forces at any given speed and condition of operation. The tractive-force diagram generally is preferable to the power diagram because, at very low speeds, the power requirement and the engine power output are very small and determination of curve intersections is difficult and inaccurate. Calculation of performance by the tractive-force method, however, gives relatively large corresponding values, even

at zero speed and permits more exact graphical analysis.

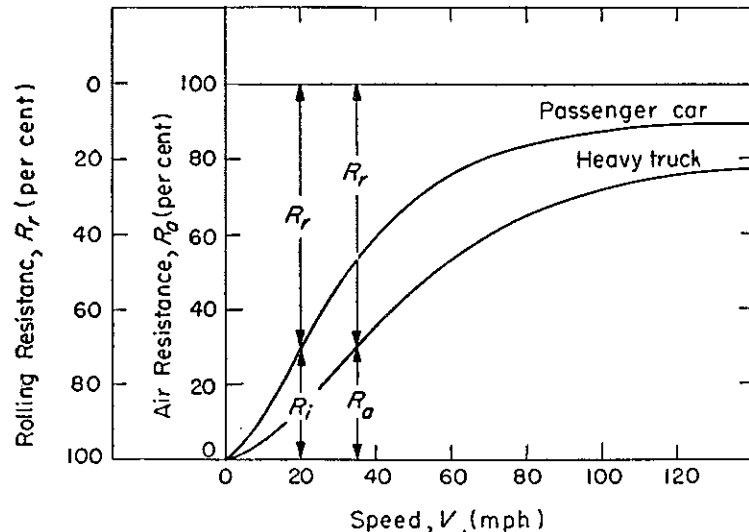
Both performance-prediction methods apply only for constant-speed driving; performance calculation in accelerated motion is more complicated and cannot be solved by a direct method. Detailed investigation of the complete subject of vehicle performance prediction in constant and accelerated motion is discussed in a subsequent article in this series.

Summary of Resistance-Force Characteristics: Comparing resistance forces, the following observations can be made:

1. Rolling and air resistance are present under all conditions of motion. Tractive force is used principally to overcome these two resistance forces. Only if excess traction is available will the vehicle accelerate or climb grades.
2. All the resistance forces except air resistance are proportional to vehicle weight. Nevertheless, a relationship between vehicle weight and frontal area (or coefficient of air resistance) is apparent, since high-capacity vehicles are usually designed for large loads and lower speeds and therefore do not require an aerodynamically clean body shape.
3. Rolling and air resistance are functions of vehicle speed, while grade and inertia resistance are independent of speed.
4. Comparison of air and rolling resistance forces, Fig. 48, shows, as a function of speed, the percentile share of these resistances in the total. Generally, it can be observed that the effect of the air resistance at a certain speed is more pronounced on a light passenger car, despite its aerodynamically superior quality, than on a

Fig. 48—Comparison of rolling and air resistances for passenger car and heavy truck. For the car: $W = 3000$ lb, $c_a = 0.5$, and $A = 30$ ft 2 ; for the truck: $W = 30,000$ lb, $c_a = 0.8$, and $A = 70$ ft 2 . Coefficient of rolling resistance on both vehicles is assumed as $f = 0.01(1 + V/100)$. Assuming, arbitrarily, that air resistance is of no practical importance until it reaches 30 per cent of rolling resistance, it is

found that this value is reached at 20 mph for the passenger car and 35 mph for the truck. At a cruising speed of 70 mph, air resistance accounts for 80 per cent of the tractive force on the passenger car, but only 60 per cent on the truck. This fact justifies the emphasis placed on the aerodynamic design of passenger cars.



heavy truck. Considering the cruising speed on modern highways as 70 mph, it is found that an average passenger car will use 80 per cent of its tractive force to overcome air resistance. The necessity for aerodynamic perfection, especially on small cars operated at high speeds, is evident.

On the other hand, air resistance does not become appreciable until a certain speed is reached. Assuming that air resistance will be considered only after it reaches at least 30 per cent of rolling resistance ($R_a = 0.3 R_r$), it is found that air resistance is negligible on passenger cars for speeds below 20 mph and on trucks below 35 mph. Rolling and air resistances are equal at speeds of about 35 and 55 mph, respectively (Fig. 48).

5. Similarity of the characteristics of grade and inertia resistances enables mathematical comparisons to be made. The excess tractive force will produce either an acceleration a (ft per sec²) or enable the vehicle to climb the grade G (per cent). From Equations 61 (Part 5) and 78, the

following relation can be derived:

$$a = \frac{gG}{100\gamma} \quad (89)$$

Correspondingly, if maximum acceleration on level ground is known, the acceleration a_g while the vehicle is ascending grade G can be calculated as

$$a_g = a - \frac{gG}{100\gamma} \quad (90)$$

Therefore, the same excess tractive force will produce either a 10 per cent grade-climbing ability or an acceleration of $0.1 (g/\gamma)$ ft per sec².

In the next part of this series, the effects of weight distribution on vehicle static and dynamic stability (against tipping) are reviewed. Experimental and analytical methods for determining the vehicle center of gravity are also presented.

Mechanics of Vehicles—7

By JAROSLAV J. TABOREK*

Development Engineer
Towmotor Corp.
Cleveland

FORCES that act on a moving vehicle, reviewed in preceding articles of this series, are essential factors in performance and stability calculations. Certain static vehicle characteristics, fixed principally by the weight distribution of the vehicle (loaded and unloaded), are also significant to the vehicle designer. In this article, analytical and experimental methods for finding vehicle centers of gravity in the longitudinal, transverse and vertical directions are described.

► How to Find the CG

The relationship between static axle reactions and cg position is revealed by consideration of Fig. 49. Axle reactions W_f and W_r are obtained by writing the moment-equilibrium equations for the ground-contact points:

$$W_f = \frac{W}{L} [L_f \cos \theta + H \sin (\pm \theta)] \quad (91.1)$$

*Now Research and Development Engineer, Phillips Petroleum Co., Bartlesville, Okla.

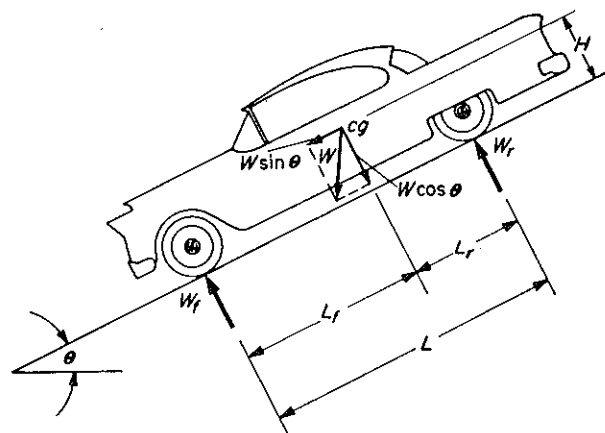


Fig. 49—Relationship between static axle reactions and position of the center of gravity. The downhill axle carries the greater load because of the raised cg.

$$W_r = \frac{W}{L} [L_r \cos \theta - H \sin (\pm \theta)] \quad (91.2)$$

$$W \cos \theta = W_f + W_r \quad (91.3)$$

In these equations, it is assumed that the longitudinal and horizontal co-ordinates (L_f , L_r , and H) of the center of gravity are known. The downhill axle carries the greater load because of the raised position of the cg. However, the sum of both axle reactions equals the normal weight component. Positive sign for angle θ is arbitrarily taken for an uphill slope.

Longitudinal and Transverse CG Location: Position of the center of gravity in the longitudinal direction can be found by weighing the vehicle, Fig. 50a. With one axle of the vehicle on a scale at a time, the other supported on firm ground, front and rear axle weights, W_f and W_r , can be obtained. The longitudinal position of the cg is calculated from the two relations

Nomenclature

- H = Height of center of gravity, ft
 H_g = Height of cg of load, ft
 I = Mass moment of inertia around cg of body, lb-ft-sec²
 J = Mass moment of inertia around oscillation point, lb-ft-sec²
 L = Wheelbase, ft
 L_f = Distance between front axle and cg of vehicle, ft
 L_g = Load action arm, ft
 L_r = Distance between rear axle and cg of vehicle, ft
 Q = Load, lb
 r_f = Front-tire radius, ft
 r_r = Rear-tire radius, ft
 S = Wheel tread, ft
 S_1, S_2 = Distances determining lateral cg position in relation to vehicle tread, ft
 T = Oscillation time, sec
 W = Vehicle weight, lb
 W_f = Front-axle-weight (static), lb
 W_r = Rear-axle weight (static), lb
 W_1, W_2 = Static weight on the left and right-side wheels, lb

Center of Gravity

- static axle reactions
- side-tilting
- weighing with elevated axle
- vehicle pendulum

$$L_f = \frac{LW_r}{W}$$

$$L_r = \frac{LW_f}{W} \quad (92)$$

Addition of co-ordinates L_f and L_r should give wheelbase L , affording a check on the accuracy of the measurements.

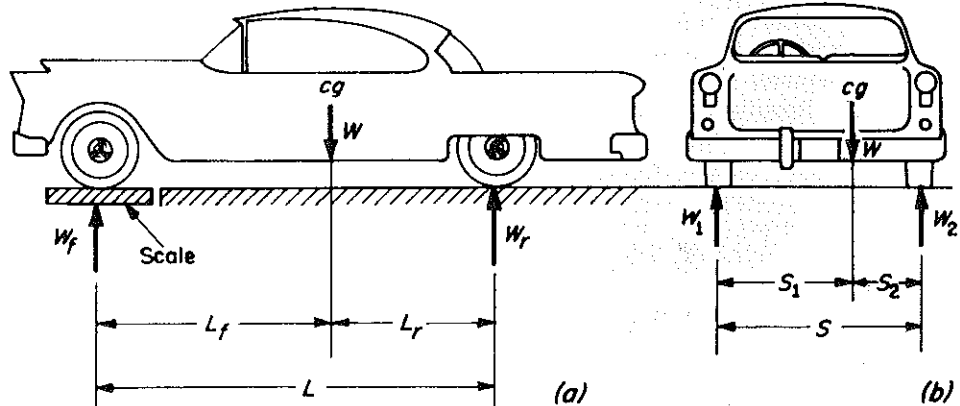
The transverse position of the center of gravity can be assumed to lie on the axis of symmetry of the vehicle only when vehicle weight is uniformly distributed on each side of the longitudinal axis. For accurate results, or on vehicles with asymmetrical weight distribution, the transverse position of the center of gravity can be determined by a method similar to that described. In this case, weights of the right and left-side wheels (W_1 and W_2) are found by weighing, Fig. 50b, and the co-ordinates of the transverse center of gravity location are determined from

$$S_1 = \frac{SW_2}{W}$$

$$S_2 = \frac{SW_1}{W} \quad (93)$$

As a check, again $S_1 + S_2 = S$.

Fig. 50—Weighing front and rear axles one at a time, a, gives the longitudinal position of the cg. Where the cg is not on the longitudinal axis of symmetry, b, right-side and left-side wheels can be weighed to fix the transverse position of the cg.



Height of CG: Determination of the vertical position of the center of gravity, distance H in Fig. 51, is more difficult. Following are the principal methods: (1) Side tilting, (2) Weighing with one axle elevated, and (3) The pendulum method.

SIDE TILTING: The vehicle is tilted sideways (Fig. 51) and the angle of inclination β is measured when the vehicle balances. By inspection of the geometry of the tilted vehicle,

$$H = r + \frac{S_1}{\tan \beta} \quad (94)$$

This method presupposes a round tire cross section (point contact with the ground) and assumes an exact knowledge of S_1 , the lateral position of the center of gravity. Accuracy of this method is highly questionable, since not all of these conditions are fulfilled in the usual case. Also, the necessary angular measurement may offer a problem. To create the best possible experimental conditions, high tire-inflation pressure should be used, and springs should be locked in position to prevent uneven deflection. Unavoidable tire distortion will, in any case, give uncontrollable errors. If higher than normal working tire pressure is used, correction for the effective tire radius should be made in the final result. This method of fixing cg loca-

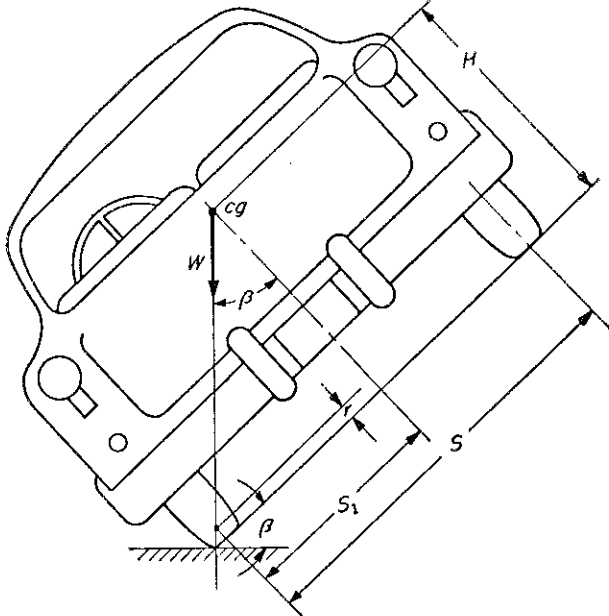


Fig. 51—By tilting the vehicle to one side until it balances, vertical height of the cg can be calculated from a measurement of tilt β . This method of locating the cg requires that front and rear wheels have the same tread.

tion is limited to vehicles with front and rear tires in line. Other wheel arrangements do not have the tilt axis parallel to the axis of symmetry of the vehicle, a condition which is necessary for use of the method.

WEIGHING WITH ONE AXLE ELEVATED: This method requires measurement of the weight of one axle; the other axle is raised to arbitrary height, n , Fig. 52. Actual height of the axle elevation is unimportant. The angle of tilt must be measured accurately, usually by determining one or both longitudinal distances L' and n . Springs should be locked in normal position, and the location of the center of gravity in the longitudinal direction (distance L_r) must be known. In elevating the axle, care should be taken that the hoist does not touch any part of the vehicle except the axle, since additional moments might be introduced that would disturb the results.

This method can be used irrespective of the wheel arrangement on the vehicle, for example, on three-wheel vehicles and with unequal tire diameters. Results can be obtained by the graphical or analytical methods described in the following.

Graphical Method: In many applications, a simple graphical method gives H quickly and with sufficient accuracy. Measuring the height of elevation n , and obtaining the corresponding weight of the lower axle, W'_f (Fig. 52), distance L'_r can be calculated from the expression

$$L'_r = \frac{W'_f L'}{W} = \frac{W'_f}{W} \sqrt{L^2 - N^2} \quad (95)$$

where $N = n - r$.

This establishes a vertical line which crosses the known longitudinal position of the center of gravity and determines the cg position in the horizontal direction. Height H is next scaled from the layout, giving sufficient accuracy for the usual performance calculation.

Analytical Method: Evaluation of the vertical position of the cg for the difficult case of unequal front and rear tire diameters, Fig. 53, is illustrated by the following development.

Let the difference in loaded effective tire radii on rear and front axles be designated by Δr , where

$$\Delta r = r_r - r \quad (96)$$

and r_f and r_r are radii of front and rear wheels. By inspection (Fig. 53),

$$L'_r = L_r \cos \beta + h \sin \beta$$

$$L' = x \cos \beta = (L - \Delta r \tan \beta) \cos \beta \quad (97)$$

Dividing both equations by $\cos \beta$ and substituting L'_r and L' into Equation 95, it follows that

$$W'_f L - W'_f \Delta r \tan \beta = WL_r + Wh \tan \beta \quad (98)$$

For easier calculation, L_r can be eliminated by substituting

$$WL_r = W_f L \quad (99)$$

from Equation 92. Height of the cg above the rear axle center is then

$$h = \frac{L(W'_f - W_f)}{W \tan \beta} - \frac{W_f \Delta r}{W} \quad (100)$$

Angle β cannot be measured directly and will be

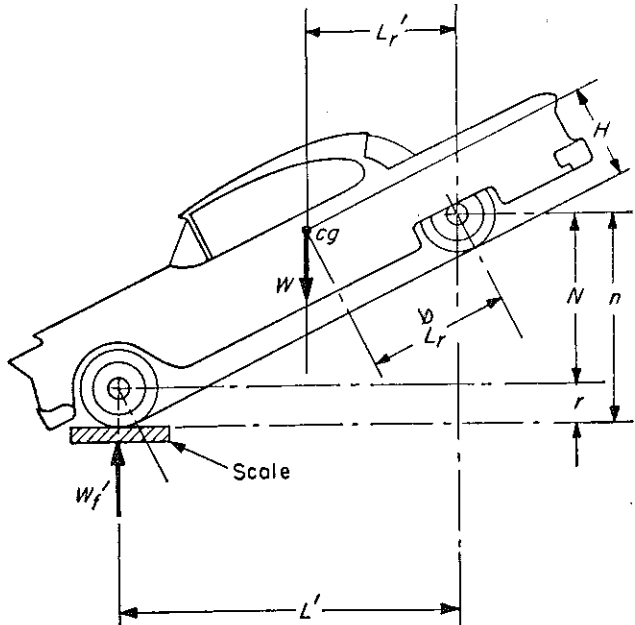


Fig. 52—Height of the cg can be determined by weighing one axle with the other elevated to arbitrary height n . With longitudinal cg position L_r known, L'_r is calculated from Equation 95. This allows two lines to be drawn that intersect at the vehicle cg. Height H can be scaled from the layout.

calculated from $\beta = \alpha - \gamma$, where the component angles are

$$\begin{aligned}\tan \alpha &= \frac{N}{L'} \\ \tan \gamma &= \frac{\Delta r}{L} \end{aligned}\quad (101)$$

Consequently,

$$\begin{aligned}\tan \beta &= \tan (\alpha - \gamma) = \frac{\tan \alpha - \tan \gamma}{1 + \tan \alpha \tan \gamma} \\ &= \frac{LN - \Delta r L'}{LL' + \Delta r N} \end{aligned}\quad (102)$$

Finally, for the cg height above the ground,

$$\begin{aligned}H &= r_f + h = r_f + \frac{L(LL' + \Delta r N)}{(LN - \Delta r L')} \times \\ &\quad \frac{W_f' - W_f}{W} - \frac{\Delta r W_f'}{W} \end{aligned}\quad (103)$$

To limit length measurements in the elevated position to n only, L' can be eliminated by use of the relation

$$\begin{aligned}L' &= \sqrt{L^2 - N^2 + (\Delta r)^2} \\ &= \sqrt{L^2 - (n - r_f)^2 + (\Delta r)^2} \end{aligned}\quad (104)$$

Only the following measurements are then necessary: W_f = Weight of the front axle with vehicle on level ground, W_f' = Weight of the front axle

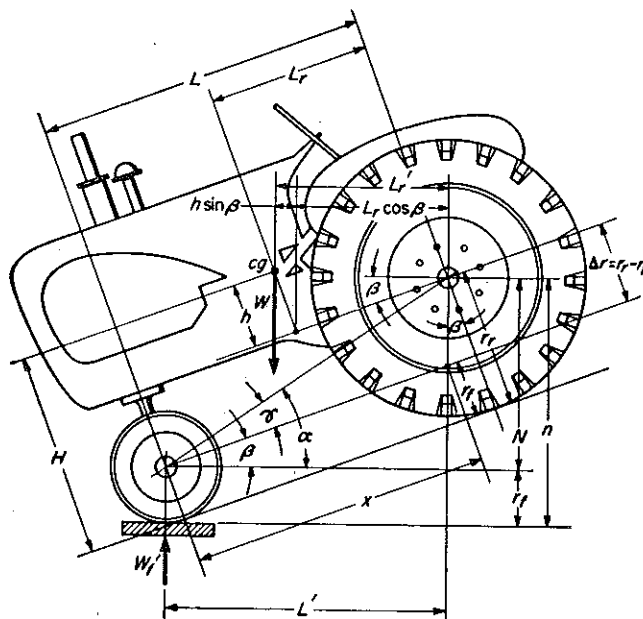


Fig. 53—When front and rear wheels have different diameters, height of the cg can be determined from Equations 100 and 103. Measurements required are: (1) Weight of front axle with the vehicle level, W_f ; (2) Weight of front axle with rear axle elevated, W_f' ; and (3) Height of rear axle, n .

HOW TO FIND THE CG

with rear axle elevated, and n = Height of elevation of the rear-axle center.

For vehicles with equal tire radii on front and rear axles, Equation 103 is simplified, since $\Delta r = 0$ and $\gamma = 0$, giving

$$H = r_f + \frac{(W_f' - W_f)L\sqrt{L^2 - N^2}}{WN} \quad (105)$$

Calculation of the height of the center of gravity by this method requires no special equipment, and accuracy is superior to the side-tilting method. It is recommended, however, that several calculations be made at different heights of rear-axle elevation and with front and rear axles alternately raised.

PENDULUM METHOD: This method of finding vertical cg position is based on the physical law that determines the oscillation period of a compound pendulum as a function of the center of gravity position of the swinging mass. The measuring arrangement consists of two pendulum structures of lengths h_s and h_v , carefully suspended on knife edges, Fig. 54. Location of the pendulum centers of gravity (unloaded) and their oscillation times are known. The vehicle is placed, successively, on both long and the short pendulums, and the oscillation times of the combined systems are measured. Height of the center of gravity is then calculated from oscillation times.

Described in detail in Reference 40, derivation of the expression for H , the vertical position of

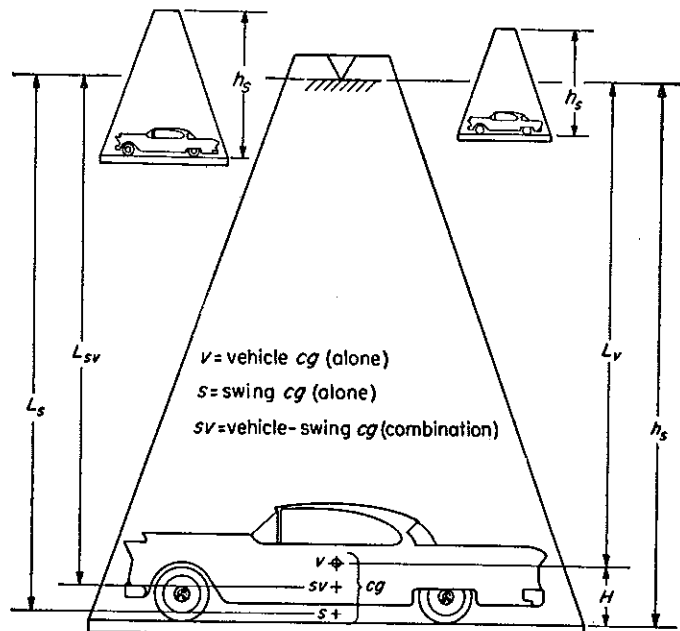


Fig. 54—Determination of center-of-gravity height by the pendulum method. Two "swing" structures (heights h_s and h_v) are used, and the oscillation time of each is measured with the vehicle on the platform. With all other pendulum data known, cg height can be calculated.

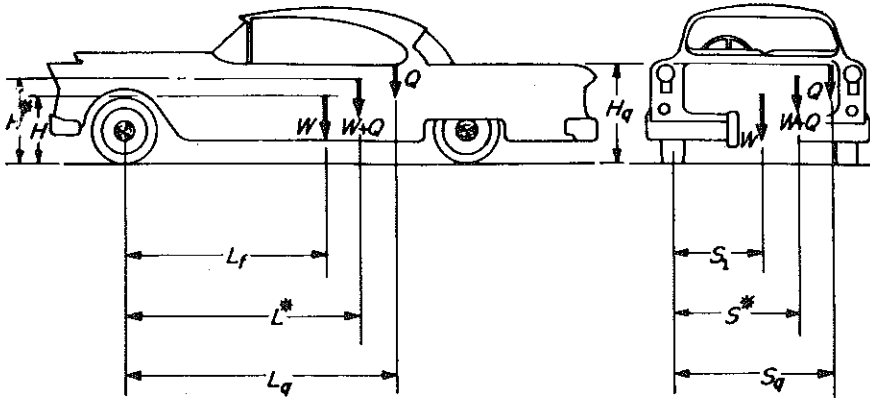


Fig. 55—Position of cg of loaded vehicle (cg of load and cg of empty vehicle known) can be calculated from Equation 106.

the vehicle cg, is not given here. Form of the equation, where cap and lower-case subscripts refer to the long and short swings, is

$$H = \frac{1}{W_v(T_{sv}^2 - T_{sv}^2) - 8\pi^2 m_v(h_s - h_s)} \times \\ [W_s L_s(T_s^2 - T_{sv}^2) - W_s L_s(T_s^2 - T_{sv}^2) + \\ W_v(T_{sv}^2 h_s - T_{sv}^2 h_s) - 4\pi^2 m_v(h_s^2 - h_s^2)] \quad (106)$$

Containing, for the most part, known swing and vehicle constants, Equation 106 requires only the measurement of T_{sv} and T_{sv} , which are the oscillation times of the short and long pendulums, respectively, with the vehicle in place.

For extreme accuracy in measurement, the buoyancy of the vehicle in the air and the increase of mass due to the entrapped air volume should be taken into consideration. Buoyancy of the swing structure is considered negligible.

From this brief description, it is seen that the pendulum method requires quite elaborate equipment and therefore finds use only in well equipped laboratories. Accuracy claimed is within ± 1 per cent, which is the highest of all methods.

Center of Gravity of a Loaded Vehicle: For practical reasons, the center of gravity of a vehicle is often determined in the empty condition. Performance calculations, however, usually require the cg position to be known in the loaded state. For vehicles, which operate under changing loads, both conditions are of importance: the minimum traction and braking performance will be realized with ve-

hicle empty, while other performance and stability calculations will use the loaded-vehicle data.

Center of gravity of the load can usually be calculated without difficulty. Designating the position of the center of gravity of any load Q , as positioned on the vehicle with co-ordinates L_q , H_q and S_q , Fig. 55, the location of the loaded-vehicle cg can be calculated from

$$L^* = \frac{WL_f + \Sigma QL_q}{W + \Sigma Q} \\ H^* = \frac{WH + \Sigma QH_q}{W + \Sigma Q} \\ S^* = \frac{WS_1 + \Sigma QS_q}{W + \Sigma Q} \quad (107)$$

Starred values designate the cg co-ordinates of the loaded vehicle.

Knowledge of vehicle cg position leads to an evaluation of static and dynamic stability against tipping. Discussed in the next article of this series, the problem is particularly important on a vehicle that is designed to carry a load outside of its wheelbase. Fork lift trucks, front-end loaders, scoops and cranes are typical examples.

REFERENCES

37. P.M. Heldt—*The Automotive Chassis*, Chilton Co., 1952.
38. R. Dean-Averns—*Automobile Chassis Design*, Iliffe, London, 1952.
39. R. Bussien—*Automobiltechnisches Handbuch*, Cram Verlag, Berlin, 1952.
40. R. S. Brink—"The Solution of the Center of Gravity and Moment of Inertia Problem," *GM Engineering Journal*, Nov.-Dec., 1953.
41. Timoshenko and Young—*Advanced Dynamics*, McGraw-Hill Book Co. Inc., New York, 1948.
42. Kamm and Schmidt—*Das Versuchs und Messwesen auf dem Gebiete des Kraftfahrzeugs*, (Experimentation and Measuring on Automotive Vehicles), Springer Verlag, Berlin, 1939.

Mechanics of Vehicles—8

Longitudinal Stability

By JAROSLAV J. TABOREK*

Development Engineer
Towmotor Corp.
Cleveland

dynamic moments •
static moments •
axle reactions •
moments of inertia •

STABILITY against tipping—in either lateral or longitudinal directions—is an essential characteristic of any well-behaved vehicle. The problem of predicting tipping stability assumes special importance where the vehicle center of gravity is high, or where the vehicle is designed to carry a load outside of its wheelbase. Representative of the latter case are fork lift trucks, loaders, scoops and cranes.

front-axle ground-contact point gives the equation:

$$L_f W \cos \theta = L_q Q \cos \theta + H_q Q \sin \theta + \frac{QaH_q}{g} + \\ HW \sin \theta + \frac{WaH}{g} + \frac{Qa_q L_q}{g} \quad (108)$$

This equation applies, of course, for the state of balance. In practice, stabilizing moments must be

Dynamic and Static Moments

Part 4 of this series (July 11, 1957) dealt with vehicle side tipping on a curve resulting from the action of centrifugal forces. In the following section, stability of a vehicle in straight-line motion is examined and related to the position of its center of gravity. As a special case, stability of a load-carrying vehicle while stationary is also investigated.

Dynamic Stability in the Drive Direction: In the general case, moments affecting the dynamic longitudinal stability of a vehicle are:

1. Static moments of the load and of the empty vehicle on level ground.
2. Static moments due to ground inclination.
3. Moments due to acceleration of the vehicle in the drive direction.
4. Moments due to forces of acceleration on the lifted or lowered load.

One of the worst possible combinations of forces is represented in Fig. 56 where a fork-lift truck is shown being decelerated on a down-hill slope and the load is being decelerated while moving downward. Equilibrium of moments around the

a	= Acceleration, ft per sec ²
a_q	= Load acceleration, ft per sec ²
D	= Drawbar pull, lb
f	= Coefficient of rolling resistance
H	= Height of cg from ground, in.
H_a	= Height of action point of the air-resistance force, in.
H_d	= Height of the hitch point, in.
I	= Polar moment of inertia, ft-lb-sec ²
L	= Wheelbase, in.
L_f, L_r	= Distances of cg from front and rear axles, in.
M_d	= Torque on drive axle, lb-ft
M_e	= Engine torque, lb-ft
P	= Tractive force, lb
P_f, P_r	= Tractive forces of front and rear-wheel drives, lb
R_a	= Air resistance, lb
R_g	= Grade resistance, lb
R_i	= Inertia resistance, lb
R_{it}	= Inertia resistance of translatory mass, lb
R_r	= Rolling resistance, lb
W_{df}, W_{dr}	= Dynamic weights on front and rear axles, lb
ΔW_d	= Dynamic weight transfer in driving, lb
α	= Angular acceleration, rad per sec ²
ξ	= Reduction ratio
η	= Transmission efficiency
μ	= Road adhesion coefficient
θ	= Horizontal slope, deg
σ	= Stability factor

*Now Research and Development Engineer, Phillips Petroleum Co., Bartlesville, Okla.

made larger by a stability or safety factor σ , defined as the ratio of the stabilizing to the overturning moment.

Stability can be expressed either as a ratio or as a percentage margin, the two being connected by the relation

$$\text{Stability Margin, per cent} = (\sigma - 1) \times 100 \quad (109)$$

Rearranging Equation 108 so that every stability influencing factor forms its own group,

$$\sigma = \frac{1}{A + B + C + D} \quad (110)$$

where

A = Static Level Moments

$$= \frac{QL_q}{WL_f}$$

B = Moments due to Slope

$$= \frac{\tan \theta (WH + QH_q)}{WL_f}$$

C = Moments due to Vehicle Acceleration

$$= \frac{a(WH + QH_q)}{gL_f W \cos \theta}$$

D = Moments due to Load Acceleration

$$= \frac{a_q Q L_a}{gL_f W \cos \theta}$$

Terms containing grade or acceleration can have either a tipping or a stabilizing effect, depending on the direction of the slope and the direction of the acceleration. Convention for assigning signs is as follows: $+ \theta$, downhill; $+ a$, braking; $+ a_q$, deceleration.

Static Stability: Equation 110 is difficult to work

with and requires that values of θ , a and a_q be assumed. In practice, stability is often determined for static level-ground conditions only. In such cases, it is sufficient to know cg locations of the vehicle and of the load. Values of the static stability factor are then selected on an experience basis. Adjustments, of course, are made for each specific application so as to provide sufficient safety margin for anticipated dynamic conditions and horizontal slope.

In Fig. 57, a lift truck is shown in level-ground position. The stability factor is

$$\sigma = \frac{L_f W}{L_q Q} \quad (111)$$

which is identical to Equation 110 if interpreted for stationary conditions and level ground.

It is apparent that stability is determined not only by the weight of the load alone but, in addition, by its moment around the tipping point. For a given stability factor, the product of load Q and action arm L_q is constant. Graphically such a relation is represented by a hyperbolic curve, Fig. 57. While values of both variables are theoretically unlimited where the stability effect is concerned, the load magnitude is restricted by the strength of vehicle structural parts, and practical considerations will limit the length of the action arm.

Stability Calculations: The techniques employed in stability calculations are best demonstrated by an example:

Assume that a lift truck has empty weight $W = 12,200$ lb and cg location at $L_f = 46$ in. and $H = 30$ in. The nominal load capacity is 11,000 lb at $L_q = 40$ in. The relation between the load and its corresponding permissible distances from the support point is to be determined for a stability margin range of zero (tipping limit), 25 per cent, and 50 per cent.

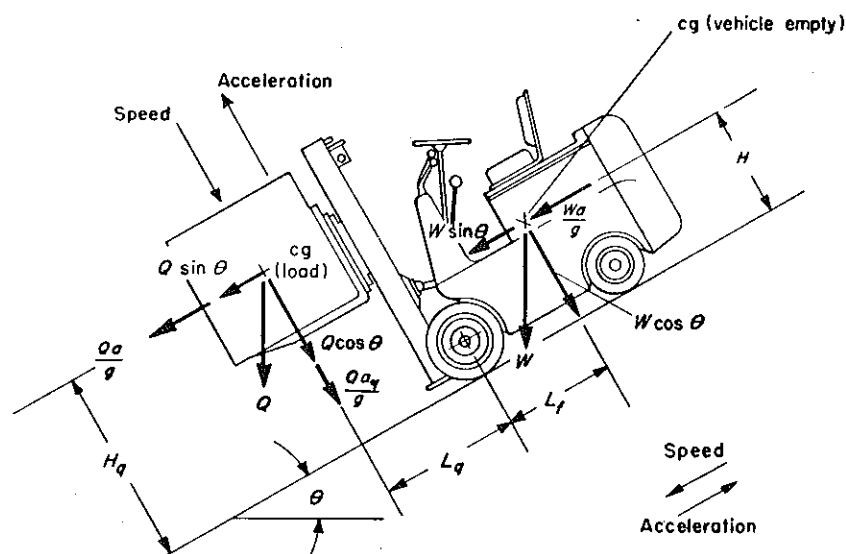


Fig. 56—The fork lift truck is representative of vehicles designed to carry loads outside of their wheelbases. The sketch illustrates the stability-affecting factors for the general case: downhill slope, deceleration of the vehicle in translatory motion and deceleration of the load while being lowered.

STATIC STABILITY ON LEVEL GROUND: The rearranged stability equation is

$$L_q Q = \frac{L_f W}{\sigma} = \frac{(46)(12,200)}{\sigma} \quad (112)$$

From the desired stability margins, the corresponding stability factors, σ , are 1.00, 1.25 and 1.50, respectively. With an assumed series of Q values, the corresponding distances L_q can be calculated. Results are plotted as a family of curves in Fig. 57.

For the nominal capacity of the truck, the stability factor is

$$\sigma = \frac{(46)(12,200)}{(40)(11,000)} = 1.27 \text{ or } 27\% \text{ margin} \quad (113)$$

If the absolute load limit Q is 14,000 lb, the truck can carry 6,300 lb at $L_q = 70$ in. (tips of the forks) and maintain a nominal stability margin of 27 per cent.

STABILITY ON UNBANKED SLOPES AND UNDER DYNAMIC CONDITIONS: For the same nominal capacity data, a stability check will be made for static and dynamic grade conditions. The cg height of the load is assumed variable between 40 in. (load lowered) and 100 in. (load elevated). For the stationary condition, the grade is first calculated for which the truck would tip over ($\sigma = 1$). Rearranged, Equation 110 is written as

$$\begin{aligned} \tan \theta_{max} &= \frac{L_f W - L_q Q}{H_q Q + HW} \\ &= \frac{(46)(12,200) - (40)(11,000)}{H_q(11,000) + (30)(12,200)} \end{aligned} \quad (114)$$

For the assumed conditions, results are as follows:

1. Load lowered ($H_q = 40$ in.), $\tan \theta_{max} = 0.15$ and $\theta_{max} = 8.5$ deg, or a 15 per cent grade.
2. Load elevated ($H_q = 100$ in.), $\tan \theta_{max} = 0.082$ and $\theta_{max} = 4.79$ deg, or an 8.2 per cent grade.

Maximum translatory deceleration of the vehicle at the point of tipping ($\sigma = 1$) on level ground is next established. From Equation 110,

$$\begin{aligned} a_{max} &= \frac{g(L_f W - L_q Q)}{H_q Q + HW} \\ &= \frac{g[(46)(12,200) - (40)(11,000)]}{H_q(11,000) + (30)(12,200)} \end{aligned} \quad (115)$$

Substituting again for H_q , results are as follows:

1. Load lowered ($H_q = 40$ in.), $a_{max} = 0.15 g = 4.8 \text{ ft-sec}^{-2}$.
2. Load elevated ($H_q = 100$ in.), $a_{max} = 0.082 g = 2.6 \text{ ft-sec}^{-2}$.

Maximum safe deceleration ($\sigma = 1$) of the load when it is lowered is

$$\begin{aligned} a_{q max} &= \frac{g(L_f W - L_q Q)}{L_q Q} \\ &= \frac{g[(46)(12,200) - (40)(11,000)]}{(40)(11,000)} \\ &= 0.27 g = 8.7 \text{ ft sec}^{-2} \end{aligned}$$

LONGITUDINAL STABILITY

Any combination of values for grade and acceleration can, of course, be assumed and the actual stability calculated from Equation 110.

Finding Moments of Inertia

There are several occasions in the study of vehicle dynamics where calculation of moments of inertia is required:

1. In the determination of the kinetic energy of rotating parts, such as wheels and tires, gears, flywheels, clutches, crankshafts and connecting rods.
2. In the design of suspension systems.
3. In the calculation of directional stability and curve behavior. In such cases, the inertia moment of the whole vehicle with respect to all three axes is required.

Mass moment of inertia, designated I_m , is defined by

$$I_{(m)} = mk^2 = \frac{Wk^2}{g} \text{ ft-lb-sec}^2 \quad (117)$$

where k is the radius of gyration. The mass mo-

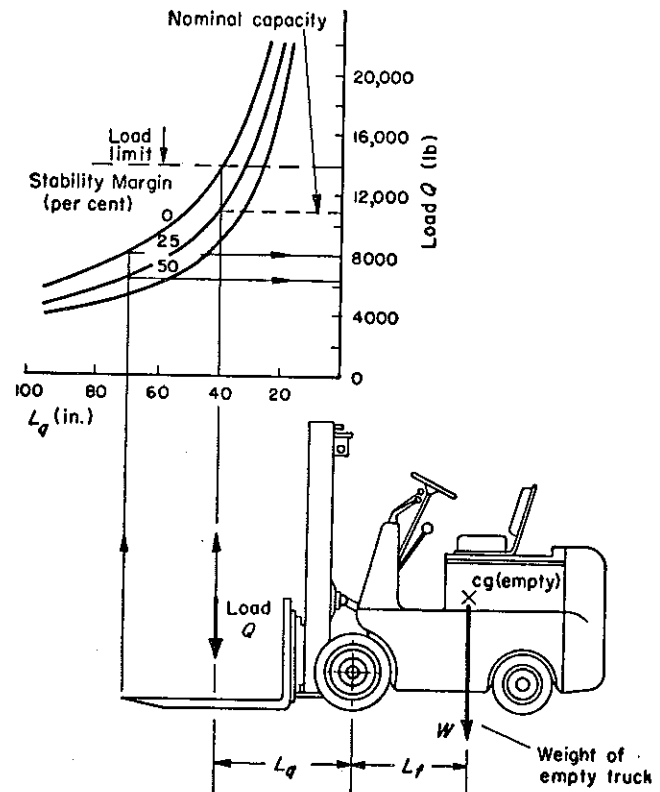


Fig. 57—Capacity-rating technique for a vehicle with load carried outside of the wheelbase. The stability factor σ is defined as the ratio of stabilizing to overturning moments. The relation between the load Q and load moment arm L_q plots as a family of hyperbolas with σ as a parameter.

ment is used commonly in Great Britain and on the continent. In U.S. automotive practice, the weight moment of inertia $I_{(w)}$, which is the product of the weight and the square of the radius of gyration, is widely used. By definition,

$$I_{(w)} = Wk^2 \text{ lb-ft}^2 \quad (118)$$

Mass and weight moments of inertia are related by the simple relationship

$$I_{(w)} = I_{(m)}g \quad (119)$$

The moment of inertia of symmetrical parts, for example, wheels and gears, can be calculated by conventional mathematical methods supplemented by sensible approximations. For irregular parts, one of the following experimental methods can be used:

1. Pendulum method, introduced in Part 7 as a means for determining the height of the vehicle center of gravity, can also be used to find the inertia moment around the transverse axis.

2. Torsional oscillation method, used to determine inertia moments around a vertical axis, requires that the body be rigidly fastened at its center of gravity to a torsion wire. For a known twisting moment D (lb-ft per rad) producing unit deflection, the inertia moment can be calculated from the measured oscillation time T . The relationship is

$$I = D \left[\frac{T}{2\pi} \right]^2 \text{ lb-ft-sec}^2 \quad (120)$$

The value of D for the torsion pendulum can be found by applying Equation 120 to a body of known

inertia moment.

3. A third method also uses the weight of the body as an initiating force for torsional oscillations. Suspended freely on two flexible wires of length L , spaced distance A apart, the body of weight W is given a torsional motion of small angular displacement. Time of one complete oscillation T is then measured. The inertia moment around the vertical axis is

$$I = \frac{W}{L} \left[\frac{AT}{4\pi} \right]^2 \text{ lb-ft-sec}^2 \quad (121)$$

Direct suspension of the body itself is a useful technique for small parts. However, if the inertia moment of the entire vehicle is to be measured, a platform is usually constructed. The inertia moment of the platform is deducted from the calculated inertia moment of the car-platform combination.

Dynamic Axle Reactions

Tractive force between vehicle driving wheels and the ground is a function of the road-adhesion coefficient μ and the effective weight on the driving wheels. When axle reactions are found by weighing or are calculated from the cg position, results apply only for the stationary vehicle. The moving vehicle, on the other hand, is subject to the action of motion-resisting forces which cause a weight shift toward one of the axles. The resulting effective axle reaction is herein designated the dynamic axle weight, and is the factor which ultimately determines the maximum transferable

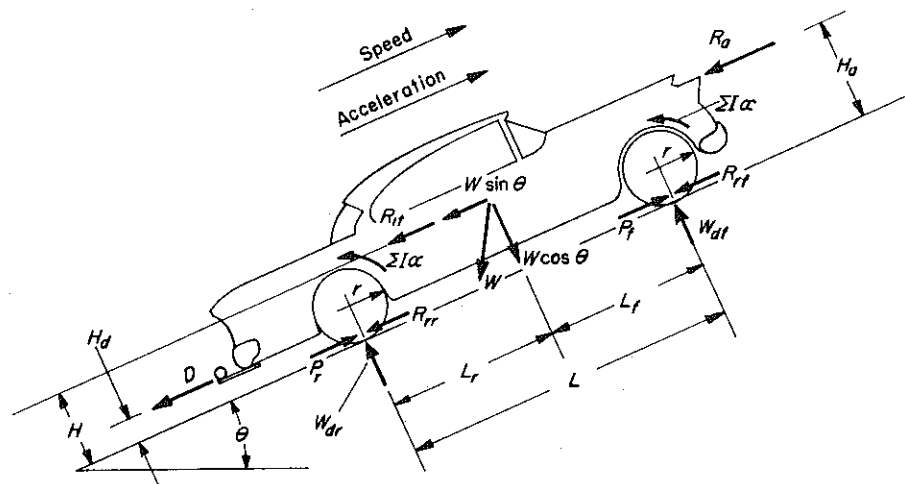


Fig. 58—Vehicle in accelerated motion uphill.
All possible forces are represented.

- D = Drawbar pull
- P_f, P_r = Traction forces on front and rear axles
- R_a = Air resistance
- R_{tt}, R_{rr} = Inertia resistance of translatory mass
- W_{dt}, W_{dr} = Dynamic axle reactions
- I = Inertia moment of rotating parts

tractive force.

All other vehicle performance factors, such as acceleration, gradability, speed and drawbar pull, depend directly on the available tractive force. In following sections of this article, dynamic axle reactions are examined and are related in the next article to the performance limits of front, rear and four-wheel drive vehicles.

Dynamic Axle Weights: A vehicle in accelerated motion up-hill with all possible forces represented is shown in Fig. 58. Dynamic axle reactions are best determined by forming moment equations around the tire-ground contact points. This procedure eliminates all forces acting in the ground plane. Resulting relationships are

$$W_{df} = \frac{1}{L} \left[L_f W \cos \theta - HW \sin (\pm \theta) - H_a R_a - Hma - H_d D \right] \quad (122.1)$$

$$W_{dr} = \frac{1}{L} \left[L_f W \cos \theta + HW \sin (\pm \theta) - H_a R_a - Hma - H_d D \right] \quad (122.2)$$

$$W \cos \theta = W_{dr} + W_{df} \quad (122.3)$$

where W_{df} is the dynamic weight on the front axle and W_{dr} is the dynamic weight on the rear axle.

Rolling resistance, tractive force and the inertia-resistance torque of rotating parts do not appear in these equations since they form no moment with respect to the tire-ground contact point. By inspection of the equations and from common experience, it is apparent that the weight transfer for the vehicle in Fig. 58 is toward the rear axle.

Results identical to those of Equations 122.1 to 122.3 are obtained when moments are taken around the axle centers. Ground-plane forces, that is, rolling resistance, tractive force and inertia torques of rotating parts, would enter such calculations. Additional moments would therefore be created with the rolling radius of the tire as a lever arm. These additional terms would be canceled out in the final form of the moment equation.

From an analysis of the influences of different forces affecting dynamic axle weight, it is seen that:

1. Weight of the vehicle appears in the normal-to-ground (cosine) component of the grade angle θ . The influence of the cosine factor, however, is usually negligible. For example, for a gradability limit of 30 per cent or 17 deg, the corresponding cosine has a value of 0.96; for the usual maximum road grades of 12 per cent, the cosine equals 0.993. Therefore, in subsequent calculations, the approximation $W \cos \theta \approx W$ has been adopted. Where the $\cos \theta$ factor still appears, it is only to show relationships in theoretically correct form.

2. The effect of grade resistance R_g is to give a weight increase on the down-hill axle proportional to the sine of the grade angle and to the

LONGITUDINAL STABILITY

height of the vehicle cg. The grade angle θ is considered positive if grade resistance is motion opposing (uphill travel). Conversely, grade resistance becomes a motion-promoting force as the grade angle changes sign from positive to negative, since

$$\sin (-\theta) = -\sin \theta \quad (123)$$

3. Air resistance tends normally to increase the rear-axle reaction by a weight proportional to H_a , the height of the air resistance action point. Determination of exact relationships, however, is difficult at high vehicle speeds where air lift forces of unpredictable characteristics appear. Such forces diminish axle weight, particularly on the front axle. To counteract this effect, high-speed vehicle bodies are designed to create a vertical component of the air-resistance force which will balance the lift force and provide further additions to axle weight.

4. Inertia resistance that affects dynamic axle weights is that portion of the total force resulting from acceleration of the translatory vehicle mass. Acting at the mass center of the vehicle, effect of this force is proportional to the height of the cg. The inertia torque of rotating parts, M_i , which can be imagined as a resistance force acting at the ground contact point, is similar to all ground-plane forces in that there is no influence on dynamic axle weights.

5. Drawbar pull D , acting at the hinge point, also increases rear-axle weight by an amount proportional to H_d , the height of the drawbar action point.

For a stationary vehicle, motion-dependent resistance forces disappear, and dynamic axle weights equal static weights.

Simplified Method: While Equations 122.1 through 122.3 are mathematically exact, they are unhandy to work with. This is because air resistance is a function of speed and inertia resistance is a function of acceleration. Furthermore, the state of motion must be known, and the calculation is limited to instantaneous values. A simplification can be introduced by the approximation

$$H = H_a = H_d \quad (124)$$

This implies that all resistance forces are assumed to act at a height equal to that of the center of gravity of the vehicle. Such a condition is very nearly true for the air-resistance force, but for drawbar pull, the approximation should be employed with discretion.

With this simplification, Equations 122.1 through 122.3 can be rewritten as

$$W_{df} = \frac{1}{L} \left[L_f W - H(R_g + R_a + R_{it} + D) \right] \quad (125.1)$$

$$W_{dr} = \frac{1}{L} \left[L_f W + H(R_g + R_a + R_{it} + D) \right] \quad (125.2)$$

From the equilibrium of forces parallel to the ground, the following equation results:

$$P - (R_{rf} + R_{rr}) = R_g + R_a + R_{it} + D \quad (126)$$

The right side of this equation is identical with the terms in parenthesis in Equations 125.1 and 125.2. Further, total rolling resistance of the vehicle is unaffected by dynamic weight transfer and equals the sum of the front and rear-axle components, or

$$R_{rf} + R_{rr} = R_r = fW \cos \theta \approx fW \quad (127)$$

When Equations 125, 126 and 127 are combined, an equation results where the dynamic axle weights are a function of the tractive force P , or

$$W_{df} = \frac{L_r W}{L} - \frac{H(P - fW)}{L} \quad (128.1)$$

$$W_{dr} = \frac{L_f W}{L} + \frac{H(P - fW)}{L} \quad (128.2)$$

From these equations, dynamic axle weight can be readily calculated for any vehicle operating

condition if the tractive force is known. It is of interest to note that the first term on the right side of each equation is the static level axle weight, while the second term represents the actual change in the axle weights, or the so-called dynamic weight transfer ΔW_d . It is also of importance to note that the equations are independent of the state of motion (speed or acceleration), the only variable being tractive force P . Further, the form of motion-resisting forces is unimportant, and the equations are applicable whether the vehicle is equipped with front, rear, or four-wheel drive.

Using the dynamic weight transfer term ΔW_d , the axle weight equations can be written

$$W_{df} = W_f - \Delta W_d \quad (129.1)$$

$$W_{dr} = W_r + \Delta W_d \quad (129.2)$$

where W_f and W_r are static level axle weights. For determination of ΔW_d , the value of tractive force P is required. It can be calculated from M_d , the torque on the driving axle which, in turn, is a function of engine torque M_e , total reduction ratio ζ and transmission efficiency η . The expression is

Example 2—Dynamic Axle Weight

A vehicle has gross weight of 3000 lb and is driven by an engine delivering a maximum torque of 200 lb-ft. The differential ratio is 3.9 and low-gear ratio 2.8. Transmission efficiency is assumed as 90 per cent in direct drive and 85 per cent in low gear. The weight is distributed to the axles as follows, $L_f = (0.55)(L)$, $L_r = (0.45)(L)$ and cg height H is (0.35) (L). Rolling radius r of the tire is 1.1 ft, and coefficient of rolling resistance f is 0.02.

The dynamic axle weights for max. engine torque output are to be determined for direct drive and for low gear.

Static axle weights are given by the cg location; or

$$W_f = L_r W = \frac{(0.45)LW}{L} = (0.45)(3000) = 1350 \text{ lb}$$

$$W_r = W - W_f = 3000 - 1350 = 1650 \text{ lb}$$

The effective torque on the drive axle, M_d , is found from Equation 130. Results are:

1. In direct drive,

$$M_d = (200)(3.9)(0.9) = 700 \text{ lb-ft}$$

2. In low gear,

$$M_d = (200)(3.9)(2.8)(0.85) = 1860 \text{ lb-ft}$$

The dynamic weight transfer is then calculated from Equation 131. Results are:

1. In direct drive,

$$\begin{aligned} \Delta W_d &= \frac{(0.35)L}{L} \left[\frac{700}{1.1} - (0.02)(3000) \right] \\ &= 200 \text{ lb} \end{aligned}$$

2. In low gear,

$$\begin{aligned} \Delta W_d &= \frac{(0.35)L}{L} \left[\frac{1860}{1.1} - (0.02)(3000) \right] \\ &= 570 \text{ lb} \end{aligned}$$

which is a 42 per cent weight decrease on the front axle, or a 34.5 per cent weight increase on the rear axle over the static load.

Dynamic axle weights are then:

1. In direct drive,

$$W_{df} = 1150 \text{ lb}$$

$$W_{dr} = 1850 \text{ lb}$$

2. In low gear,

$$W_{df} = 780 \text{ lb}$$

$$W_{dr} = 2220 \text{ lb}$$

It is apparent that weight transfer is considerable, especially in high-reduction drive. Results are the same whether the tractive force produces motion acceleration or drawbar pull.

$$P = \frac{M_d}{r} = \frac{M_e \xi \eta}{r} \quad (130)$$

The dynamic weight transfer term is then

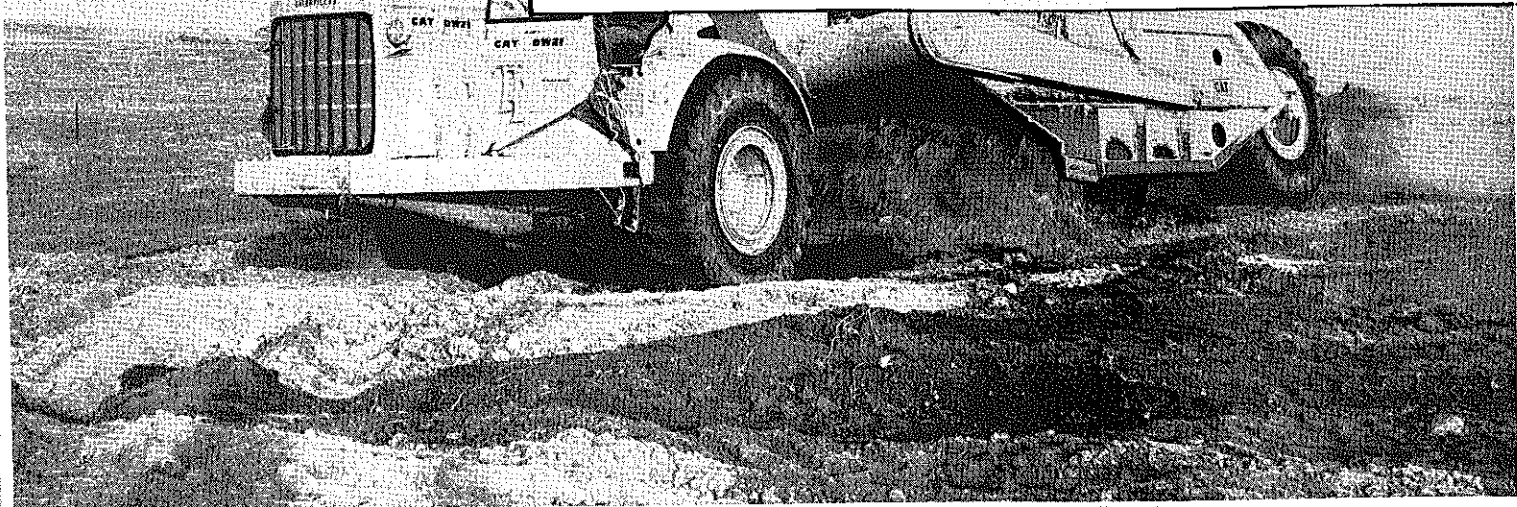
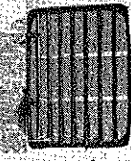
$$\Delta W_d = \frac{H}{L} \left(\frac{M_d}{r} - fW \right) \quad (131)$$

It is seen that the weight transfer term is merely a function of wheelbase L and cg height H ; it is

independent of cg position and almost independent of weight (fW term is small). Example 2 illustrates the calculation technique.

The next part of this series examines the performance limits of a vehicle, that is, traction, speed, gradability, acceleration and drawbar limits, and relates these factors to the fundamental propulsive force.

Mechanics of Vehicles—9



MAIMUM transferable tractive force—as determined by the nature of the wheel-ground connection—sets a fundamental limit to vehicle performance. It follows, therefore, that the type of drive employed in the vehicle—front, rear, or four-wheel—influences its ultimate capacity for speed, acceleration, gradability, and drawbar pull.

In this article, the performance-limit concept is reviewed, and the relative advantages of the three common drive systems are compared.

Equation of Motion: Performance of a vehicle can be predicted from its equation of motion. When interpreted for a moving vehicle, the energy theorem gives the differential expression

$$dE = (P - \Sigma R) ds \quad (132)$$

where P is tractive force and $\Sigma R = R_r + R_a + R_g + D$. When both rotating and translating vehicle masses are considered,

$$E = \frac{mv^2}{2} + \sum \frac{I\omega^2}{2} \quad (133)$$

As detailed in Part 6 (Aug. 8, 1957), this expression is differentiated and the following substitutions are made:

$$\omega = \omega_d \xi$$

$$\omega_d = \frac{v}{r}$$

$$m\gamma = m + \frac{\Sigma I \xi^2}{r^2}$$

In these equations, ω_d is the angular speed of the driving wheels, ξ is the reduction ratio between each rotating part and the driving axle and γ is the factor giving the equivalent inertial effect of rotating parts (Part 6). After these operations are performed, the resulting expression for dE is

$$\begin{aligned} dE &= mvdv + \Sigma I\omega d\omega \\ &= vdv \left(m + \frac{\Sigma I \xi^2}{r^2} \right) \\ &= v m \gamma dv \end{aligned} \quad (135)$$

Since $v = ds/dt$, and $a = dv/dt$, combining Equations 132 and 135 gives

$$am\gamma = P - (R_r + R_a + R_g + D) \quad (136)$$

which is the general equation of vehicle motion.

► Performance Limits

Calculation of vehicle performance limits is based on the fundamental relation

$$P_{max} = W_d \mu \quad (137)$$

This equation shows that the maximum tractive force that can be transmitted by the driving wheels is a function of both the effective dynamic axle weight W_d and the coefficient of road adhesion μ , as determined by existing road conditions (Part 1).

The type of drive—front, rear, or four-wheel—exerts a decisive influence on the magnitude of the transferable tractive force. Dynamic weight shift, for example, generally decreases front-axle weight,

*Now Research and Development Engineer, Phillips Petroleum Co., Bartlesville, Okla.

Limits of Vehicle Performance

- tractive force
- speed
- gradability
- acceleration
- drawbar pull

By JAROSLAV J. TABOREK*

Development Engineer
Towmotor Corp.
Cleveland

making the front-wheel drive system generally less effective than the rear-wheel system. The four-wheel drive, on the other hand, theoretically utilizes full vehicle weight.

In following calculations, it is assumed that the vehicle operates on a road without side elevation (no bank) and that the coefficients of road adhesion μ and rolling resistance f are identical for all vehicle wheels. With these assumed conditions, limits of performance can be calculated for all three drive types.

Tractive-Force Limits: The basic tractive-force relationship (Equation 137) can be employed to give vehicle tractive-force limits as outlined in the following section.

FRONT-WHEEL DRIVE: Designating maximum force and dynamic axle weight on the front wheels by $P_{f\max}$ and W_{df} , respectively,

$$P_{f\max} = W_{df} \mu \quad (138)$$

Substituting this expression into Equation 128.1 (Part 8),

$$W_{df} = \frac{L_r W}{L} + \frac{H}{L} (W_{df} \mu - fW) \quad (139)$$

After rearrangement, dynamic axle weight becomes

$$W_{df} = \frac{W(L_r + fH)}{L + \mu H} \quad (140)$$

Maximum transferable tractive force is then

$$P_{f\max} = \mu W \left[\frac{L_r + fH}{L + \mu H} \right] \quad (141)$$

To simplify its handling in subsequent calculations, the bracketed term in Equation 141 can be designated by the symbol w , which is interpreted as the weight-distribution factor W_d/W . This is the ratio of effective weight on the driving axle to total vehicle weight. For the front-wheel drive vehicle, Equation 140 shows that the weight-distribution factor has the form

$$w_f = \frac{W_{df}}{W} = \frac{L_r + fH}{L + \mu H} \quad (142)$$

Equations 140 and 141 can then be written

$$W_{df} = W w_f \quad (143)$$

and

$$P_{f\max} = \mu W w_f \quad (144)$$

REAR-WHEEL DRIVE: The basic equation for tractive force on the rear-wheel drive vehicle is

$$P_{r\max} = \mu W_{dr} \quad (145)$$

Substituting this expression into Equation 128.2 and rearranging terms,

$$W_{dr} = \frac{W(L_r - fH)}{L - \mu H} \quad (146)$$

In this case, the weight-distribution factor w_r is identified as

$$w_r = \frac{L_r - fH}{L - \mu H} \quad (147)$$

The maximum transferable traction force is then

Example 3—Performance Limit Calculation

A vehicle has a gross weight of 3000 lb with the following weight distribution: $L_f = (0.55)(L)$, $L_r = (0.45)(L)$. Height of the center of the center of gravity H is $(0.35)(L)$; coefficient of rolling resistance f is 0.02. Performance limits, that is, maximum traction, maximum speed as limited by available friction, maximum gradability and maximum acceleration, are calculated in this example.

Maximum Traction Force: With an assumed value of 0.8 for the road-adhesion coefficient μ , maximum transferable traction forces for the three vehicle drive types are calculated in following sections.

FRONT-WHEEL DRIVE: Equation 142 gives the weight-distribution factor w_f as

$$w_f = \frac{(0.45)(L) + (0.02)(0.35)(L)}{L + (0.8)(0.35)(L)} = 0.357$$

From Equation 141, the maximum transferable tractive force is then

$$P_{f\ max} = (0.08)(3000)(0.357) = 860 \text{ lb}$$

REAR-WHEEL DRIVE: Equation 147 gives the weight-distribution factor as

$$w_r = \frac{(0.55)(L) - (0.02)(0.35)(L)}{L - (0.8)(0.35)(L)} = 0.755$$

From Equation 148, the maximum tractive force is

$$P_{r\ max} = (0.8)(3000)(0.755) = 1830 \text{ lb}$$

FOUR-WHEEL DRIVE: Equation 149, which assumes that full vehicle weight is utilized in producing traction, gives the result

$$P_{4\ max} = (0.8)(3000) = 2400 \text{ lb}$$

This equation is used with the understanding that tractive forces (and engine torque) are distributed to front and rear wheels according to the requirements of Equation 153, or

$$\frac{P_{4f}}{P_{4r}} = \frac{(0.45)(L) - (0.35)(L)(0.8 - 0.02)}{(0.55)(L) + (0.35)(L)(0.8 - 0.02)} = \frac{17}{83}$$

Meaning of this result is that the front axle produces 17 per cent and the rear axle 83 per cent of the total tractive effort. For comparison, the distribution is recalculated for a slippery road where $\mu = 0.2$:

$$\frac{P_{4f}}{P_{4r}} = \frac{(0.45) - (0.35)(0.2 - 0.02)}{(0.55) + (0.35)(0.2 - 0.02)} = \frac{38}{62}$$

These results show that the front axle utilizes 38 per cent and the rear axle 62 per cent of effective engine torque when the road surface becomes slippery. It is apparent that changes in optimum torque distribution for a four-wheel vehicle are appreciable when road surface conditions change from dry to wet.

Speed Limits: With an assumed coefficient of air resistance $c_a = 0.5$ and projected frontal area $A = 25 \text{ sq ft}$, maximum vehicle speed as limited by available friction is calculated by use of Equation 158 in the following sections.

FRONT-WHEEL DRIVE:

$$V_{max} = 20 \sqrt{\frac{3000[(0.357)(0.8) - 0.02]}{(0.5)(25)}} = 159 \text{ mph}$$

REAR-WHEEL DRIVE:

$$V_{max} = 20 \sqrt{\frac{3000[(0.755)(0.8) - 0.02]}{(0.5)(25)}} = 240 \text{ mph}$$

FOUR-WHEEL DRIVE:

$$V_{max} = 20 \sqrt{\frac{3000[(0.8) - (0.02)]}{(0.5)(25)}} = 278 \text{ mph}$$

Gradability Limits: Maximum gradability for dry concrete ($\mu = 0.8$) and for a slippery surface ($\mu = 0.2$) is calculated from Equation 162.

FRONT-WHEEL DRIVE: Value of the weight-distribution factor, found in a preceding part of the example, is $w = 0.357$.

For the dry surface ($\mu = 0.8$),

$$G_{max} = 100[(0.0357)(0.8) - 0.02] = 27 \text{ per cent}$$

For slippery surface ($\mu = 0.2$),

$$G_{max} = 100[(0.357)(0.2) - 0.02] = 5 \text{ per cent}$$

REAR-WHEEL DRIVE:

(Dry surface)

$$G_{max} = 100[(0.755)(0.8) - 0.02] = 58 \text{ per cent}$$

(Slippery surface)

$$G_{max} = 100[(0.755)(0.2) - 0.02] = 13 \text{ per cent}$$

FOUR-WHEEL DRIVE:

(Dry surface)

$$G_{max} = 100[(0.8) - (0.02)] = 78 \text{ per cent}$$

(Slippery surface)

$$G_{max} = 100[(0.2) - (0.02)] = 18 \text{ per cent}$$

It is interesting to note that under slippery surface conditions the front-wheel drive vehicle is not able to negotiate grades above 5 per cent, a value well within the range of grades encountered on normal highways.

Acceleration Limits: For vehicle operation on a level road in direct drive, acceleration limits are calculated from Equation 165. Assume γ is 1.1.

FRONT-WHEEL DRIVE:

$$a_{max} = \frac{g}{1.1} [(0.357)(0.8) - (0.02)] = 0.26g = 8.3 \text{ ft per sec}^2$$

REAR-WHEEL DRIVE:

$$a_{max} = \frac{g}{1.1} [(0.755)(0.8) - (0.02)] = 0.55g = 17.4 \text{ ft per sec}^2$$

FOUR-WHEEL DRIVE:

$$a_{max} = \frac{g}{1.1} [(0.8) - (0.02)] = 0.73g = 23.3 \text{ ft per sec}^2$$

$$P_{r \max} = \frac{\mu W (L_f - fH)}{L - \mu H} = \mu W w_r \quad (148)$$

PERFORMANCE LIMITS

FOUR-WHEEL DRIVE: Substituting the expression

$$P_{4 \max} = \mu W \quad (149)$$

alternately into Equations 128.1 and 128.2, dynamic axle weights on front and rear axles are

$$W_{4f} = \frac{W}{L} [L_r - H(\mu - f)] \quad (150)$$

$$W_{4r} = \frac{W}{L} [L_f + H(\mu - f)] \quad (151)$$

For the four-wheel drive arrangement, full vehicle

Nomenclature

- A = Projected vehicle area in drive direction, sq ft
- a = Acceleration, ft per sec²
- c_a = Coefficient of air resistance
- D = Drawbar pull, lb
- E = Kinetic energy, ft-lb
- f = Coefficient of rolling resistance
- g = Acceleration of gravity, ft per sec²
- H = Height of cg from ground, in.
- H_a = Height of action point of air-resistance force, in.
- H_d = Height of hitch point, in.
- I = Polar moment of inertia, ft-lb-sec²
- L = Wheelbase, in.
- L_f, L_r = Distances of cg from front and rear axles, in.
- M_d = Torque on drive axle, lb-ft
- M_e = Engine torque, lb-ft
- m = Mass, lb-sec²-ft⁻¹
- P = Tractive force, lb
- P_f, P_r = Tractive forces of front and rear-wheel drives, lb
- P_{4f}, P_{4r} = Tractive forces on front and rear-wheel axles of a vehicle with four-wheel drive, lb
- R_a = Air resistance, lb
- R_g = Grade resistance, lb
- R_i = Inertia resistance, lb
- R_{it} = Inertia resistance of translatory mass, lb
- R_r = Rolling resistance, lb
- r = Rolling radius of tire, ft
- V = Speed, mph
- v = Speed, ft per sec
- W = Vehicle weight, lb
- W_d = Dynamic weight, lb
- W_{df}, W_{dr} = Dynamic weights on front and rear axles, lb
- W_d = Dynamic weight transfer in driving, lb
- w = Weight distribution factor
- w_f, w_r, w_4 = Weight distribution factors for front, rear and four-wheel drives
- α = Angular acceleration, rad per sec²
- ξ = Reduction ratio
- η = Transmission efficiency, per cent
- γ = Mass factor of rotating parts
- μ = Road-adhesion coefficient
- σ = Stability factor
- ω = Angular speed, rad per sec
- θ = Slope angle, deg

weight is theoretically utilized in producing tractive forces. The weight distribution factor is

$$w_4 = 1 \quad (152)$$

Such an ideal condition is realized, however, only when tractive forces (and engine torque) are distributed to the axles in the same proportion as are the dynamic weights on the respective axles. This condition can be expressed by the equation

$$\frac{P_{4f}}{P_{4r}} = \frac{W_{4f}}{W_{4r}} = \frac{L_r - H(\mu - f)}{L_f + H(\mu - f)} \quad (153)$$

It is evident that on a four-wheel drive vehicle, optimum distribution of tractive forces is a function of the road adhesion coefficient μ . This means, however, that for theoretically maximum vehicle performance, the distribution of tractive forces must be adjusted to suit varying road conditions. Design attempts in this direction have been made but, because of the complexity of the mechanism required, no really satisfactory solution has been obtained. For the purposes of this article, tractive force distribution for the four-wheel drive vehicle is computed in Example 3 for a medium value of μ equal to 0.4.

Speed Limits: On level ground and at constant vehicle speed, tractive force is resisted by rolling and air resistances only. For this condition of motion,

$$P_{\max} = W_d \mu = R_r + R_a \quad (154)$$

Substituting for the air-resistance term the following expression (Part 6),

$$R_a = 0.26 c_a A \left(\frac{V}{10} \right)^2 \quad (155)$$

and for the rolling-resistance term

$$R_r = W_f \quad (156)$$

Equation 154 can be written

$$W_d \mu = W_f + 0.0026 c_a A V_{\max}^2 \quad (157)$$

When this equation is divided by W , the weight distribution factor $w = W_d/W$ can be substituted. The maximum speed in mph, as limited by available friction, is then

$$V_{\max} = 20 \sqrt{\frac{W(w\mu - f)}{c_a A}} \quad (158)$$

where the corresponding values of w for front, rear, or four-wheel drive vehicles can be taken from Equation 142, 147, and 152.

The coefficient of rolling resistance f , which in an accurate calculation should be increased with speed, is considered constant in Example 3. The resulting error is negligible.

Gradability Limits: Because gradability limits are reached at low speeds, air resistance is con-

sidered negligible. At constant speed, therefore, tractive force balances only rolling and grade resistances, and

$$P_{max} = R_r + R_g \quad (159)$$

After substitution of Equation 137 and the rolling and grade-resistance Equations 53 and 61 (Part 5), the resulting expression is

$$P_{max} = W_d \mu = fW + W \tan \theta_{max} \quad (160)$$

where θ_{max} is the maximum gradability angle. Dividing this equation by W , and substituting again for W_d/W the weight distribution factor w ,

$$\tan \theta_{max} = w\mu - f \quad (161)$$

In place of the slope angle θ , the more practical value of G (per cent) (Equation 60, Part 5) can be substituted giving maximum gradability as

$$G_{max} = 100 (w\mu - f) \quad (162)$$

Again w is substituted for front, rear, and four-wheel drive arrangements.

Acceleration Limits: Since maximum acceleration is reached at relatively low speeds, air resistance is again negligible and the tractive force balances the inertia resistance R_i , the rolling resistance R_r and the grade resistance R_g . The equation of vehicle motion, Equation 136, is then

$$am\gamma = P - (R_r + R_g) \quad (163)$$

Substituting the established values for R_r and R_g (Equations 53 and 61) and using $P = P_{max} = \mu W_d$,

$$\frac{a_{max} W \gamma}{g} = \mu W_d - Wf - W \sin (\pm \theta) \quad (164)$$

Dividing by W and introducing the weight-distribution factor w ,

$$a_{max} = \frac{g}{\gamma} [w\mu - f - \sin (\pm \theta)] \quad (165)$$

Corresponding values of w for front, rear, and four-wheel drive vehicles can be substituted. For the correct value of sine θ , the approximate expression $G/100$ can be substituted.

Drawbar Pull Limits: If tractive force is used to produce drawbar pull D , equilibrium of forces (acceleration and air resistance neglected) is ex-

pressed as

$$W_d \mu = P_{max} = D_{max} + R_r + R_g \quad (166)$$

In this case, however, the simplified equations for dynamic axle weights W_d (Equations 128.1 and 128.2) cannot be applied since the height of the hinge point H_d is different from the cg height H . The correct equations for dynamic axle weights (Equations 125.1 and 125.2) with corresponding adjustments, $R_a = 0$, $R_{at} = 0$, are used for W_d , giving

$$W_{df} = \frac{1}{L} [L_r W - HW \sin (\pm \theta) - H_d D] \quad (167)$$

$$W_{dr} = \frac{1}{L} [L_f W + HW \sin (\pm \theta) + H_d D] \quad (168)$$

When these results are substituted into Equation 166, the following expressions are obtained for front, rear, and four-wheel drive vehicles:

FRONT-WHEEL DRIVE:

$$\frac{\mu}{L} [L_r W - HW \sin (\pm \theta) - H_d D_{max}] = D_{max} + fW + W \sin (\pm \theta) \quad (169)$$

and, for the maximum drawbar pull,

$$D_{max} = W \left[\frac{(\mu L_r - fL)}{L + \mu H_d} - \frac{(L + \mu H) \sin (\pm \theta)}{L + \mu H_d} \right] \quad (170)$$

REAR-WHEEL DRIVE:

$$\frac{\mu}{L} [L_f W + HW \sin (\pm \theta) + H_d D_{max}] = D_{max} + fW + W \sin (\pm \theta) \quad (171)$$

and

$$D_{max} = W \left[\frac{(\mu L_f - fL)}{L - \mu H_d} - \frac{(L - \mu H) \sin (\pm \theta)}{L - \mu H_d} \right] \quad (172)$$

FOUR-WHEEL DRIVE:

$$W\mu = D_{max} + fW + W \sin (\pm \theta) \quad (173)$$

and

$$D_{max} = W[\mu - f - \sin (\pm \theta)] \quad (174)$$

These equations include the horizontal grade term θ . For level ground, the sine term becomes zero and equations are correspondingly simplified.

In the next part of this series, the study of performance limits is continued and a roundup of equations used in such calculations is presented.

Mechanics of Vehicles—10

PERFORMANCE LIMITS

- performance vs. weight distribution
- performance vs. gross weight
- engine-torque limits
- drive-system comparison

By JAROSLAV J. TABOREK*

Development Engineer
Towmotor Corp.
Cleveland

MAXIMUM transferable tractive force was shown in Part 9 (Sept. 19, 1957) to set a fundamental limit to vehicle performance, regardless of whether the performance criterion of significance is acceleration, gradability, speed or drawbar pull. Determining factors for maximum tractive force were also shown to be: 1. Available road friction. 2. Effective or dynamic weight on the driving wheels.

This article continues the study of vehicle-performance limits, distinguishing between those performance qualities that are independent of vehicle gross weight and those that are weight dependent. For reference, a roundup of equations for calculating vehicle axle reactions and performance limits (developed in Parts 8 and 9) is given in Table 6.

Weight-Independent Limits: Maximum acceleration and gradability, two performance limits determined by maximum transferable tractive force, are independent of vehicle gross weight. For these qualities, weight distribution alone is the significant condition.

Physical interpretation of this fact is simple. Assume that two vehicles with identical weight distributions but with different gross weights are compared. Obviously, the higher transferable friction force available to the heavier vehicle (because of its greater driving-axle reaction) is exactly balanced by the greater force required to accelerate the vehicle or to push it uphill.

Quite apparently, no gain in tractive-force limited acceleration or gradability is realized when vehicle weight is increased. These performance limits can be improved only by changing vehicle weight distribution, that is, by loading the driving axle with a greater proportion of vehicle gross weight.

Weight-Dependent Limits: Contrary to the case for acceleration and gradability, maximum speed

and drawbar-pull are functions of vehicle gross weight. Explanation is that gain in available friction (due to a vehicle weight increase) overbalances the need for a higher tractive force in the heavier vehicle. Consequently, the heavier vehicle can attain a higher speed and can develop a greater drawbar pull.

Tractive-Force Chart: The functional relation-

Nomenclature

a	= Acceleration, ft per sec ²
c_a	= Coefficient of air resistance
D	= Drawbar pull, lb
f	= Coefficient of rolling resistance
g	= Acceleration of gravity, ft per sec ²
H	= Height of cg from ground, in.
H_d	= Height of hitch point, in.
L	= Wheelbase, in.
L_f, L_r	= Distances of cg from front and rear axles, in.
M_d	= Torque on drive axle, lb-ft
M_e	= Engine torque, lb-ft
m	= Mass, lb-sec ² -ft ⁻¹
P	= Tractive force, lb
P_f, P_r	= Tractive forces of front and rear-wheel drives, lb
P_{4f}, P_{4r}	= Tractive forces on front and rear-wheel axles of vehicle with four-wheel drive, lb
r	= Rolling radius of tire, ft
V	= Speed, mph
W	= Vehicle weight, lb
W_d	= Dynamic weight, lb
W_{df}, W_{dr}	= Dynamic weights on front and rear axles, lb
W_d	= Dynamic weight transfer in driving, lb
w	= Weight distribution factor
w_f, w_r, w_4	= Weight distribution factors for front, rear and four-wheel drives
ξ	= Reduction ratio
η	= Transmission efficiency, per cent
γ	= Mass factor of rotating parts
μ	= Road-adhesion coefficient

*Now Research and Development Engineer, Phillips Petroleum Co., Bartlesville, Okla.

Table 6 — Axle-Reaction and Performance-Limit Equations

	Front-wheel drive	Rear-wheel drive	Four-wheel drive
Static drive-axle weight, W_f, W_r (lb)	$W_f = W \frac{L_r}{L}$	$W_r = W \frac{L_f}{L}$	$W_f = W \frac{L_r}{L}$ $W_r = W \frac{L_f}{L}$
Dynamic axle-weight transfer, ΔW_d (lb)		$\Delta W_d = \frac{H}{L} (P - fW)$	
Dynamic axle reaction due to tractive force, W_d (lb)	$W_{df} = W_f - \Delta W_d$	$W_{dr} = W_r + \Delta W_d$	$W_{df} = W - \Delta W_d$ $W_{dr} = W + \Delta W_d$
Maximum dynamic axle weight, W_d (lb)	$W_{df} = W \frac{L_r + fH}{L + \mu H}$	$W_{dr} = W \frac{L_f - fH}{L - \mu H}$	$\frac{W_{4f}}{W_{4r}} = \frac{L_r - H(\mu - f)}{L_f + H(\mu - f)}$
Weight-distribution factor, $w = \frac{W_d}{W}$	$w_f = \frac{L_r + fH}{L + \mu H}$	$w_r = \frac{L_f - fH}{L - \mu H}$	$w_4 = 1$
Maximum tractive force transferable, P_{max} (lb)	$P_{fmax} = w_f \mu W$	$P_{rmax} = w_r \mu W$	$\frac{P_{4f}}{P_{4r}} = \frac{W_{4f}}{W_{4r}}$
Maximum speed*, W_{max} (mph)	$20 \sqrt{\frac{W}{C_a A} (w_f \mu - f)}$	$20 \sqrt{\frac{W}{C_a A} (w_r \mu - f)}$	$20 \sqrt{\frac{W}{C_a A} (\mu - f)}$
Maximum gradability, G_{max} (percent)	$100 (w_f \mu - f)$	$100 (w_r \mu - f)$	$100 (\mu - f)$
Maximum acceleration*, a_{max} (ft per sec ²)	$\frac{g}{\gamma} (w_f \mu - f)$	$\frac{g}{\gamma} (w_r \mu - f)$	$\frac{g}{\gamma} (\mu - f)$
Maximum drawbar pull*, D_{max} (lb)	$W \frac{\mu L_f - fL}{L + \mu H_d}$	$W \frac{\mu L_r - fL}{L - \mu H_d}$	$W (\mu - f)$

* On level ground

ship between tractive force, road-adhesion coefficient and weight distribution can be plotted in the form shown in Fig. 59. Containing only dimensionless factors, the chart has general validity for all vehicles. Mathematical basis for the chart construction is as follows:

1. Influence of rolling resistance on dynamic axle weight is neglected. This assumption is permissible for concrete or a similar surface where $f = 0.02$ is a common value. The error introduced by omitting f from the weight-distribution equations is about 1 per cent.

2. To make the chart construction independent of the absolute geometrical dimensions of the vehicle, equations for the weight-distribution factor w (Table 6) were rearranged as follows:

FRONT-AXLE DRIVE,

$$w_f = \frac{\frac{L_r}{L}}{1 + \frac{\mu H}{L}} \quad (175)$$

REAR AXLE DRIVE,

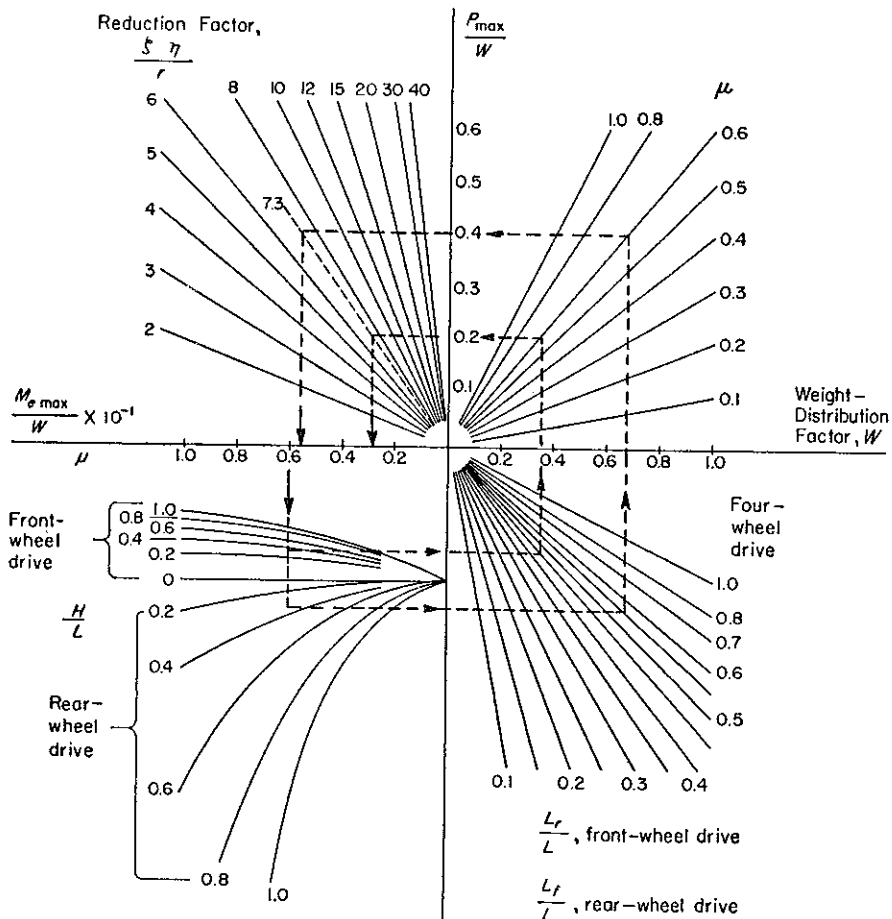


Fig. 59—Graphical relationship between the road-adhesion coefficient μ , the vehicle weight distribution, given by the factors H/L , L_r/L , L_f/L , and the specific values of maximum transferable traction P_{max}/W and corresponding engine torque M_{max}/W . Only dimensionless quantities are plotted, and the chart is therefore applicable to all vehicles.

$$w_r = \frac{\frac{L_f}{L}}{1 - \frac{\mu H}{L}} \quad (176)$$

Values appearing in Equations 175 and 176 are dimensionless ratios L_r/L , L_f/L , and H/L .

3. Weight of the vehicle is eliminated by dividing the tractive-force equation (Table 6) by W , giving

$$\frac{P_{max}}{W} = w\mu \quad (177)$$

The dimensionless quantity P_{max}/W represents the tractive force per unit of vehicle weight (lb per lb).

4. The effective tractive force on the driving wheels is a product of various combinations of the following elements: engine torque M_e , transmission reduction ratio ζ , efficiency of the reduction mechanism η and rolling radius of the tires r . Consequently, a value of maximum engine torque per unit vehicle weight can be found, where

Example: A vehicle has eg position $H/L = 0.35$, $L_f/L = 0.55$, and $L_r/L = 0.45$. Maximum transferable traction on dry concrete ($\mu = 0.60$) for both front and rear-wheel drives is required. Maximum engine torque for a low-gear reduction factor $\zeta\eta/r = 7.3$ (ft^{-1}) is also desired.

Solution: In the lower left quadrant, the $\mu = 0.60$ ordinate is projected to intersect the H/L curves at a value of 0.35. From the intersection, the heavy example lines are followed, giving $P_{fmax} = (0.21)(W)$ and $P_{rmax} = (0.405)(W)$ as the values for maximum transferable traction.

When the example lines are then followed to the left-hand abscissa axis, maximum engine torques are: $M_{emax} = (0.056)(W)$ for the front-wheel drive, and $M_{emax} = (0.028)(W)$ for the rear-wheel drive.

Assuming vehicle weight is 4000 lb: $P_{max} = 1620$ lb and $M_{emax} = 224$ lb-ft for the rear wheel drive; and $P_{max} = 840$ lb and $M_{emax} = 112$ lb-ft for the front-wheel drive.

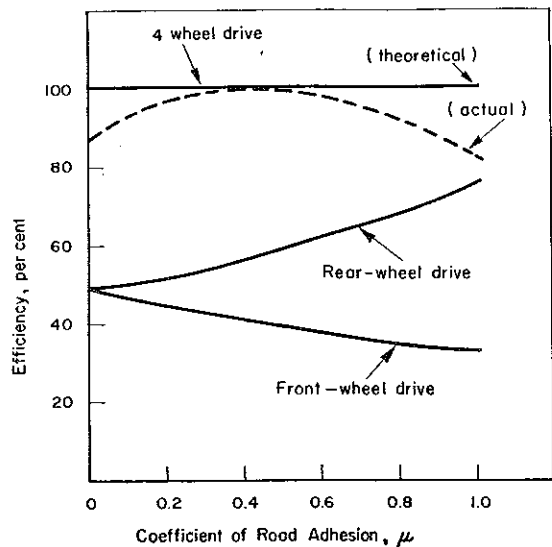


Fig. 60—Efficiency of front, rear and four-wheel drive systems as functions of the road-adhesion coefficient. Diagram represents the weight-distribution factor w in per cent ($w \times 100$) for a car with identical weights on front and rear axles. Front and rear-wheel drives have the same efficiency at low friction values. With increasing friction, the rear-wheel drive arrangement becomes more efficient and front-wheel drive efficiency decreases. Effectiveness of the four-wheel drive is maintained at the theoretical 100 per cent value throughout the range of frictional adhesion only if torque distribution to the axles is adjustable for varying μ values. Actual performance reaches the theoretical maximum only at that frictional value for which the drive is calculated.

$$\frac{M_{emax}}{W} = \frac{\frac{P_{max}}{W}}{\frac{\xi\eta}{r}} \quad (178)$$

These equations are graphically represented in Fig. 59. The chart makes it possible to find with ease and acceptable accuracy the values of P_{max} and M_{emax} for any vehicle weight and for all possible combinations of wheelbase, cg position and road-adhesion coefficient. The technique of using the diagram is illustrated by the example shown with the figure.

Practical Engine-Torque Limits: An interesting example of performance-limits calculation is presented by the often repeated question: what are the limits of the trend toward more powerful engines on passenger cars?

As a basis for analysis, a representative weight distribution (loaded car) of $L_f = 0.55L$, cg height $H = 0.35L$ and road-adhesion coefficient $\mu = 0.6$ are assumed. For these values and for the usual rear-wheel drive, Fig. 59 gives $P_{max} = 0.4W$. Maximum possible acceleration, one of the main criteria for judging performance of a passenger car, is unalterably given by the cg position. Value of a_{max} is calculated directly from the P_{max} value by use of the relation

$$a_{max} = \frac{Pg}{W\gamma} \quad (179)$$

In this example, the rotating-parts inertia factor in direct gear is assumed to be $\gamma = 1.1$. Therefore,

$$a_{max} = \frac{(0.4)(g)}{1.1} = 0.36g = 11.5 \text{ ft per sec}^2 \quad (180)$$

Assume further that the tractive force is produced through a total reduction ratio of 9.5:1 in low gear (common usage on passenger cars), an overall transmission efficiency of 85 per cent and a rolling radius of the tires of $r = 1.1$ ft. Then

$$\frac{\xi\eta}{r} = \frac{(9.5)(0.85)}{1.1} = 7.3 \quad (181)$$

For this value, the diagram gives $M_e/W = 0.056$ and, for an assumed vehicle gross weight of 4000 lb, the maximum engine torque that can be transferred by use of the 9.5:1 reduction ratio is

$$M_{emax} = (4000)(0.056) = 224 \text{ lb-ft} \quad (182)$$

Passenger-car engine torques in the 200 lb-ft range are now becoming common. Apparently, then, the drive-wheel frictional limits in low gear have been nearly reached. Higher engine torques can be used effectively only in combination with lower gear reductions, with probably no improvement in actual performance. Should the demand for higher accelerations continue, passenger-car weight distribution will have to be changed by shifting the cg toward the driving axle.

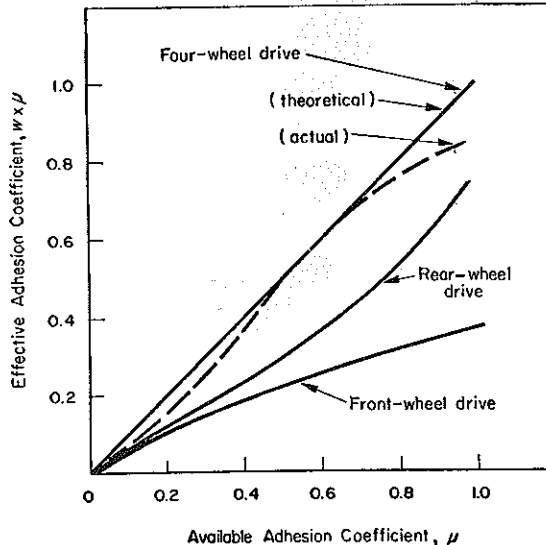


Fig. 61—Comparison of the utilization of available road friction by different drive systems. Diagram represents effective μ values ($w \times \mu$) as functions of available μ values. The four-wheel drive reaches the theoretical 100 per cent utilization only for the value of μ for which torque distribution to the axles corresponds to the theoretically required condition. Difference in friction utilization between front and rear-wheel drives increases with higher friction values.

Drive-System Comparison: Theoretical performance limits are not always reached because, with high values of road friction, engine power is often the determining factor. Obviously, in such cases, dynamic weight distribution is of no importance where the tractive performance of the vehicle is concerned. On the other hand, where high tractive-force values are a necessity, or where the vehicle must operate under poor frictional conditions, weight distribution does become a critical factor, and the performance differences between front, rear and four-wheel drive systems become apparent.

A fair measure for comparing effectiveness of the three drive-systems is the degree to which they utilize the available friction. Such a comparison is given by the ratios

$$\begin{aligned} P_4 : P_r &= \mu : \mu \frac{\frac{L_f}{L}}{1 - \frac{\mu H}{L}} \\ P_r : P_f &= \mu \frac{\frac{L_f}{L}}{1 - \frac{\mu H}{L}} : \mu \frac{\frac{L_r}{L}}{1 + \frac{\mu H}{L}} \end{aligned} \quad (183)$$

Or, in combined form

$$P_4 : P_r : P_f = \mu : \mu \frac{\frac{L_f}{L}}{1 - \frac{\mu H}{L}} : \mu \frac{\frac{L_r}{L}}{1 + \frac{\mu H}{L}} \quad (184)$$

The right side of this expression represents ratios of the effective friction coefficients utilized by the three drive systems. These values are plotted against the available road-adhesion coefficient μ in Fig. 60 for an assumed vehicle static weight distribution corresponding to $L_r = L_f = 0.5L$, and $H = 0.35L$.

At any point, the four-wheel drive offers the theoretical maximum of effectiveness, that is 100 per cent. Efficiencies of front and rear-wheel drive systems, calculated as function of the available road-adhesion coefficient, are also shown in Fig.

60. With increasing friction values, efficiency of the rear-wheel drive also increases. In contrast, front-wheel drive efficiency declines. For the usual road-adhesion coefficient of $\mu = 0.6$, ratios of maximum transferable tractive forces for the three drives are

$$P_4 : P_r : P_f = 100 : 61 : 39$$

The same proportion applies for maximum engine torques usable by each particular drive type.

The potential usability of the different drive systems can be deduced from the foregoing comparison. Front-wheel drives can support only light engines and will therefore find use only on lightweight cars. In such applications, the superior curve behavior, increased interior roominess and compact power plant construction provided by the front-wheel system are important advantages.

The rear-wheel drive accounts for a majority of present-day designs and, most probably, will maintain its leading position. However, the trend toward the use of heavier and more powerful passenger-car engines has resulted in a steady weight shift to the front axle. Aside from other disadvantages offered by heavier engines, the trend directly opposes the urgent need for more frictional weight on the driving rear axle, a requirement that permits the axle to transfer high torques made available by more powerful engines. An improvement in this situation can be achieved by locating the engine in the rear of the car. Used in several highly successful designs, rear-engine location is likely to find increasing use in the future.

Advantages of the four-wheel drive are more pronounced when friction values are low. The higher manufacturing cost of a four-wheel drive vehicle is therefore justified, only if maximum possible traction is the objective, or if the vehicle is designed to operate under poor frictional conditions. Off-the-road or military vehicles offer examples of such applications. Should the trend toward more powerful engines continue, the four-wheel drive may also provide a practicable design solution.

Dynamics of Braking

By JAROSLAV J. TABOREK*

Development Engineer
Towmotor Corp.
Cleveland

REAR BRKS ONLY ON TRACTOR, CHANGE DUE TO h_{eq} X-FER

$$M_{eff} = \frac{M_{act} \frac{a}{a+b}}{1 + \frac{M_{act} b}{a+b}}$$

BRAKING capacity, which determines the ability of a vehicle to slow down or stop, ranks as a major factor in the study of vehicle performance. This article—the first of two surveying the mechanics of decelerated motion—re-examines the principal motion-resisting and motion-aiding forces and evaluates their relationship to the braking problem.

Braking Forces: All possible forces that act on a decelerating vehicle on a downhill grade are shown in Fig. 62. As the primary motion-resisting force, braking force B originates in the frictional engagement between brake shoes and drums. The basic relationship is

$$B = \frac{F_b \mu_b r_b}{r} \quad (185)$$

where F_b is the effective force on the shoe, μ_b is the coefficient of friction between shoe and drum, r_b is the drum radius, and r is the rolling radius of the tire. In calculations that follow, B is considered to be the sum of front and rear-axle braking forces, or $B = B_f + B_r$.

Ultimately, braking force B acts at the frictional connection between the tire and the ground. Governed by the same physical relationships that set

vehicle tractive-force limits, maximum braking force B_{max} is given by the expression

$$B_{max} = W_b (\mu + f) \quad (186)$$

For the rolling wheel, therefore, maximum transferable braking force is a function of the static road-adhesion coefficient μ , the rolling-resistance coefficient f , and the effective or dynamic axle weight W_b . Should the wheel lock during braking, skidding occurs, and B_{max} is then determined by the coefficient of sliding resistance μ_s . With locked wheels, maximum transferable braking force is

$$B_{max} = W_b \mu_s \quad (187)$$

Complete analysis of the braking vehicle requires study of all forces and moments that are dependent on its state of motion. As shown in sections that follow, some of these factors are significant, others can be safely ignored.

DYNAMIC WEIGHT TRANSFER: The action of vehicle braking forces causes a dynamic weight transfer which increases the weight on the front axle and decreases it by the same amount on the rear axle. The effective axle weight, called the dynamic braking weight W_b , has a basic influence on the limits of braking performance and on the optimum distribution of braking forces to front and rear axles.

*Now Research and Development Engineer, Phillips Petroleum Co., Bartlesville, Okla.



- decelerating forces
- engine-braking effects
- stopping time and distance

GRADE EFFECT: For a vehicle braking on a grade, the significant vehicle weight is the normal-to-ground or cosine component. In braking calculations, the influence of the cosine factor is negligible, and the simplification $\cos \theta = 1$ is justified.

The sine component of vehicle weight (grade resistance R_g) is motion-supporting if the vehicle is moving downhill. In subsequent braking calculations, positive value for θ will be arbitrarily assumed as indicating a downhill slope.

ROLLING RESISTANCE: Always motion-opposing, total rolling resistance is independent of weight distribution on the axles. The basic relationship is

$$R_{rr} + R_{rf} = R_r = fW \cos \theta \approx Wf \quad (188)$$

AIR RESISTANCE: Influence of air resistance R_a as a decelerating force is small at normal vehicle speeds, especially for streamlined vehicles. In braking calculations, therefore, the decelerative effect of air resistance is often neglected. In a sense, this simplification provides an additional safety factor in the calculations, since air resistance aids braking action when it is needed most, that is, at high vehicle speeds.

For very fast vehicles, special devices known as air-resistance brakes are sometimes used. The air brakes expand the projected area of the vehicle

and simultaneously increase the air-resistance coefficient c_a .

INERTIA: The inertia force due to vehicle deceleration is given by an expression that first appeared in acceleration computations (Part 6):

$$R_i = bm \gamma_b \quad (189)$$

In Equation 189, γ_b expresses the inertia effect of vehicle rotating parts. Its value is often different from that used in acceleration calculations because, in braking, the engine may be declutched, leaving only wheels and transmission parts to be decelerated. In such cases, γ_b for conventional automotive vehicles can be taken as about 1.04, that is, the translatory mass of the vehicle is increased 4 per cent to incorporate the rotating-mass effect of wheels and other permanently engaged rotating parts.

TRANSMISSION RESISTANCE: Transmission resistance torque M_t is the torque necessary to overcome friction of gears, bearings and joints plus torque due to churning of oil in the transmission. In the calculation of accelerated motion, these factors were taken care of by transmission-efficiency factor η , which expresses the loss of power between engine and drive axle. In braking, how-

ever, with the engine clutch disengaged, torque necessary to overcome transmission resistance is derived from the kinetic energy of the vehicle.

Compared to actual braking forces, magnitude of transmission resistance is small and can be neglected in braking performance calculations. However, where accurate results are required, transmission resistance may exert a significant effect.

ENGINE BRAKING POWER: Under certain circumstances, drag of a throttled engine is an important factor in the braking of vehicles. An engine running with closed throttle has a certain idling speed. To make the engine run faster with the throttle remaining closed, power must be supplied from an external source, for example, through consumption of part of the vehicle kinetic energy. In such cases, the engine acts as a brake. Engine braking power is proportional to engine speed and therefore to the reduction ratio used. For this reason, heavy vehicles on long downhill grades depend directly on the drag of the engine to aid braking, thereby reducing heat generated in the brake drums.

Torque M_{db} on the drive axle, derived from the engine braking effect, is given by

$$M_{db} = \frac{M_e \xi}{\eta} \quad (190)$$

Torque M_e required to drive the engine is measured experimentally at the engine output shaft, ξ is the total reduction ratio between engine and the drive axle, and η is the efficiency of the transmission. Since the efficiency term η appears in the denominator, lower efficiency means higher torque and therefore greater braking effect at the drive axle. A plot of braking torque M_{db} as a function of vehicle speed is represented for different gear reduction ratios in Fig. 63.

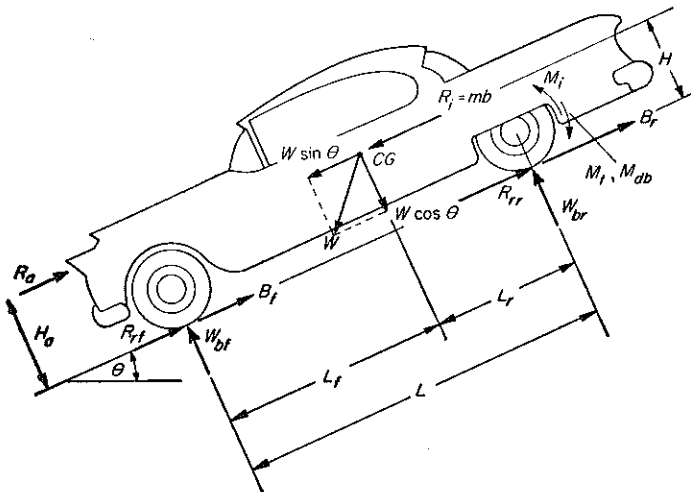


Fig. 62—Forces acting on a vehicle in decelerated motion downhill.

On heavy trucks it is sometimes necessary to increase the engine-braking effect by using the engine as compressor. This can be achieved by controlling valve timing, or by using restrictor valves in the exhaust system to increase the effective pressure in the cylinders.

Torque-Converter Transmissions: Braking potential of an engine can be utilized only in transmission trains that utilize a positive connection between engine and drive axle. Hydraulic transmissions and torque converters usually transfer power only from engine to drive axle, not from drive axle to engine. In such case, only the transmission resistance serves as a decelerating torque.

To permit use of hydraulic transmissions in heavy road vehicles, braking power of the engine can be replaced by other adjustable power-consuming devices, for example, by using flow restrictors in internal torque-converter circuits.

Optimum Engine Braking Performance: The foregoing discussion of braking by a driven engine applies strictly for low values of deceleration—for example, where a vehicle is being continuously braked downhill. To achieve high decelerations,

Nomenclature

B_f, B_r	= Braking forces, represented as frictional forces at the tire-ground contact point, lb
b	= Deceleration, ft per sec ²
c_a	= Coefficient of air resistance
F_b	= Effective force on brake shoe, lb
f	= Coefficient of rolling resistance
g	= Acceleration of gravity, ft per sec ²
M_{db}	= Resistance moment of driven engine, lb-ft
M_i	= Inertia moment of rotating parts, lb-ft
M_t	= Resistance moment of transmission, lb-ft
m	= Mass, lb-sec ² -ft ⁻¹
R_a	= Air resistance, lb
R_i	= Inertia resistance of the translatory mass, lb
R_{rf}, R_{rr}	= Rolling resistances, lb
r	= Rolling radius of tire, ft
s	= Braking distance, ft
t	= Time, sec
V	= Speed, mph
V_i, V_f	= Initial and final speeds, mph
V_m	= Mean vehicle speed, mph
v	= Speed, fps
v_i, v_f	= Initial and final speeds, fps
W	= Vehicle weight, lb
W_b	= Dynamic weight, lb
W_{bf}, W_{br}	= Dynamic axle weights on front and rear axles, lb
W_{dr}	= Weight of brake drum, lb
W_f, W_r	= Static axle weights on front and rear axles, lb
W_{4f}, W_{4r}	= Dynamic axle weights in four-wheel brake system, lb
W_b	= Dynamic weight transfer in braking, lb
γ_b	= Inertia mass factor of rotating parts in braking
ω	= Angular speed, rad per sec
μ	= Coefficient of road adhesion
η	= Efficiency factor

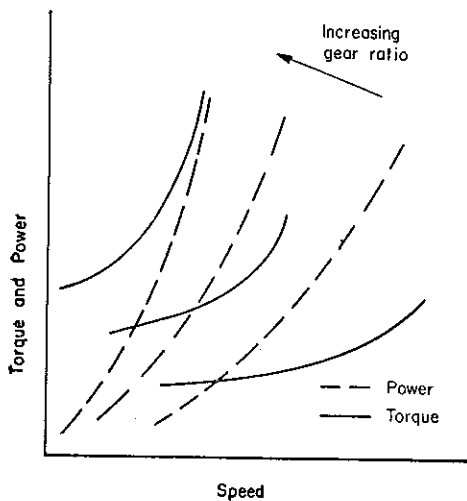


Fig. 63—Braking potential of a throttled engine. Three sets of torque and power-consumption curves show the effect of gear ratio on engine braking capacity. Quite obviously, "shifting down" helps retard the vehicle on downhill runs

brakes are applied very suddenly. In this case, the engine not only produces no braking effect but, to the contrary, consumes part of the mechanical braking effort to absorb kinetic energy of rotating engine parts.

Depending on the inertia of the engine as represented by factor γ , and consequently on reduction ratio ζ , a critical value of deceleration can be calculated above which the engine should be always disengaged for optimum braking effect.⁴³ For passenger cars the critical value is about 5 ft per sec.² As a general rule, therefore, it appears that the engine should be disengaged during most brake applications.

Dynamic Axle Weights During Braking: Forces acting on a vehicle during braking cause a weight shift toward the front axle. Knowledge of resulting dynamic axle weights is necessary for determination of maximum transferable frictional forces.

Dynamic axle reactions are best determined by writing moment-equilibrium equations around tire-ground contact points, thereby eliminating from the calculation all forces that act in the ground plane. Ground-plane forces are the braking force B , rolling resistance R_r , braking forces originating in engine and transmission, and the inertia torque M_i of rotating parts.

For a vehicle decelerating on a downgrade slope, Fig. 62, the equilibrium equations give the results:

$$W_{bf} = \frac{1}{L} (L_f W + HW \sin \theta + mbH - R_a H_a) \quad (191)$$

$$W_{br} = \frac{1}{L} (L_f W - HW \sin \theta - mbH + R_a H_a) \quad (192)$$

To transform these equations into a more workable form, use is made of the following assumptions: 1. The action point of the air resistance is considered to fall at the cg of the vehicle, or $H = H_a$. 2. The simplified equilibrium-of-force expression is sufficiently accurate, where

$$mb - R_a + W \sin \theta = B + fW \quad (193)$$

Dynamic axle weights during braking then become

$$W_{bf} = \frac{L_f W}{L} + \frac{H(B + fW)}{L} \quad (194)$$

$$W_{br} = \frac{L_f W}{L} - \frac{H(B + fW)}{L} \quad (195)$$

Designating dynamic weight transfer during braking as ΔW_b ,

$$\Delta W_b = \frac{H(B + fW)}{L} \quad (196)$$

Dynamic axle weights can then be written as

$$W_{bf} = W_f + \Delta W_b \quad (197)$$

$$W_{br} = W_r - \Delta W_b \quad (198)$$

where W_f and W_r are static level axle weights.

Equations of Decelerated Motion: Equations of decelerated motion for a vehicle are derived in a manner similar to that used for accelerated motion. According to the energy theorem, change in kinetic energy of a moving body equals work produced by external forces. Applying this principle to a vehicle in decelerated motion, change of kinetic energy in differential distance ds is

$$dE = (B + \sum R) ds \quad (199)$$

where the effective retarding force is obtained through summation of the actual braking force B and all external resistance forces acting on the vehicle at that instant. Kinetic energy of translatory and rotating parts is given by

$$E = \frac{mv^2}{2} + \sum \frac{I\omega^2}{2}$$

Differentiated, the expression becomes

$$dE = mv dv + \sum I\omega d\omega \quad (200)$$

By use of the technique developed in Part 6 of this series, the effect of rotating parts is represented by an equivalent translatory mass. Equation 200 then becomes

$$dE = vdv \left(m + \frac{1}{r^2} \sum I_r^2 \right) = vm \gamma_b dv \quad (201)$$

where γ_b is the factor expressing the inertia effect of wheels and other rotating parts.

When Equation 201 is substituted in Equation 199 and with $b = dv/dt$, the general equation

*References are tabulated at end of article.

of decelerated motion becomes

$$B = bm \gamma_b - \sum R \quad (202)$$

From the foregoing equation, the state of motion of a vehicle and the forces involved in the braking process can be readily calculated.

Stopping Distance: For calculation of stopping distances, Equations 199 and 201 are equated, or

$$ds \left(B + \sum R \right) = vm \gamma_b dv \quad (203)$$

In integral form, Equation 203 becomes

$$s = \gamma_b m \int_{v_i}^{v_f} \frac{v dv}{B + \Sigma R} \quad (204)$$

Here, v_i is initial speed, and v_f is final speed. In the integration of Equation 204, either of two assumptions can be made: 1. Air resistance is negligible. 2. Air resistance is significant. The following sections show the effects of these assumptions.

AIR RESISTANCE NEGLECTED: When air resistance is neglected, deceleration is constant during braking, and the solution of Equation 204 is

$$s = \frac{\gamma_b m}{B + \Sigma R} \left[\frac{v_i^2 - v_f^2}{2} \right] \quad (205)$$

Therefore, minimum full-stop braking distance with four-wheel brakes ($B_{max} = W\mu$) is

$$\begin{aligned} s_{min} &= \frac{v_i^2 \gamma_b}{2g(\mu + f)} = \frac{V_i^2 \gamma_b}{64(\mu + f)} \left[\frac{5280}{3600} \right]^2 \\ &= \frac{\gamma_b V_i^2}{30(\mu + f)} \end{aligned} \quad (206)$$

where dimensions of s are in ft, v in ft per sec, and V in mph.

It is seen, therefore, that if air resistance is neglected, stopping distance is independent of vehicle weight.

AIR RESISTANCE CONSIDERED: Since air resistance is a function of speed, vehicle deceleration changes continuously during the braking process. Before substitution in Equation 203, the familiar air-resistance equation can be rearranged to read

$$R_a = 0.0012 c_a A v^2 = C v^2$$

where v is instantaneous speed in ft per sec. Solving for C ,

$$C = \frac{c_a A}{840} \quad (207)$$

On level ground only air and rolling resistances act on the vehicle, and the stopping-distance equation becomes

Example 4—Braking Distance and Time

Problem: Determine minimum stopping distance on dry concrete ($\mu = 0.6$, $f = 0.02$) from initial speed $V_i = 100$ mph. The vehicle weighs 4000 lb, has projected frontal area $A = 25$ sq ft and air resistance coefficient $c_a = 0.5$. The engine is disengaged during deceleration, and the inertia factor for wheels and transmission parts is $\gamma_b = 1.05$.

NEGLECTING AIR RESISTANCE: From Equation 206, minimum stopping distance with air resistance neglected is

$$s_{min} = \frac{1.05(100^2)}{30(0.6 + 0.02)} = 570 \text{ ft}$$

INCLUDING AIR RESISTANCE: From Equation 211, minimum stopping distance including the effect of air resistance is

$$\begin{aligned} s_{min} &= \frac{13.1(1.05)(4000)}{0.5(25)} \log_e \left[1 + \right. \\ &\quad \left. \frac{0.5(25)(100^2)}{390(4000)(0.6 + 0.02)} \right] \\ &= 4400 \log_e 1.129 = 532 \text{ ft} \end{aligned}$$

Stopping distances with and without the air-resistance effect are of approximately the same magnitude, differing by about 7 per cent. This difference, of course, is greater at higher initial speeds.

Coasting: For a free-rolling vehicle acted on

only by rolling and air resistance, $B = 0$ and Equation 210 gives the coasting-distance as

$$s = \frac{13.1 \gamma_b W}{c_a A} \log_e \left[1 + \frac{c_a A V_i^2}{390(Wf)} \right]$$

Substituting numerical values,

$$\begin{aligned} s &= \frac{13.1(1.05)(4000)}{0.5(25)} \log_e \left[1 + \right. \\ &\quad \left. \frac{0.5(25)(100^2)}{390(4000)(0.02)} \right] \\ &= 4400 \log_e 6.0 = 7100 \text{ ft} \end{aligned}$$

Stopping time for the free-rolling vehicle ($B = 0$) is given by Equation 215 as

$$t = \frac{0.9 \gamma_b \sqrt{W}}{\sqrt{f c_a A}} \tan^{-1} \frac{V_i}{19.7} \sqrt{\frac{c_a A}{Wf}}$$

Substituting numerical values,

$$\begin{aligned} t &= \frac{0.9(1.05)\sqrt{4000}}{\sqrt{0.02(12.5)}} \tan^{-1} \frac{100}{19.7} \sqrt{\frac{12.5}{4000(0.02)}} \\ &= 120 \tan^{-1} 5.1 \sqrt{0.156} = 133 \text{ sec} \end{aligned}$$

Average deceleration b is therefore

$$b = \frac{1.47(100)}{133} = 1.11 \text{ ft per sec}^2$$

$$s = \gamma_b m \int_{v_f}^{v_i} \frac{v \, dv}{B + R_r + Cv^2} \quad (208)$$

Letting $z = v^2/2$ and $dz = v \, dv$, integration gives

$$s = \frac{\gamma_b m}{2C} \log_e \left[\frac{B + R_r + Cv_i^2}{B + R_r + Cv_f^2} \right] \quad (209)$$

Braking to a full stop ($v_f = 0$) from initial speed V (mph),

$$s = \frac{\gamma_b m}{2G} \log_e \left[1 + \frac{C V_i^2}{B + R_r} \left(\frac{5280}{3600} \right)^2 \right] \quad (210)$$

With the substitution of C from Equation 207 and $B_{max} = W\mu$ for maximum braking force, the minimum-stopping distance expression becomes

$$s_{min} = \frac{13.1 W \gamma_b}{c_a A} \log_e \left[1 + \frac{c_a A V_i^2}{390 W(\mu + f)} \right] \quad (211)$$

Stopping distance where air resistance serves as a braking aid is therefore a function of vehicle weight. This is because the same air-resistance force acts on vehicles of the same aerodynamic form regardless of weight. Therefore the effect of air resistance on a lighter vehicle is more pronounced.

Stopping Time: Time required to reduce speed of a vehicle from v_i to v_f is calculated from Equation 203. With the substitution $v = ds/dt$, Equation 203 can be rearranged to give

$$t = \gamma_b m \int_{v_f}^{v_i} \frac{dv}{B + R_r + Cv^2} \quad (212)$$

After integration,

$$t = \frac{\gamma_b m}{\sqrt{C(B + R_r)}} \tan^{-1} \sqrt{\frac{C}{B + R_r}} (v_i - v_f) \quad (213)$$

After substitution of C from Equation 207, braking time to a full stop ($v_f = 0$) is given as

$$t = \frac{\gamma_b W}{g} \sqrt{\frac{840}{(B + R_r)c_a A}} \times \tan^{-1} 1.47 V_i \sqrt{\frac{c_a A}{840(B + R_r)}} \quad (214)$$

Minimum stopping time ($B_{max} = W\mu$) is

$$t_{min} = 0.9 \gamma_b \sqrt{\frac{W}{(\mu + f)c_a A}} \tan^{-1} \frac{V_i}{19.7} \sqrt{\frac{c_a A}{W(\mu + f)}} \quad (215)$$

When air resistance is neglected, the kinematic equation for decelerated motion applies, and

$$t = \frac{v_i}{b} = \frac{1.47 V_i}{b} \quad (216)$$

Representative calculations for stopping distance and time are given in Example 4.

In the next part of this series, braking-performance limits as established by maximum transferable friction and by thermal considerations are examined.

REFERENCES

43. A Jante—"Muss man beim Bremsen auskuppeln" (When to Disengage the Engine in Braking), Automobiltechnische Zeitschrift (ATZ), 1942.

Mechanics of Vehicles—12

By JAROSLAV J. TABOREK*

Towmotor Corp.
Cleveland

AVAILABLE friction at the tire-ground contact point sets a basic limitation to the stopping capacity of a vehicle braking system. Assuming that such frictional contact is adequate, a further braking limit is set by the ability of brake-system mechanical components to absorb or dissipate heat generated during vehicle deceleration. Continuing the study of the braking vehicle, this article examines fundamental limits to brake performance and presents design criteria that lead to optimum system performance.

Braking-Force Limits: Maximum transferable braking force, since it is dependent upon frictional ground reaction, is a function of dynamic axle weight and the available coefficient of road ad-

hesion. The mathematical relationship is

$$B_{max} = W_b \mu \quad (217)$$

where W_b is the dynamic weight on the braking axle. When this equation is substituted into equations for dynamic axle weights (Equations 194 and 195, Part 11), braking-force limits for front, rear, and four-wheel systems can be derived as follows:

FRONT-WHEEL BRAKES:

$$B_{fmax} = W_{bf} \mu \quad (218)$$

$$W_{bf} = \frac{L_r W}{L} + \frac{H}{L} (W_{bf} \mu + fW) \quad (219)$$

$$W_{bf} = \frac{W(L_r + fH)}{L - \mu H} \quad (220)$$

$$B_{fmax} = \frac{\mu W(L_r + fH)}{L - \mu H} \quad (221)$$

*Now Research and Development Engineer, Phillips Petroleum Co., Bartlesville, Okla.

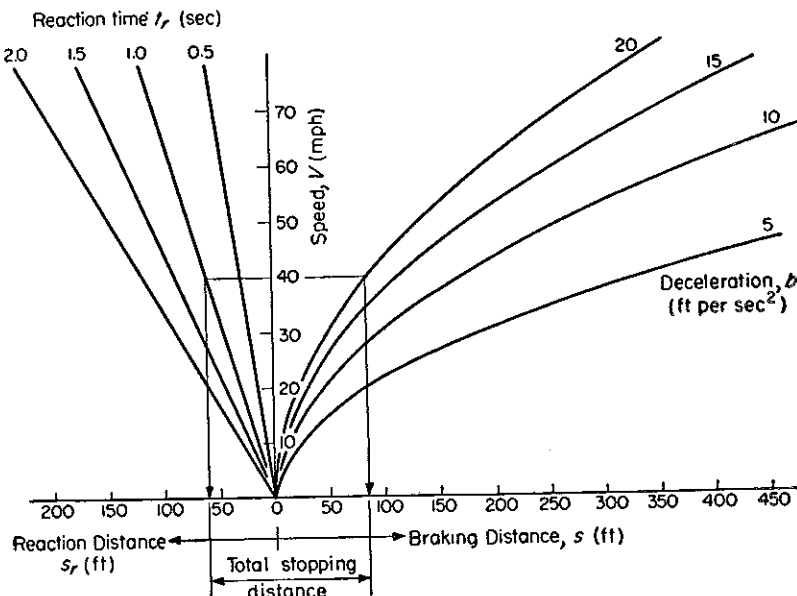


Fig. 64—Braking-performance chart

Example: Assuming a vehicle speed of 40 mph, determine distance traveled during a driver reaction time of 1 sec. Find also the total stopping distance for an assumed maximum deceleration of 20 ft per sec².

SOLUTION: On the left-hand side of the chart, projection of the 40-mph ordinate through the 1-sec reaction-time line shows that the vehicle travels 59 ft before the brakes are applied. A similar projection through the 20 ft per sec² maximum deceleration line on the right-hand side of the chart shows distance traveled during braking to be 85 ft. Total stopping distance from the point of emergency is therefore 144 ft.

Braking Performance Limits

transferable braking forces
tractor-trailer braking
heat dissipation
heat storage

REAR-WHEEL BRAKES:

$$B_{rmax} = W_{br} \mu \quad (222)$$

$$W_{br} = \frac{L_f W}{L} - \frac{H}{L} (W_{br} \mu + fW) \quad (223)$$

$$W_{br} = \frac{W(L_f - fH)}{L + \mu H} \quad (224)$$

$$B_{rmax} = \frac{\mu W(L_f - fH)}{L + \mu H} \quad (225)$$

FOUR-WHEEL BRAKES: Since the effective axle weight equals the full vehicle weight, then

$$B_{4max} = \mu W \quad (226)$$

Substituting this expression into Equations 194 and 195:

$$W_{4f} = \frac{W}{L} [L_r + H(\mu + f)] \quad (227)$$

$$W_{4r} = \frac{W}{L} [L_f - H(\mu + f)] \quad (228)$$

The condition of maximum brake performance as expressed by Equation 228 is realized only when distribution of braking forces to the axles is in proportion to their respective dynamic weights. That is,

$$\frac{B_{4f}}{B_{4r}} = \frac{W_{4f}}{W_{4r}} = \frac{L_r + H(\mu + f)}{L_f - H(\mu + f)} \quad (229)$$

In a subsequent development (Equation 236),

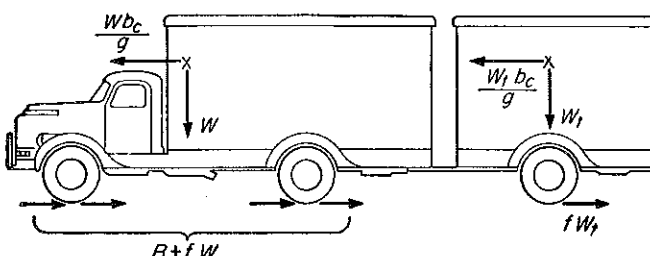


Fig. 65—Forces acting on a tractor-trailer rig when braking is provided by tractor only.

a simplified expression for maximum deceleration is derived as

$$b = g(\mu + f)$$

Combining this expression with Equation 229,

$$\frac{B_{4f}}{B_{4r}} = \frac{L_r g + bH}{L_f g - bH} \quad (230)$$

Both equations for braking-force distribution (Equations 229 and 230) are functions of the widely changing variables of road adhesion μ and deceleration b . As a consequence, the braking-force distribution ratio would ideally have to be adjust-

Nomenclature

A	= Projected vehicle area in drive direction, sq ft
B	= Brake force at tire-ground contact point, lb
B_{4f}, B_{4r}	= Brake forces on front and rear axles, four-wheel brakes, lb
c_a	= Air resistance coefficient
E	= Kinetic energy, ft-lb
E_t	= Energy in thermal units, Btu
G	= Grade or gradability, per cent
H	= Height of vehicle cg from ground, in.
I	= Polar moment of inertia, lb-sec ² -ft
L	= Wheelbase, in.
L_f, L_r	= Distance between vehicle cg and front and rear axles, in.
M_e	= Engine torque, lb-ft
N_a	= Power required to overcome air resistance, hp
N_{ad}	= Braking power supplied by additional sources, hp
N_b	= Energy conversion rate in brake, hp or Btu per hr
N_g	= Power required to overcome grade resistance, hp
N_r	= Power required to overcome rolling resistance, hp
Q_b	= Thermal capacity of brake drum, Btu
R_a	= Air resistance, lb
R_g	= Grade resistance, lb
R_i	= Total inertia resistance, lb
R_r	= Rolling resistance, lb
R_{rf}, R_{rr}	= Rolling resistances on front and rear axle wheels, lb
ΣR	= Summation of resistance forces, lb

Example 5—Braking-Force Distribution

Problem: Determine distribution on a vehicle with design configuration $L_f = L_r = 0.5L$ and $H = 0.35L$. With an average value $\mu = 0.35$, Equation 229 gives

$$\frac{B_{4f}}{B_{4r}} = \frac{0.5 + 0.35(0.35 + 0.02)}{0.5 - 0.35(0.35 + 0.02)} = \frac{63}{37}$$

In other words, for the assumed weight distribution, braking-force distribution is 63 per cent to the front wheels and 37 per cent to the rear wheels.

able to assure optimum braking effect. This condition, however, has not been realized in practice, and in the design of brake systems an average value of road adhesion $\mu = 0.35$ is usually assumed as compromise. This corresponds to deceleration $b = 11.5$ ft per sec.² As deceleration increases, or as values of road adhesion coefficient increase, the braking effort exerted by the front wheels increases. Example 5 illustrates a typical calculation of brake-force distribution.

Limits of Deceleration: Substituting Equation 217, the braking force limit expression, into the equation of decelerated motion (Equation 202, Part 11, then

$$B_{max} = \mu W_b = \gamma_b mb - R_r \pm R_g - R_a \quad (231)$$

Deceleration b then becomes b_{max} , where

$$b_{max} = \frac{g}{\gamma_b} \left[\frac{W_b \mu}{W} + f - \sin(\pm\theta) + \frac{R_a}{W} \right] \quad (232)$$

When the dynamic axle weight term W_b is replaced by the values given in Equations 220, 224, and 226 (front, rear, and four-wheel brakes), the maximum decelerations obtainable under given friction conditions are as follows:

FRONT WHEEL BRAKES:

$$b_{max} = \frac{g}{\gamma_b} \left[\frac{(L_r + fH)\mu}{L - \mu H} + f - \sin(\pm\theta) + \frac{R_a}{W} \right] \quad (233)$$

REAR-WHEEL BRAKES:

$$b_{max} = \frac{g}{\gamma_b} \left[\frac{(L_f - fH)\mu}{L + \mu H} + f - \sin(\pm\theta) + \frac{R_a}{W} \right] \quad (234)$$

FOUR-WHEEL BRAKES:

$$b_{max} = \frac{g}{\gamma_b} \left[\mu + f - \sin(\pm\theta) + \frac{R_a}{W} \right] \quad (235)$$

The above equations include the effects of rolling, grade, and air resistances, and show that deceleration is independent of vehicle weight only when air resistance can be neglected, that is, at low speeds. The loaded vehicle, therefore, is at a

Example 6—Parking-Brake Calculations

Problem: Determine the maximum grade on which a rear-axle parking brake will hold a vehicle with dimensions $L_f = L_r = 0.5L$ and $H = 0.35L$. Assume the surface is slippery with friction coefficient $\mu = 0.2$.

Equation 246 gives the maximum grade G_{max} as

$$G_{max} = \frac{100[0.2(0.5) + 0.02]}{1 + 0.35(0.2)} = 11 \text{ per cent}$$

for the downhill-pointing vehicle, and

$$G_{max} = \frac{100[0.2(0.5) + 0.02]}{1 - 0.35(0.2)} = 13 \text{ per cent}$$

for the uphill-pointing vehicle.

Problem: Determine the minimum coefficient of friction required to hold the vehicle stationary on a slope of 30 per cent.

From Equation 247, required values are

$$\mu_{min} = \frac{30 - 2}{100(0.5) + 0.35(30)} = 0.71$$

for the downhill-pointing vehicle, and

$$\mu_{min} = \frac{30 - 2}{100(0.5) - 0.35(30)} = 0.46$$

for the uphill-pointing vehicle.

disadvantage when compared to the same vehicle in the empty condition. This is because the retarding effect of air resistance (per unit weight) is smaller and the resulting deceleration is therefore lower.

When air resistance (which can be considered as a safety factor) is neglected, Equation 235 can be simplified to the form

$$b = \frac{g}{\gamma_b} (\mu + f) \approx g (\mu + f) \quad (236)$$

The road-adhesion coefficient value $\mu = 0.6$ is usually assumed for dry concrete, leaving a sufficient margin for directional side forces. Maximum deceleration is then

$$b_{max} = 32.2(0.6 - 0.02) = 20 \text{ ft per sec}^2 \quad (237)$$

Such decelerations have been actually measured experimentally and can usually be attained by most passenger cars with properly adjusted brakes. Practical considerations, such as passenger comfort and the shifting of loads, usually impose much lower limits on deceleration. Deceleration values over 10 ft per sec² are considered unpleasant; values higher than 15 ft per sec² are used only in emergencies.

Deceleration values are often expressed in terms of the gravitational constant g . Maximum deceleration on dry concrete (20 ft per sec²) then becomes $0.64g$, and the average deceleration 10 ft

per sec² equals 0.32g.

An average automobile collision, which is essentially an extremely abrupt stop, is about 1 to 4g in terms of deceleration. Limits of human survival seem to be somewhere around 20g and, as an example, a head-on collision at 40 mph produces a deceleration of about 16g or 510 ft per sec.²

As stated in a foregoing section, deceleration limits on dry concrete are seldom reached in everyday driving. The superiority of the four-wheel brake system is, therefore, more apparent when the vehicle is driven on slippery surfaces of low μ values, since the braking work is distributed over more application points.

Actual Stopping Distance: In an emergency stop, a certain time elapses before the driver can take his foot from the accelerator and depress the brake pedal. Called the reaction time, the time interval has been measured experimentally as falling between 0.5 and 2.0 sec. Actual stopping distance, $S = s_r + s$, can be calculated from the relationship

$$S = vt_r + \frac{v^2}{2b}$$

In this equation, the first term on the right side is the distance traveled during the reaction time before the brake is applied. The second term, which results from combination of Equation 236

Example 7—Braking-Power Calculation

Problem: Determine the energy that must be absorbed by the brake system in a vehicle which is descending a slope of 10 per cent at a steady speed of 50 mph. Vehicle weight is 20,000 lb.

Rate at which potential energy is converted in the descending vehicle is given by the expression

$$N_g = \frac{WGV}{37,500} = \frac{20,000(10)(50)}{37,500} = 266 \text{ hp}$$

Assuming $f = 0.02$, the power consumed by rolling resistance is

$$N_r = \frac{WfV}{375} = \frac{20,000(0.02)(50)}{375} = 53 \text{ hp}$$

For an assumed $c_a = 0.8$ and $A = 70 \text{ sq ft}$, power consumed by air resistance is

$$N_a = \frac{0.26 c_a A V^3}{37,500} = \frac{0.8(70)(50)^3}{144,000} = 47 \text{ hp}$$

Power that must be absorbed by the brake system is therefore

$$N_b + N_{ad} = N_g - (N_r + N_a) \\ = 266 - (53 + 47) = 166 \text{ hp}$$

Despite the relatively high speed of 50 mph, air resistance counteracts only about 18 per cent of the total energy converted on the grade.

and Equation 206 (Part 11), is the braking distance. The importance of reaction time in braking calculations is graphically illustrated in Fig. 64.

Special Applications: Solution of any particular braking-performance problem can be easily calculated from combination of the equation of decelerated motion (Equation 202), the equations for static and dynamic axle weights (Equations 194 and 195), and the equation of maximum transferable braking force. The procedure is demonstrated for two special applications in the following sections.

DECELERATION OF TRACTOR-TRAILER COMBINATION: If, on a tractor-trailer combination, brakes are provided only on the tractor, braking power of the tractor must obviously decelerate both vehicles. From Fig. 65, the force balance is

$$B = \frac{b_c}{g} (W + W_t) - f (W + W_t) \quad (238)$$

where subscript t applies to the trailer only, and c refers to the combination.

Limit of braking force produced by the tractor is given by the relation

$$B_{max} = W\mu \quad (239)$$

When Equations 238 and 239 are equated, maximum deceleration of the combination becomes

$$b_{cmax} = g \left[\frac{W\mu}{W + W_t} + f \right] \quad (240)$$

Often a certain allowable minimum deceleration of the tractor-trailer combination is required for safety reasons. In such case, the maximum permissible weight of the trailer can then be calculated as

$$W_{tmax} = W \left[\frac{g(\mu + f) - b_c}{b_c - gf} \right] \quad (241)$$

After substitution of Equation 236 for maximum deceleration of the tractor alone, and neglecting rolling resistance which, in this case, is of little importance, Equation 241 becomes

$$W_{tmax} = W \left[\frac{b}{b_c} - 1 \right] \quad (242)$$

As an example of such a calculation, assume that the weight of the trailer must be determined if the minimum required deceleration on dry concrete is 15 ft per sec². From Equation 237, the deceleration of the tractor alone is $b = 20$ ft per sec². From Equation 242,

$$\frac{W_{tmax}}{W} = \frac{20}{15} - 1 = 0.33$$

This shows that the trailer can have a maximum weight equal to 33 per cent of that of the tractor.

PARKING BRAKE HOLDING POWER: Parking-brake action represents a special form of the braking problem since it concerns the stationary vehicle.

The function of a parking brake is to retain the vehicle on a grade at least equal to vehicle gradability, usually by restraining the driving axle. The force equation in this case is

$$W \sin \theta - fW \cos \theta = B \quad (243)$$

Here, plus and minus signs of the different terms do not change in relation to each other, if the slope either is downhill or uphill.

Braking force is limited by available ground friction which, in turn, is a function of weight acting on the braking axle. For a rear-axle parking brake, the equation for stationary axle weights applies (Equation 91, Part 7):

$$W_r = \frac{W}{L} [L_f \cos \theta - H \sin (\pm \theta)] \quad (244)$$

where $\pm \theta$ applies to the vehicle pointing downhill. This represents the worst case possible, since weight transfer is away from the rear or braking axle. Combining Equations 243 and 244 with the applicable limit equation

$$B_{max} = W_r \mu$$

the resulting expression is

$$W \sin \theta - fW \cos \theta = \frac{\mu W}{L} [L_f \cos \theta \pm H \sin \theta] \quad (245)$$

After rearrangement and substitution of $G = 100 \tan \theta$, then

$$G_{max} = 100 \left[\frac{\frac{\mu L_f}{L} + f}{1 \pm \frac{\mu H}{L}} \right] \quad (246)$$

where G in per cent and the plus sign in the denominator refers to a downhill pointing vehicle.

Minimum coefficient of friction required to hold the vehicle on a grade of G per cent is obtained by rewriting Equation 246 as

$$\mu_{min} = \frac{G - 100f}{\frac{100 L_f}{L} \pm \frac{HG}{L}} \quad (247)$$

It is interesting to note that the maximum grade on which the parking brake is able to hold is independent of vehicle weight and is a function of weight distribution and friction coefficient only. Example 6 illustrates typical parking-brake holding-power calculations.

Braking-Heat Effects: In foregoing sections, elementary equations of motion and the relationships between forces acting on a vehicle in decelerated motion were established. These equations, however, did not consider braking-performance limitations imposed by the energy conversion rate in the brake and the accompanying temperature rise in both drum and lining.

Basically, a brake performs an irreversible conversion of potential or kinetic energy into heat. This conversion is a frictional process, which can

take place in the brake drum or, undesirably, at the tire-ground contact area when the braked wheel skids. In following sections, braking calculations are carried out from the viewpoint of energy conversion, and basic equations and design criteria are established.

Heat created in the brake raises the temperature of the friction surfaces, which, in turn, sets the limiting factor on brake performance. This is because the friction coefficient value of the brake lining decreases rapidly with higher temperatures, and braking torque falls off correspondingly. Furthermore, resistance of the linings against abrasion also declines at higher temperatures, affecting the service life of the brakes. Design of a brake system must be carried out so that lining operating temperatures, even under the most severe anticipated performance requirements, will stay below limits for which frictional and abrasive properties are acceptable.

From an energy conversion standpoint, braking calculations described here are based on two different operational conditions:

1. Moderate brake application of long duration, for example, on a vehicle descending a long downhill grade. For such brake operation at constant temperature, equilibrium must be established be-

Example 8—Braking-Heat Calculation

Problem: Determine average energy-conversion rate and temperature rise in the brakes of an aircraft decelerating at a 10 ft per sec² rate from an initial speed of 100 mph. Gross weight of the aircraft is 80,000 lb; brake weight is 400 lb. Effects of air resistance and kinetic energy of rotating parts are neglected.

Equation 255 gives the average energy-conversion rate as

$$\begin{aligned} N_b &= \frac{WV_m}{375} \left[\frac{b}{g} - f \right] \\ &= \frac{80,000(100)}{375(2)} \left[\frac{10}{32} - 0.02 \right] \\ &= 3050 \text{ hp} \end{aligned}$$

Total work performed in stopping the aircraft equals the kinetic energy converted, or from Equation 257

$$\begin{aligned} E &= \frac{80,000(100)^2}{30(778)} \\ &= 34,500 \text{ Btu} \end{aligned}$$

Assuming specific heat of the brake-drum material is $c = 0.11$, temperature rise in the drums is given by Equation 260 as

$$\Delta t = \frac{34,500}{0.11(400)} = 780^{\circ}\text{F}$$

tween the frictional heat generated in the brake and the heat dissipated by the brake to the outside air.

2. Severe brake application of short duration, for example, in an emergency stop. In this case the total kinetic energy converted during deceleration must be absorbed by the heat storage capacity of the brake. This is because heat dissipation during the short braking period is negligible.

The following sections give further details on these brake-application conditions.

Braking-Heat Dissipation: The heat-dissipation rate of the brake is the performance determining factor where braking is intermittent but frequent. This is the case in bus service, for example, or during braking of extended duration.

Basis for the heat-dissipation calculation is the energy-conversion rate and heat-flow balance at the brake drum. Temperature of the brakes of a vehicle descending a grade at constant speed increases until it reaches a constant value where equilibrium between energy conversion and heat dissipation has been reached. Obviously, as heat conduction from the lining contact area improves, energy-handling capabilities of the brake also increase.

Heat exchange in the brake is brought about by the usual processes:

1. *Conduction* through the shoe and brake drum to the adjoining parts in direct contact.

2. *Radiation*, which takes place between all brake parts and surrounding surfaces. Since radiation

is a function of absolute temperature, it is usually neglected because of the relatively low brake operating temperatures.

3. *Convection*, especially from the outside surface of the drum, to the ambient air. This accounts for the largest part of the heat exchange in the brake. The amount of heat convected is a function of the size and quality of the contact surface and the velocity and turbulence of the air flow. Diagonal ribs are usually provided on the drums of high-capacity brakes, and an air stream is diverted to them from openings in the tire rims, or by proper shaping of surrounding sheetmetal body parts. When special cooling provisions are not made, brakes hidden deep in the tire rim often show poor performance because of inadequate convection cooling.

Because of the many variables influencing heat flow from the brake, no systematic mathematical analysis has yet been made. Instead, the problem is handled by measurements in wind tunnels, or by towing the vehicle to obtain characteristic heat-dissipation curves. These curves usually form a family, Fig. 66, each curve representing a certain constant brake temperature plotted against vehicle speed, which is the important heat-convection influencing factor. On new designs, estimates are made on a basis of similarity to comparable existing types.

Energy-Conversion Equations: The equation of forces acting on a vehicle descending a downhill slope with constant speed is derived from Equation 202 (Part 11) setting $b = 0$,

$$B + B_{ad} = R_g - R_r - R_a \quad (248)$$

In other words, the sum of B , the actual braking force, and B_{ad} , the braking force derived from the engine or other additional sources, equals the algebraic sum of grade resistance and rolling and air resistances.

Expressed in power units, Equation 248 becomes

$$N_b + N_{ad} = \frac{V}{375} (R_g - R_r - R_a) \quad (249)$$

After substituting the terms for the resistance forces,

$$N_b + N_{ad} = \frac{VWG}{37,500} - \frac{VWF}{375} - \left[\frac{0.26 c_a A}{37,500} \right] \cdot V^3 \quad (250)$$

where N_b is the energy conversion rate in the brake (hp) and N_{ad} is braking power supplied by additional sources.

A general solution for this equation, which would be applicable to all vehicles, cannot be found, since the air-resistance factors c_a and A are particular to each vehicle. The effect of vehicle weight can, however, be eliminated by considering the product $W(G - 100f)$ as the variable. In other words, the same energy conversion rate is

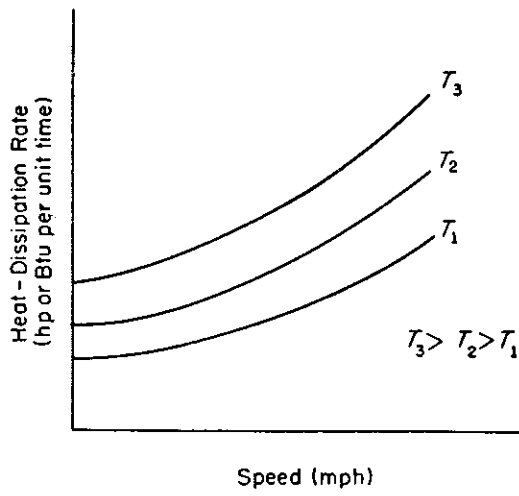


Fig. 66—Heat dissipation or energy-conversion rate in a brake as a function of vehicle speed. Rate of heat dissipation from the brake is proportional to temperature and to vehicle speed. Higher speeds improve the convective transfer of heat from brake components. Energy-conversion rate in the braking system of a vehicle descending a grade must remain below the heat-dissipation capacity of the system if equilibrium brake temperatures are to be established.

reached when a vehicle of 2000 lb descends a grade of 5 per cent as for the case of a 10,000 lb vehicle on a 1 per cent grade. This substitution permits use of the same diagram for calculation of brake performance for all vehicles having the same product $c_a A$, regardless of weight. Rearranged, Equation 249 becomes

$$N_b + N_{ad} = \frac{VW(G - 100f)}{37,500} - \frac{c_a A V^3}{1440} \quad (251)$$

The first term on the right side of this equation represents the total net power input, while the second term is the power consumed by air resistance. To maintain temperatures within permissible limits, the energy conversion N_b in the brake must be kept below the thermal capacity of the brake, this capacity being established by its heat dissipation curve (Fig. 66). Any braking-power requirements beyond such equilibrium must be supplied by additional braking sources, represented by N_{ad} .

Equation 251 is solved by graphical methods to give, for any value of W and G , the following performance results: 1. Speed of descent of a free-rolling vehicle. 2. Maximum permissible speed of descent for a particular brake. 3. Additional braking power required and the gear ratio to be used to achieve the desired braking performance. The principles and techniques for use of the diagram are shown in Fig. 67.

As an example of the use of Fig. 67, determine the maximum grade on which an 8000 lb vehicle can be braked (at brake equilibrium temperature) without assistance from engine. Intersection of the 50-mph ordinate with the N_b curve is found at the 40,000 power-input line. Therefore, assum-

ing $f = 0.02$,

$$G = \frac{40,000}{W} + 100f = 7 \text{ per cent}$$

With the engine braking in high gear, intersection of the 50-mph ordinate and the power-input line is at 60,000. This value corresponds to a 9.5 per cent grade. Similarly, in second gear, the maximum grade is 15 per cent.

Speed of descent for a free-rolling vehicle ($N_b = 0$ and $N_{ad} = 0$) is found at the intersections of the power-input lines and the N_a curve. For example, on a grade of 4.5 per cent (20,000 line), the speed of free descent is 96 mph.

One possible simplification is to consider air resistance as a safety factor and omit it from the calculations. This is permissible with little error when the anticipated maximum speed of descent is under 50 mph, which is usually the case in most automotive applications. The simplified form of Equation 251 is then

$$N_b + N_{ad} = \frac{VW(G - 100f)}{37,500} \quad (252)$$

This equation can also be solved again by the graphical method mentioned earlier. The basic diagram has general validity for all vehicles, each particular case being solved by superimposing on the diagram the braking power of the engine and the heat dissipation curve of the brake under consideration. Example 7 illustrates the technique.

Heat-Storage Capacity: If quick deceleration of the vehicle is the main objective of brake application, duration of the process is short, and heat dissipation from the brake is negligible. The func-

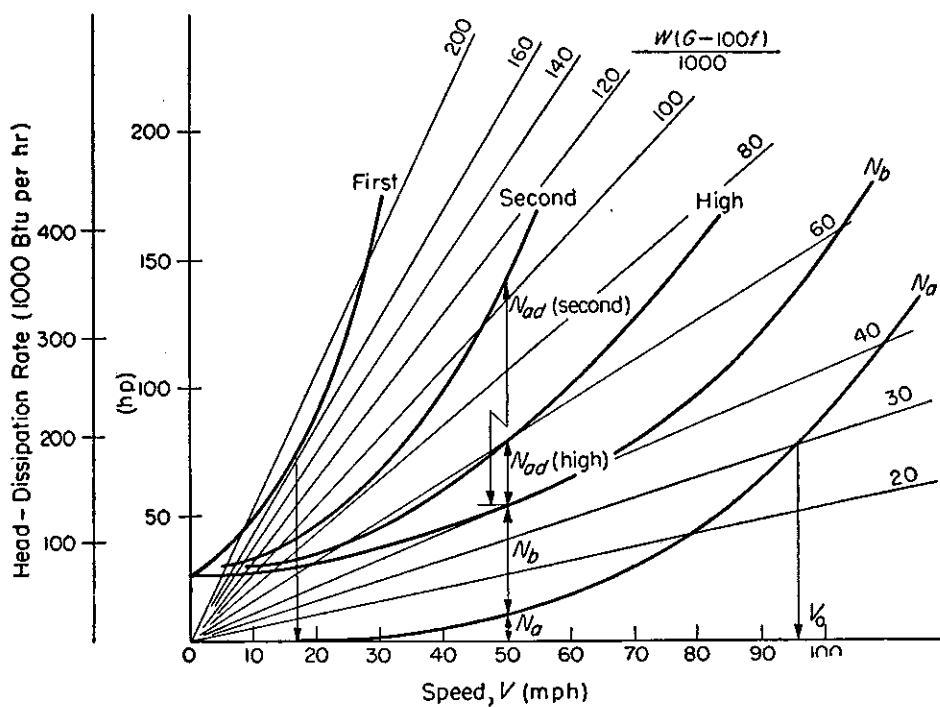


Fig. 67 — Typical brake performance of a vehicle descending long grades. Net rate of energy input, $W(G - 100f)$ has general validity for all vehicles. Air-resistance power-consumption curve N_a assumes a vehicle with $c_a A = 13$. Heat-dissipation of the assumed brake, N_b , which is added to the N_a value, represents the maximum energy-conversion rate allowed by brake-temperature limits. Braking power of the engine, represented in first, second and high gears, is similarly added to give total vehicle braking power.

tional limitation of the system is then the heat-storage capacity of the drum.

The drum must absorb a heat quantity equivalent to the maximum anticipated kinetic energy of the vehicle without reaching a critical temperature on the brake lining.

As in calculations in Part 11, the engine is considered to be disengaged, and the force equation becomes

$$B = \gamma_b mb - R_r - R_a + R_g \quad (253)$$

where the positive sign on the grade resistance term R_g applies to a downhill grade.

The instantaneous energy conversion rate in the brake N_b (hp), corresponding to deceleration from speed V (mph), can be calculated from Equation 253 as

$$N_b = \frac{V}{375} \left[\gamma_b mb + R_g - R_r - R_a \right] \quad (254)$$

Speed decreases during deceleration and so does the energy conversion rate. The calculation is therefore made for the mean speed

$$V_m = \frac{V_i + V_f}{2}$$

For a full stop, this becomes

$$V_m = \frac{V_i}{2}$$

Neglecting air resistance, the mean energy-conversion rate in decelerating a vehicle of weight W descending a downgrade slope of G per cent is

$$N_b = \frac{WV_m}{375} \left[\frac{b\gamma_b}{g} + \frac{G}{100} - f \right] \quad (255)$$

Brake calculations based on sudden braking are based on the total kinetic energy freed when the vehicle slows down from V_i to V_f . Furthermore, the power-consuming effect of rolling and air resistance is usually neglected and the assumption

is made that total kinetic energy E (ft-lb) is absorbed by the brake, or

$$\begin{aligned} E &= m \left(\frac{v_i^2 - v_f^2}{2} \right) = \frac{W(V_i^2 - V_f^2)}{2g} \left[\frac{5280}{3600} \right]^2 \\ &= \frac{W(V_i^2 - V_f^2)}{30} \end{aligned} \quad (256)$$

Expressed in thermal units, and for a full stop, Equation 256 becomes

$$E_t = \frac{WV_i^2}{30(778)} = \frac{WV_i^2}{23,200} \quad (\text{Btu}) \quad (257)$$

When the amount of heat created in the brake has been established, the temperature rise and the required weight of the brake drum can be calculated. Thermal storage capacity of the brake drum is:

$$Q_b = cW_{dr}\Delta t \quad (258)$$

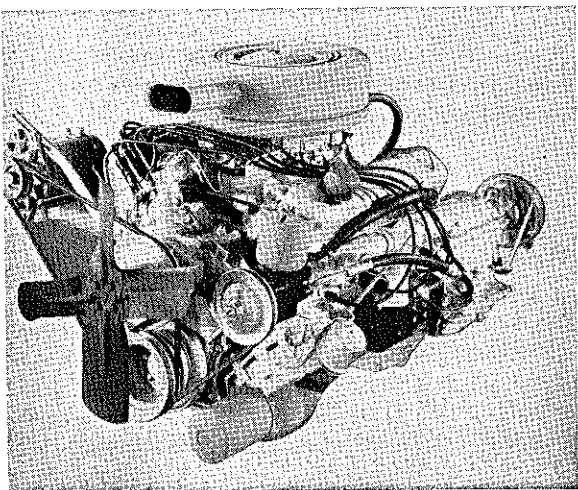
where Q_b is the thermal capacity of the brake drum, W_{dr} is the weight of the brake drum, c is the specific heat of the drum material, and Δt is the temperature rise in the drum. Letting $E_t = Q_b$, the required weight W_b of heat-absorbing material can be determined for which converted kinetic energy would raise the temperature only the permissible amount Δt . The expression is

$$W_{dr} = \frac{E_t}{c\Delta t} = \frac{WV_i^2}{23,200 c\Delta t} \quad (259)$$

Temperature rise Δt , which results from heat input that is equivalent to the kinetic energy converted, is therefore

$$\Delta t = \frac{E_t}{cW_{dr}} = \frac{WV_i^2}{23,200 cW_{dr}} \quad (260)$$

A typical calculation of these effects is illustrated in Example 8.



Mechanics of Vehicles—13

By JAROSLAV J. TABOREK*

Development Engineer
Towmotor Corp.
Cleveland

BASIC limitations to vehicle performance, reviewed in Parts 9 and 10 of this series, are set by the maximum tractive force that can be transferred by the driving wheels to the ground. In the analysis of these performance limits, it was assumed that torque supplied by the engine always equaled or exceeded the demands of the driving wheels.

In this article, the first of two that will be presented treating the subject of vehicle performance prediction, general characteristics desired of a

*Now Research and Development Engineer, Phillips Petroleum Co., Bartlesville, Okla.

vehicle powerplant are introduced, and methods for correcting standard data to existing atmospheric conditions are reviewed. Also surveyed are the power losses in accessories and drive-system components.

Vehicle Powerplants: Performance characteristics that ideally suit a powerplant for vehicle propulsion are: 1. Constant power output throughout the usable speed range. 2. Torque that peaks in the low-speed range where traction demands for grade climbing and acceleration are high. Plotted against engine speed, the characteristic curves of such a powerplant have the form of a straight line for power output P and a hyperbola for the torque M , Fig. 68. The equation of the torque characteristic has the general form

$$M = \frac{5252 P}{n}$$

Automotive powerplants in actual use have characteristics differing more or less from these ideal

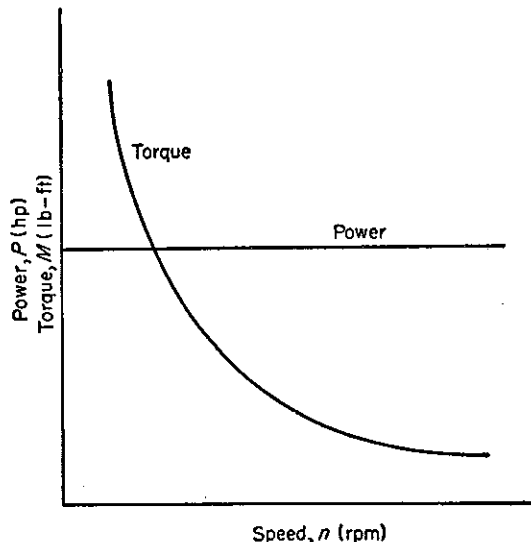


Fig. 68—Powerplant characteristics ideally suited for vehicle propulsion show constant power output over the entire speed range. This gives a hyperbolic torque curve and provides high tractive forces for vehicle acceleration at low road speeds.

Nomenclature

B	= Barometric pressure, in. Hg
B_o	= SAE standard barometric pressure ($= 29.92$ in. Hg)
B_v	= Vapor pressure of air, in. Hg
c	= Number of cylinders
D	= Cylinder bore, in.
M	= Engine torque, lb-ft
n	= Speed, rpm
P	= Power delivered at output shaft, hp
p_b	= Brake mean effective pressure, psi
Q	= Volume output of pump, gpm
s	= Piston stroke, in.
T	= Absolute temperature, °R
T_o	= SAE standard air temperature ($= 520^{\circ}\text{R}$)
x	= Revolutions per power stroke ($x = 2$ for four-stroke cycle)
η	= Efficiency

Powerplant Characteristics

- propulsion requirements
- standard performance data
- accessory losses
- transmission characteristics

requirements. In following sections, the internal-combustion engine, which powers the majority of automotive vehicles is discussed in detail; other powerplant types are reviewed briefly for comparison.

STEAM ENGINES: The steam engine, which as a rule develops peak power output at very low speeds, has characteristics that come close to satisfying requirements of the ideal automotive powerplant, Fig. 69. Such an engine would eliminate the need for a speed-change transmission and could be directly coupled to the vehicle driving axle. Despite these excellent qualities, use of the steam engine is generally limited to railroad applications, and seldom is it seen on automotive vehicles. One reason for this is the time required to put the steam engine into operation; a second disadvantage is poor power-to-weight ratio. Both these qualities are of decisive importance in road vehicles.

ELECTRIC MOTORS: The series-wound electric motor also has power-torque characteristics which approach the ideal for vehicle propulsion. There are two applications where electric powerplants are used in vehicles:

1. In battery-operated vehicles, mostly of the industrial type, requiring high tractive forces at very low speeds. These are conditions for which the electric motor is best suited. The power source is a storage battery; capacity of the battery determines the operation time for which the vehicle is independent of its base. Use of battery-powered vehicles is limited to short-range applications where weight is not objectionable. Often, in fact, battery weight is an advantage, for example, in industrial tractors and lift trucks.

2. Trolley buses, which find use in city transportation systems, operate on alternating current supplied from an overhead wiring system. The excellent adaptability of the electric motor to high-torque acceleration demands makes it an ideal powerplant for bus service with characteristically

frequent stops. The superiority of the electric motor over internal-combustion engine power is still unsurpassed in this respect.

INTERNAL-COMBUSTION ENGINE: Of all the possible power sources for propelling automotive vehicles, the internal-combustion engine has the most unfavorable power-torque characteristics, and can be used only in conjunction with a torque multiplying transmission. This is because of the inherent property of the engine to develop power in proportion to speed, giving torque-output characteristics unsuited for vehicle propulsion. Paradoxically, the internal combustion engine has nevertheless found the widest acceptance for automotive vehicles, due principally to its excellent

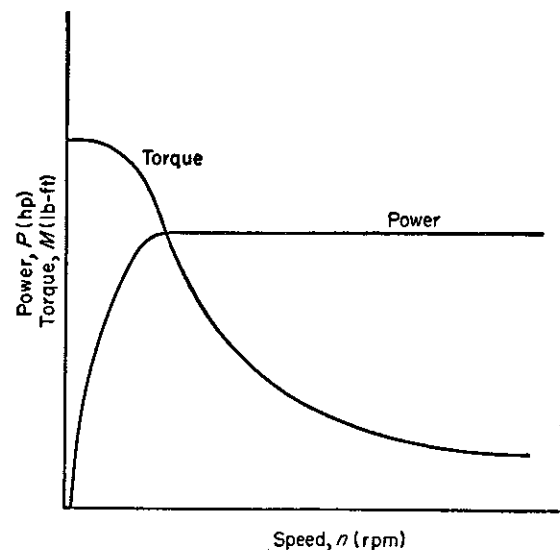


Fig. 69—Characteristics of the steam engine and the series-wound electric motor closely approximate the ideal for vehicle propulsion.

readiness for operation, high power-to-weight ratio, and wide availability of fuel.

Two different internal-combustion engine applications can be distinguished:

1. *Direct Drive*: In direct drive, which accounts for the majority of current applications, the engine is coupled through a transmission directly to the driving axle. The transmission can be mechanical (gear shift) or hydraulic (torque-converter type).

2. *Indirect Drive*: The internal combustion is merely the initial power source in the indirect-drive system; the actual driving is done by either electric or hydraulic systems.

The engine-electric drive combines the good operational properties of the combustion engine with the desirable power-torque characteristics of the electric motor. The relatively low efficiency of the combination, due to double transformation of power, is improved by running the engine at its economic optimum. Use of this type power-plant is limited at present to railroads and heavy duty industrial vehicle applications where advantages offered by the flexibility of the electric drive balance the increased cost and weight of the combination.

In the hydraulic-drive system, the engine drives a constant-displacement hydraulic pump which, in turn, supplies hydraulic fluid under pressure to a variable-displacement hydraulic motor coupled to the drive axle. Hydraulic-motor pressure and volume demands correspond to instantaneous driving conditions. Low efficiency of this combination is again justified by the excellent power-torque characteristics of the hydraulic-motor drive. The system is increasing in popularity for high-torque applications, where stepless speed regulation is essential.

Internal-Combustion Engine Characteristics: A typical power-torque diagram for a gasoline engine is shown in Fig. 70. Basic engine data are interrelated by the equation

$$P = \frac{p_b n Dsc}{396,000 x} = \frac{Mn}{5252} \quad (261)$$

Terms in Equation 261 are defined in Nomenclature.

From Equation 261, proportionality between brake mean effective pressure p_b and engine torque M can be derived as

$$M = kp_b \quad (262)$$

where k is the proportionality factor. Brake mean effective pressure is in itself not a measurable physical value, but is proportional to indicated pressure. Consequently, it is a function of a number of engine design factors and efficiencies. It is noted that power developed is a function of the product $p_b \times n$, while torque is proportional only to p_b .

The gasoline engine starts to run smoothly at a certain minimum or idle speed n_{min} and produces excess power at speeds above this point. Optimum combustion quality, and therefore maximum effec-

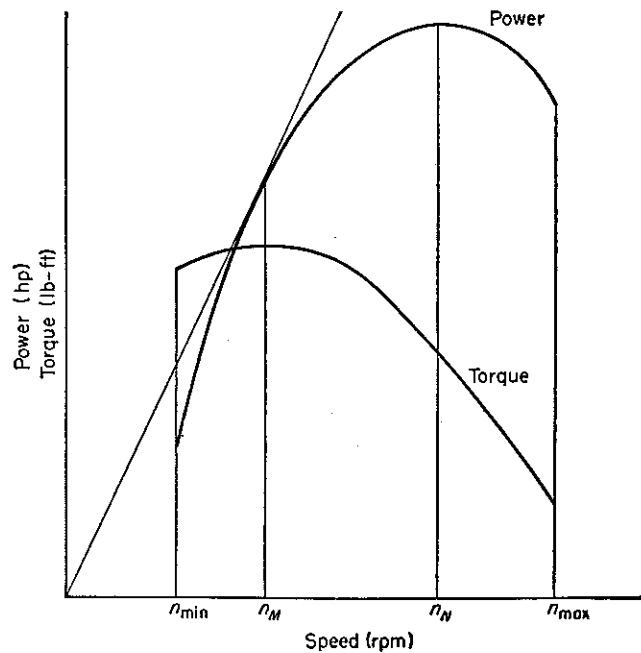


Fig. 70—Typical full-throttle characteristics of a gasoline engine. Maximum torque is given at speed n_M , which corresponds to the point of tangency of a line drawn from the origin to the power curve. Minimum speed, n_{min} , is engine idling speed; maximum torque is reached at relatively low power levels. Both of these characteristics account for the poor adaptability of the internal combustion engine for vehicle propulsion and point up the need for a change-gear transmission.

tive pressure, is reached at a medium engine speed where, as a result, maximum engine torque is developed. This point is designated in Fig. 70 as n_M . Power output at this rather low speed is also relatively low, which accounts for the poor adaptability of the combustion engine as a vehicle powerplant.

As speed increases further, brake mean effective pressure deteriorates due to the rapidly growing losses in the air-induction manifolds. Torque therefore starts to decline.

Power output is in nearly straight line proportion with speed up to the point of maximum torque. Beyond this point, the rate of power increase $\Delta P/\Delta n$ falls off until the maximum-power-output point is reached at n_N . The relative positions of n_N and n_M are often used as comparative measures of the quality and adaptability of an engine for given application.

Speed increase beyond n_N results in a fast decline in power output, determining therefore the position of maximum permissible speed n_{max} . In vehicle applications, this point is usually set just above the maximum-power-output speed. Vehicles designed for traction, however, are designed to operate at much lower engine speeds, since maximum torque and not power output determines performance limits.

The point of operation for maximum economy, corresponding to minimum specific fuel consump-

tion, coincides approximately with the speed of maximum torque. When transmission reduction ratios are properly selected, this economic optimum falls within the most frequently used part of the vehicle speed range. This is especially true for part-load operation, where differences in specific fuel consumption are particularly large.

Effects of Atmospheric Conditions: Maximum engine power developed is directly proportional to the weight of air inducted into the cylinder. Power output is therefore a function of the state of the air.

In gasoline engines, it is found that power is in direct proportion to barometric pressure (which changes with altitude) and approximately inversely proportional to the square root of absolute temperature. To permit comparison of engines on a basis that is independent of atmospheric conditions, performance data are measured experimentally on dynamometers and are recalculated to certain standard air conditions. These standards, which were established by SAE, are: 1. Temperature, $T_o = 520$ deg Rankine (60 F). 2. Barometric pressure, $B_o = 29.92$ in. Hg (dry air).

If engine power under standard air conditions is known, the effective power developed under any other set of conditions can be calculated from the equation:

$$P = \frac{P_o(B - B_v)}{B_o} \left(\frac{T_o}{T} \right) \quad (263)$$

where P is effective engine power under the given atmospheric conditions (hp), P_o is engine power under SAE standard air conditions (hp), T is ambient temperature (°R), B is barometric pressure at the carburetor air inlet (in. Hg), and B_v is vapor pressure of the air (in. Hg).

The effect of air humidity, expressed in Equation 263 as vapor pressure B_v , is, except under seasonally extreme conditions, usually negligible in performance calculations.

In Diesel engines, effects of atmospheric conditions on power output are more complicated, since not all the air inducted into the cylinders actually participates in the combustion process. Data-standardizing formulas are therefore functions of many variables that pertain to specific characteristics of a given engine, for example, engine size, quality of the fuel-air mixing process, etc. As a rough approximation, the following correction equation can be used for compression-ignition engines:

$$P = \frac{P_o(B - B_v)}{B_o} \left(\frac{T_o}{T} \right) \quad (264)$$

Atmospheric conditions can easily change engine output as much as 25 per cent. This is because air-intake temperature under the hood of an engine can rise to 200 F or higher, and air-intake pressures can be reduced substantially by increasing altitudes. Even daily variations at a given location can give a 10 per cent change in engine power.

The effects of air conditions and altitudes on engine power are graphically represented in Fig. 71. The plot allows the relative magnitude of these factors to be compared.

Engine Accessory Losses: Engine performance diagrams supplied to vehicle designers usually represent the power of the so-called "bare" engine. Since there is no generally accepted definition of this term, interpretation in each case should be carefully considered. This requires accurate knowledge of the conditions under which dynamometer measurements were actually taken in the laboratory.

Generally, the bare-engine performance diagram pertains to an engine stripped of all installations and accessories not essential to engine functioning and such accessories that are subject to in-

Fig. 71—Effects of carburetor-air intake conditions on internal-combustion engine power output. Normal power refers to engine rated power at SAE standard conditions (60 F and 29.92 in. Hg). Curve *a* shows power ratio vs. ambient pressure; curve *b* shows power ratio vs. intake temperature for gasoline engines; curve *c* shows power ratio vs. intake temperature for Diesel engines.

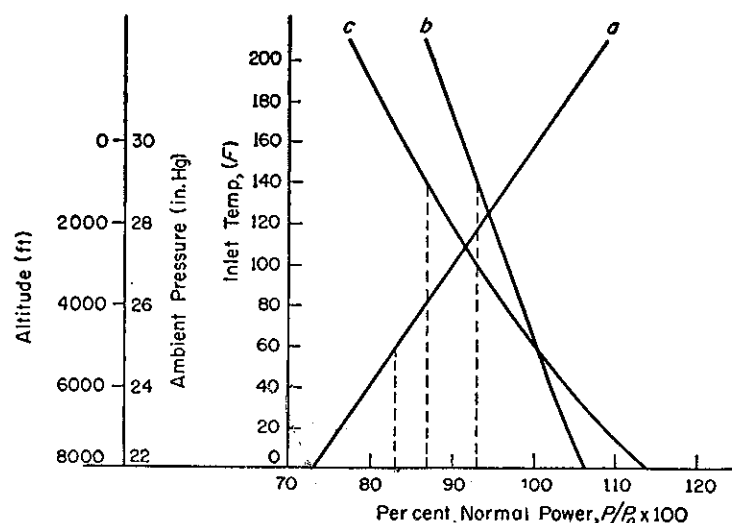
Example: Determine engine power ratio at 5000 ft altitude and 140 F air-intake temperature for gasoline and Diesel engines.

Gasoline engine:

$$P = 0.83 \times 0.93 P_o = 0.77 P_o$$

Diesel engine:

$$P = 0.83 \times 0.87 P_o = 0.72 P_o$$



dividual design and application requirements.

To obtain the power actually available at the output shaft, the power consumed by installations and accessories is subtracted from values given by the bare-engine power diagram. This gives a new diagram which represents the effective power available.

Installations and accessories found in the normal vehicle are reviewed in the following sections.

PUMPS AND DISTRIBUTOR: Water pump, fuel pump, oil pump and distributor drive form a special group since they are usually driven through internal connections from the engine block. As a rule, power requirements of these components are included in the bare-engine performance diagram. The fuel pump is sometimes an exception, since gravity feed may be used in the vehicle, making use of a fuel pump unnecessary.

MUFFLER: The muffler causes back pressure in the exhaust system and consequently power is lost in pushing through the burned gases. This power loss is proportional to the square of the engine speed and, depending on muffler resistance, reaches about 12 per cent at maximum power output. In high-performance engines, dual mufflers are used to reduce power losses to half of this value.

AIR CLEANER: Since the air cleaner is essentially a resistance element in the suction line, it causes a power loss proportional to the square of engine speed. Depending on its flow resistance, the average passenger-car air cleaner accounts for about a

3 per cent loss at maximum engine output.

GENERATOR: The generator has a varying power demand, depending on the instantaneous load in the electric circuit. At constant load, generator power-consumption characteristics have a linear relationship with speed. For the average passenger car, the generator requires about 2 hp at maximum engine power output.

FAN: Power requirement of the cooling fan is proportional to the third power of the speed and accounts for a considerable loss of power at high speeds. Shape of air-intake channels (grill) and operating speeds of the vehicle have an important effect on fan performance. On high speed vehicles, the natural flow of air often provides a substantial cooling effect. In fact, recent design developments have made it possible to automatically idle the fan when its function is not required, such as at high speeds and when starting a cold engine. On the other hand, vehicles working regularly at low speeds, or under intermittently stationary conditions, must depend entirely on the fan for cooling flow, since air flow due to vehicle speed is negligible. In rough approximation, an average passenger-car engine requires a fan with 1 hp power consumption at medium speeds. Power requirements increase about eight times when speed doubles.

HYDRAULIC PUMPS: Use of hydraulic pumps to provide power for auxiliary functions is increasing rapidly. On passenger cars fluid pressure is used for power steering, while hydraulically powered work-saving devices on agricultural and industrial vehicles are standard equipment.

The power consumption of a hydraulic pump can be calculated from the equation

$$P = \frac{Qp}{1714 \eta} \quad (265)$$

where Q is volume output (gpm), p is pressure (psi) and η is total pump efficiency, usually around 75 per cent. The power-consumption characteristic of a pump is basically in straight-line proportion with speed. At very high speeds, pump efficiency usually decreases, resulting in higher power consumption.

To determine how much of pump power should be subtracted from the bare-engine output, consideration must be given to the variation of pump-power demand with driving conditions. Power steering and other auxiliary equipment, for example, reach the peak power-consumption point when the vehicle is stationary and show reduced requirements at normal driving speeds.

Power requirement of all accessories should be carefully evaluated for each application and then plotted additively against engine speed. The final graphical summation is then subtracted from the bare-engine power diagram. The result represents effective power delivered to the transmission input shaft.

Transmission Characteristics: It has been shown in preceding sections that the internal-combustion engine is not in itself suited for vehicle propulsion,

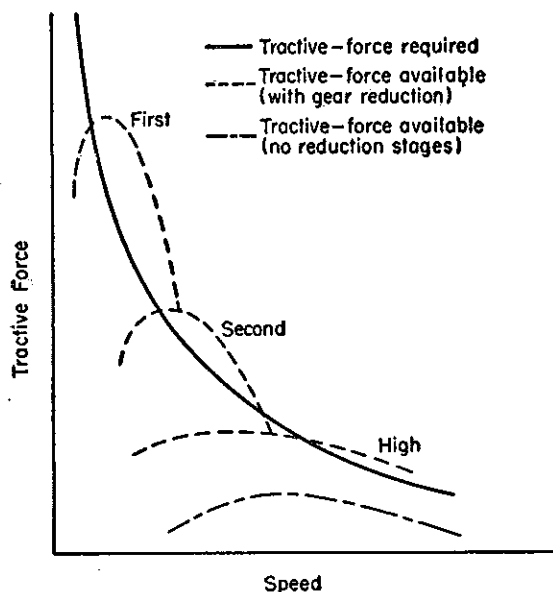


Fig. 72—Comparison of tractive force required by a typical vehicle and tractive force made available to the wheels by the engine. Plot shows that basic characteristic of the engine can be matched to the tractive force required curve by providing three or more speed-reduction steps in the transmission. Difference between "high" characteristic and "no transmission" characteristic is due to speed reduction in the vehicle differential.

since torque requirement for initial acceleration can be met only with the help of a change-gear transmission. The function of the transmission is to transform the torque-speed relationship of engine output into a form which more closely corresponds to actual driving demands, Fig. 72. This transformation is performed by the following means:

1. By the transmission itself, which can either have the form of a manual gear-shift transmission or that of a gear-reduction stage plus a hydraulic element such as a fluid coupling or a torque converter. Reduction ratios must be properly chosen in number and magnitude if the desired effect is to be obtained.
2. By a rear-axle gear, which gives, as a general rule, a constant reduction ratio of 3.5 to 6.5 through a hypoid gear pair. The rear-end ratio is determined by the usual practice requiring direct (non-reducing drive) drive through the transmission in high gear.
3. On vehicles requiring extremely high torques at low speeds, additional gear-reduction stages are usually placed at the drive wheels.

Power transmission between the engine output shaft and the driving wheels involves the following additional factors as power-consuming elements:

1. *Clutch efficiency*, amounting to about 99 per cent.
2. *Transmission power consumption*, originating in friction between gears and oil-churning losses. Gear friction is proportional to power transmitted and depends on gear-surface finish and quality of lubrication. Oil churning losses are proportional to approximately the third power of speed and are a function of oil viscosity. These factors re-

sult in an average transmission efficiency of 97 to 95 per cent for each gear pair, including final gear reductions. Torque-converter efficiencies, which vary more widely with operating conditions, are discussed in the next part of this series.

3. *Efficiencies of bearings and joints*, assumed for a passenger car to be from 98 to 99 per cent.

4. *Wheel slip*. A driving wheel in one full turn makes a translatory advance which is less than the circumference of the circle corresponding to the rolling radius of the tire. The difference is explained by the slip of the driving wheels (Part 1) and depends mainly on the nature and condition of the ground surface. This effect is expressed as drive efficiency or slip factor, with values of approximately 95 to 98 per cent for normal highway surfaces.

Total efficiency of the drive system between engine output shaft and drive wheels is the product of all component efficiency factors. The following are representative average overall efficiencies for a vehicle with a change-gear transmission:

1. In direct gear, 90 per cent
2. In other gears, 85 per cent
3. Drives with very high reductions (final drive), 75 to 80 per cent.

Power loss in the transmission is manifested as heat in the gear-box oil, bearings and other parts engaged in power transmission. The heat is eventually transmitted to the outside air by convection and radiation.

In the next part of this series, two representative vehicles—a passenger car and an industrial truck—are matched to their powerplants and detailed calculations of resulting vehicle performance are illustrated.

Mechanics of Vehicles—14

PERFORMANCE PREDICTION

By JAROSLAV J. TABOREK*

Development Engineer
Towmotor Corp.
Cleveland

effective power •
tractive forces •
gradability •
passing distance •

PERFORMANCE characteristics that suit a powerplant for use in a wheeled vehicle were surveyed in Part 13.⁴⁴ In this, the final article of the series, tentative design choice of powerplant is assumed to have been made, and the problem considered is that of predicting vehicle performance.

Performance calculations are illustrated for two representative vehicles: 1. Passenger car with a manual three-speed gear-shift transmission. 2. Industrial truck incorporating a torque-converter transmission with low and high gear stages. Methods of procedure emphasize calculation techniques and illustrate the advantages of graphical representation of performance results. Specifications for the two assumed vehicles are given in Table 7.

Effective Engine Power: Basic methods for determining effective engine power are identical for both the passenger car and the industrial truck. Power outputs P_o of bare engines at SAE standard air conditions are shown as functions of speed in Fig. 73 and 74. To establish usable power, standard engine power P_o is corrected to existing ambient air conditions. It is important to note that carburetor air-intake temperature under the hood of an engine may be substantially higher than that of the ambient air. The designer may rely on previous experience as a guide in such cases.

For both examples, air-intake temperature is assumed as 140 F, and air pressure is 29.6 in. Hg. Vapor pressure of the air is neglected ($B_v = 0$). From Equation 263 (Part 13), corrected power is

$$P = \frac{P_o(29.6)}{(29.92)} \sqrt{\frac{520}{600}} = 0.925 P_o \quad (266)$$

Or, from the correction factors plotted in Fig. 71

*References are tabulated at end of article.

⁴⁴Now Research and Development Engineer, Phillips Petroleum Co., Bartlesville, Okla.

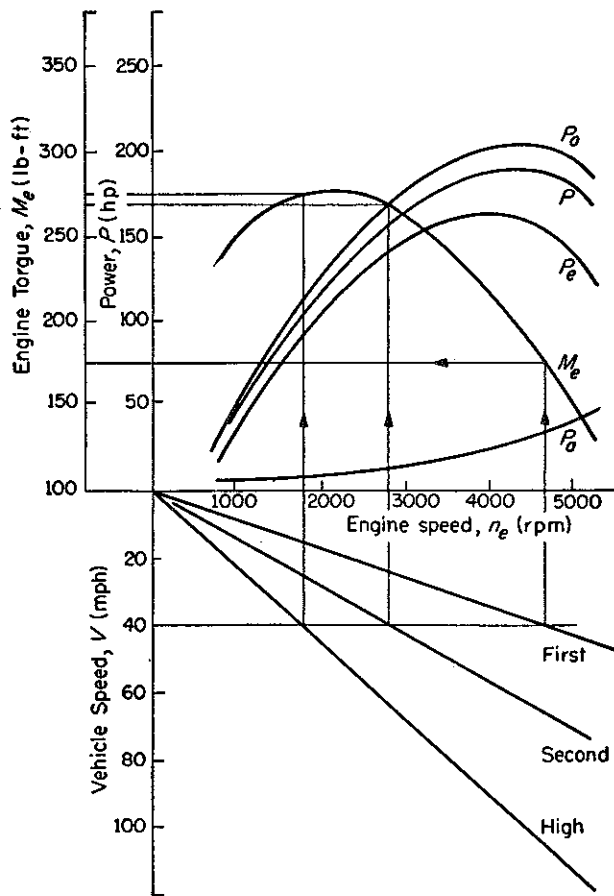


Fig. 73—Powerplant performance characteristics assumed for the passenger-car example. Upper plot shows method for obtaining effective power output P_e from SAE standard power P_o . Lower plot gives relationship between engine speed n_e and vehicle speed V in first, second and high gears.

Mechanics of Vehicles—14

PERFORMANCE PREDICTION

By JAROSLAV J. TABOREK*

Development Engineer
Towmotor Corp.
Cleveland

- effective power •
- tractive forces •
- gradability •
- passing distance •

PERFORMANCE characteristics that suit a powerplant for use in a wheeled vehicle were surveyed in Part 13.⁴⁴ In this, the final article of the series, tentative design choice of powerplant is assumed to have been made, and the problem considered is that of predicting vehicle performance.

Performance calculations are illustrated for two representative vehicles: 1. Passenger car with a manual three-speed gear-shift transmission. 2. Industrial truck incorporating a torque-converter transmission with low and high gear stages. Methods of procedure emphasize calculation techniques and illustrate the advantages of graphical representation of performance results. Specifications for the two assumed vehicles are given in Table 7.

Effective Engine Power: Basic methods for determining effective engine power are identical for both the passenger car and the industrial truck. Power outputs P_o of bare engines at SAE standard air conditions are shown as functions of speed in Fig. 73 and 74. To establish usable power, standard engine power P_o is corrected to existing ambient air conditions. It is important to note that carburetor air-intake temperature under the hood of an engine may be substantially higher than that of the ambient air. The designer may rely on previous experience as a guide in such cases.

For both examples, air-intake temperature is assumed as 140 F, and air pressure is 29.6 in. Hg. Vapor pressure of the air is neglected ($B_v = 0$). From Equation 263 (Part 13), corrected power is

$$P = \frac{P_o(29.6)}{(29.92)} \sqrt{\frac{520}{600}} = 0.925 P_o \quad (266)$$

Or, from the correction factors plotted in Fig. 71

*References are tabulated at end of article.

⁴⁴Now Research and Development Engineer, Phillips Petroleum Co., Bartlesville, Okla.

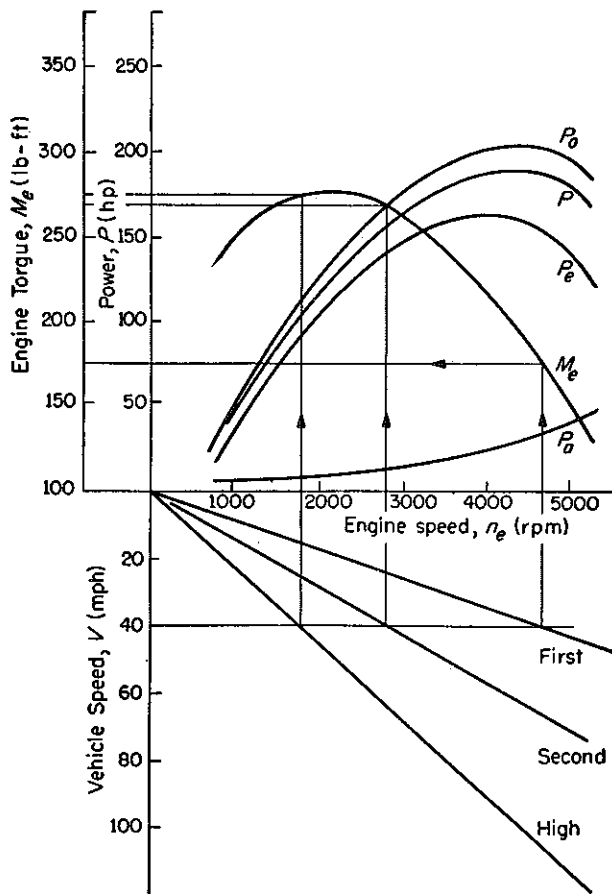


Fig. 73—Powerplant performance characteristics assumed for the passenger-car example. Upper plot shows method for obtaining effective power output P_e from SAE standard power P_o . Lower plot gives relationship between engine speed n_e and vehicle speed V in first, second and high gears.

cases fully acceptable and saves lengthy numerical calculation.

Transmission and rear-end gear reductions multiply engine torque to the value M_d at the drive axle. Designating the tractive force exerted by the driving wheels on the ground by T , the following relationship applies:

$$T = \frac{12 M_d}{r} = \frac{12 M_e \xi \eta}{r} \quad (270)$$

From this value, the motion-resisting forces encountered in constant-speed driving are next sub-

tracted, giving the free tractive force T_f , that is available for grade climbing, trailer pull or acceleration. Following are the principal motion-resisting forces:

1. Rolling resistance R_r , calculated from

$$R_r = Wf$$

can be assumed constant throughout the speed range. If greater accuracy is required, Equations 57 or 58 (Part 5) can be used. In the present example, Equation 57 gives the results tabulated in Table 8.

Table 7—Vehicle Specifications

Passenger Car

WEIGHT DATA: Gross weight of the loaded vehicle is 4000 lb. Distribution of weight to front and rear axles is equal. Height of the cg is $H = 0.25(L)$, where L is the wheelbase.

ENGINE DATA: Bare engine power output P_o is given for SAE standard conditions in Fig. 73. Power P_a consumed by accessories is plotted as a function of engine speed in the same figure.

TRANSMISSION DATA: Transmission is a three-speed, manual-shift unit. Rear-end reduction is through a hypoid gear box. Reduction ratios and efficiencies of the power train are as follows:

	Gear		
	First	Second	High
Transmission ratio	2.6:1	1.6:1	1.1
Rear-end ratio	3.6:1	3.6:1	3.6:1
Total ratio	9.4:1	5.75:1	3.6:1
Total Efficiency	0.85	0.85	0.90

TIRE DATA: Rolling radius of 6.75 x 15 tires is $r = 13.5$ in.

AIR-RESISTANCE DATA: Projected frontal area $A = 28$ sq ft. Coefficient of air resistance $c_a = 0.55$.

Truck

WEIGHT DATA: Gross weight of

loaded truck is 15,000 lb.

ENGINE DATA: Bare engine power output P_o at SAE standard conditions is plotted with accessory power consumption P_a in Fig. 74.

TRANSMISSION DATA: Transmission is a torque converter with automatic two-speed gearshift. Ratio between input and output speed and torque multiplication are plotted as functions of output speed

in Fig. 74. Torque multiplication at stall speed is 2.1. Additional speed reduction, obtained in the vehicle final-drive gear box is as follows:

	First Gear	Second Gear
Reduction	22.2:1	15:1
Total Efficiency	0.85	0.85

TIRE DATA: Rolling radius of 8.25 x 15, 12-ply tires is $r = 15.5$ in.

Table 8—Passenger-Car Performance

V (mph)	n_e (rpm)	M_e (lb-ft)	M_d (lb-ft)	T (lb)	R_r (lb)	R_a (lb)	ΣR (lb)	T_f (lb)	a (ft/sec ²)
First Gear									
7	800	230	1840	1850	44	1	45	1605	10.2
10	1150	258	2060	1840	44	4	48	1792	11.4
20	2300	275	2200	1960	44	16	60	1900	12.1
30	3450	240	1920	1710	48	36	84	1626	10.4
40	4600	175	1400	1250	52	64	116	1134	7.3
Second Gear									
11	800	230	1130	1010	44	4	48	962	6.9
20	1400	285	1300	1160	44	16	60	1100	7.9
30	2100	278	1360	1220	48	36	84	1136	8.1
40	2800	265	1300	1160	52	64	116	1044	7.5
50	3500	240	1170	1050	56	100	156	894	6.4
60	4200	200	980	875	64	144	208	667	4.8
70	4900	150	740	660	72	196	268	392	2.8
High Gear									
20	880	240	780	700	44	16	60	640	4.8
30	1320	265	860	770	48	36	84	686	5.1
40	1750	275	890	795	52	64	116	679	5.0
50	2200	278	900	800	56	100	156	644	4.8
60	2630	272	880	785	64	144	208	577	4.3
80	3500	240	780	700	88	256	344	356	2.6
100	4400	190	615	550	120	400	520	30	0.2

Table 9—Truck Performance

V (mph)	n_{tc} (rpm)	n_e (rpm)	ξ_{ts}	ξ_s	ξ_{tt}	ξ_t	M_e (lb-ft)	M_d (lb-ft)	T (lb)	R_r (lb)	T_f (lb)	ξ_γ	γ	m' (lb-sec ² /ft)	a (ft per sec ²)
Low Gear															
0	0	1400	∞	∞	2.10	46.5	168	6650	5150	300	4850	0	1.03	485	10
2	500	1400	2.80	62	1.60	35.5	168	5100	3950	300	3650	0	1.03	485	7.5
4	980	1500	1.53	34	1.27	28.2	168	4000	3100	300	2800	12	1.1	515	5.4
6	1490	1750	1.17	26	1.10	24.5	166	3460	2680	300	2380	21	1.32	620	3.8
8	1900	2100	1.10	24.4	1.02	22.7	160	3100	2400	300	2100	22	1.40	655	3.2
10	2450	2550	1.04	23	1.02	22.6	150	2820	2180	300	1880	23	1.40	655	2.9
12	2900	3000	1.03	23	1.02	22.6	127	2400	1860	300	1560	23	1.40	655	2.4
High Gear															
0	0	1400	∞	∞	2.1	31.5	168	4500	3480	300	3180	0	1.03	485	6.5
4	680	1450	2.10	31.5	1.46	21.9	168	3120	2420	300	2120	2	1.04	490	4.3
6	1000	1500	1.50	22.5	1.27	19	168	2700	2100	300	1800	7	1.05	493	3.6
8	1300	1650	1.27	19	1.15	17.3	167	2460	1900	300	1600	12	1.10	516	3.1
10	1620	1850	1.14	17.1	1.06	15.9	165	2230	1730	300	1430	14	1.12	525	2.7
12	1960	2120	1.08	16.2	1.02	15.3	160	2080	1610	300	1310	15.3	1.13	530	2.5
14	2250	2350	1.04	15.6	1.02	15.3	156	1970	1530	300	1230	15.3	1.13	530	2.3
18	2930	3000	1.03	15.5	1.02	15.3	127	1620	1250	300	950	16.3	1.13	530	1.8

2. Air resistance R_a , calculated from Equation 64 (Part 6), is

$$R_a = 0.26 c_a A \left(\frac{V}{10} \right)^2 = 0.26(0.55)(28) \left(\frac{V}{10} \right)^2 = 0.04 V^2$$

Values of c_a , the air-resistance coefficient, and A , the projected area, are usually known for existing vehicles or, in case of new designs, are assumed on grounds of similarity.

Both R_r and R_a are additively plotted against vehicle speed V and their sum is subtracted from tractive force T . This operation gives the free tractive force T_f , plotted for the passenger car in Fig. 75.

Tractive forces transferable by the driving wheels are limited by available friction, which, in turn, is a function of both the dynamic weight on the driving axle and the frictional properties of the ground (Part 9). For the rear-wheel drive system used on the passenger car, Equation 148, which has the form

$$T_{max} = \frac{\mu W(L_f - fH)}{(L - \mu H)}$$

can be evaluated for representative road surfaces with the following coefficients: $\mu = 0.75$ (dry concrete); $\mu = 0.60$ (gravel); $\mu = 0.40$ (wet asphalt). Weight-distribution data (Table 7) are $L_f = 0.5L$ and $H = 0.25L$. For dry concrete, then

PERFORMANCE PREDICTION

$$T_{max} = \frac{0.75(4000)[0.5 - 0.02(0.25)]}{[1 - 0.75(0.25)]} = 1840 \text{ lb}$$

Other traction values are 1410 lb for the gravel surface and 890 lb for wet asphalt. These results are plotted in Fig. 75. The downward trend of the curves with increasing vehicle speed is caused by the decline of μ values at higher speeds (Part 1).

INDUSTRIAL TRUCK: Unlike the geared transmission, which forms a positive coupling between engine and drive wheels, the torque converter is essentially a hydraulic coupling that gives values for torque multiplication and speed reduction that depend on converter speed, Fig. 74.

Torque-Converter Characteristics: Torque ratio of the converter reaches maximum at stall output speed, with a value around 2.2:1. The ratio gradually falls off as output speed increases, the converter eventually acting as a hydraulic coupling with 1:1 torque ratio.

Speed ratio of a torque converter is infinite at stall condition, where the vehicle is stationary and the engine is working at a certain predetermined design speed. As the vehicle begins to move, the engine speeds up, first very slowly, then at an increasing rate until the converter becomes a

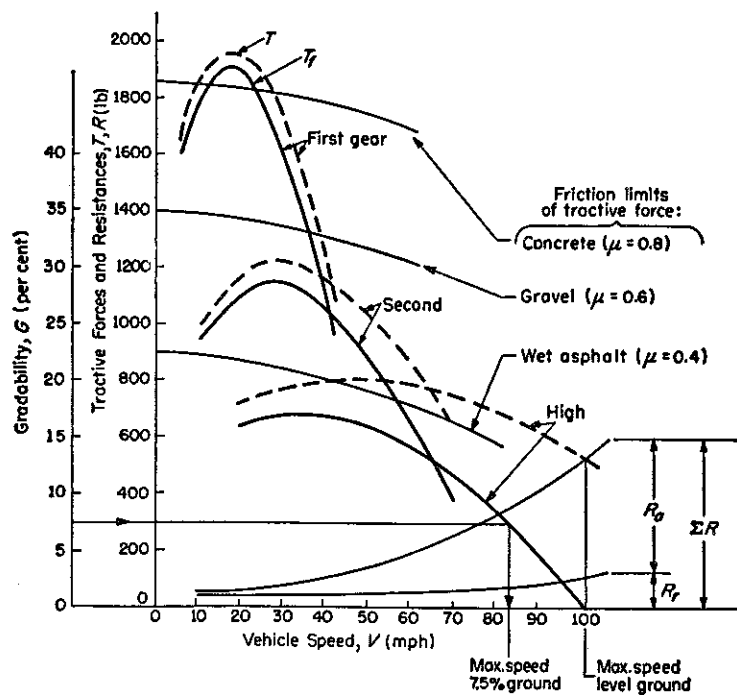


Fig. 75—Tractive force and gradability for the passenger-car example. Free tractive force T_f , is obtained by subtracting motion-resisting forces from the gross tractive force T which corresponds to engine effective torque output. Gradability is proportional to free tractive force and therefore can be represented on the same diagram by recalculating the scale.

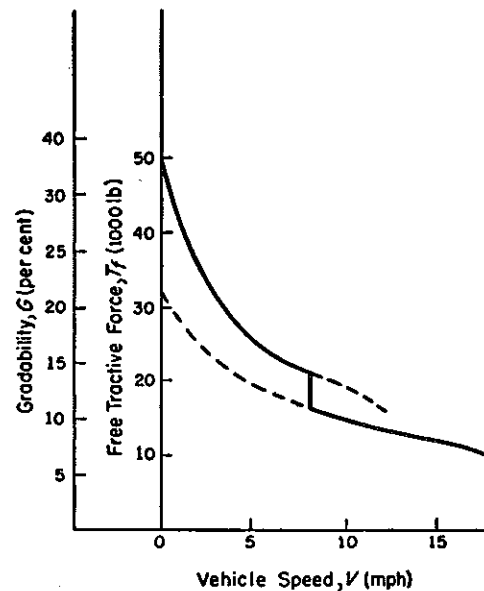


Fig. 76—Free tractive force and gradability as functions of vehicle speed for the truck example.

coupling. Here the proportionality between input and output speeds is re-established. At this point, however, a small difference between input and output speeds remains because of internal slip in the hydraulic element.

Principal advantages of the torque-converter transmission can be summarized as follows:

1. It creates an elastic connection between engine and driving wheels, cushioning the engine from sudden loads and shocks that are unavoidable with gear-shift transmissions.
2. It prevents engine operation at uneconomical low speeds and power outputs.
3. The torque-output characteristic of a torque-converter transmission approaches closely the torque-speed demands of a vehicle.

Characteristics of the converter used in the

truck example are given in Fig. 74. When combined with the reduction in the geared stages, the plot leads to a complete graphical equivalence between vehicle speed, engine speed, converter torque ratio, and engine torque output.

Speed and tractive force equations developed in foregoing sections for a geared transmission must be adjusted for use with the torque-converter transmission. The basic relationship, which has a form similar to that of Equation 269, is therefore

$$V = \frac{n_e r}{168 \xi_{ts} \xi} = \frac{n_e r}{168 \xi_s} \quad (271)$$

Tractive Forces: Calculation of tractive forces is carried out by means of a modified form of Equation 270:

Nomenclature

A	Projected vehicle area, sq ft
a	Acceleration, ft per sec ²
B	Barometric pressure, in. Hg
B_o	SAE standard barometric pressure (29.92 in. Hg)
B_v	Vapor pressure of air, in. Hg
c_a	Coefficient of air resistance
f	Coefficient of rolling resistance
G	Grade or gradability, per cent
H	Height of vehicle cg from ground, in.
L_f	Distance between vehicle cg and front axle, in.
M_d	Torque on drive axle, lb-ft
M_e	Engine torque, lb-ft
m	Mass, lb-sec ² -ft ⁻¹
m'	Total effective inertia mass, lb-sec ² -ft ⁻¹
n	Speed, rpm
n_d	Drive-axle speed, rpm
n_e	Engine speed, rpm
n_M	Engine speed at maximum torque, rpm
n_{max}	Maximum engine speed permissible, rpm
n_{min}	Minimum engine speed, rpm
n_N	Engine speed at maximum power output, rpm
n_{tc}	Torque-converter output speed, rpm
P	Power, hp
P_o	Engine power output at SAE standard air conditions, hp
R_a	Air resistance, lb
R_g	Grade resistance, lb
R_r	Rolling resistance, lb
r	Rolling radius of tire, in.
T	Tractive force, lb
T_f	Free tractive force, lb
t	Time, sec
V	Vehicle speed, mph
W	Vehicle gross weight, lb
ΣR	Summation of motion resistance forces, lb
η	Efficiency factor
η_{sl}	Tire-slip factor
γ	Inertia mass factor of rotating parts
ξ	Total reduction ratio
ξ_s	Total speed ratio
ξ_t	Total torque ratio
ξ_{ts}	Torque-converter speed ratio
ξ_{tt}	Torque-converter torque ratio
ξ_γ	Ratio of change in engine speed to change in vehicle speed
μ	Coefficient of road adhesion

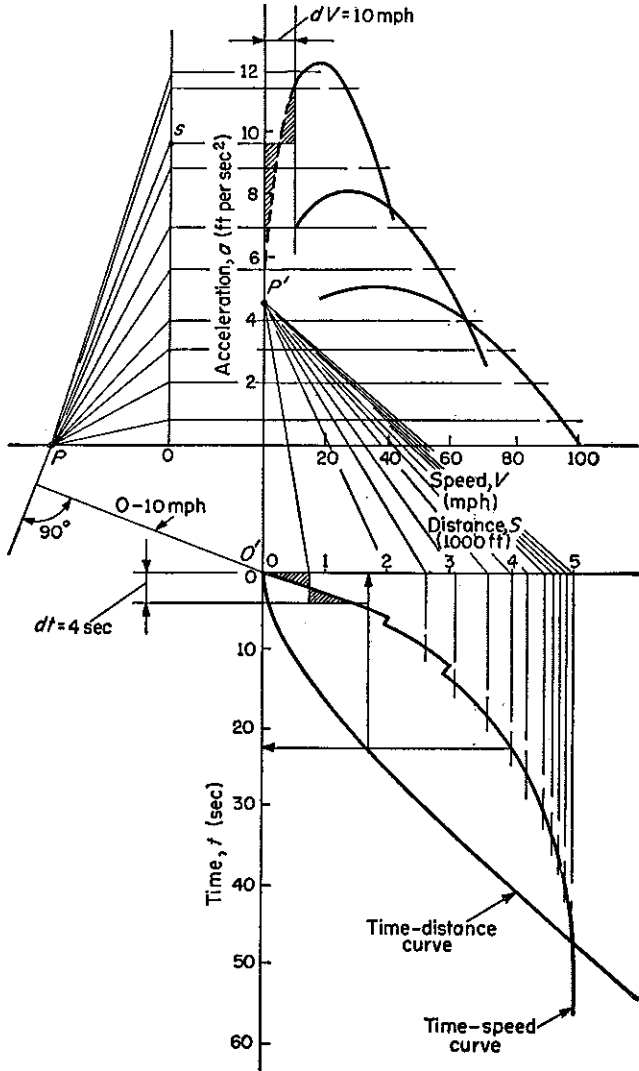


Fig. 77—Construction of time-speed and time-distance curves for the passenger car by graphical integration of the acceleration-speed curve. Diagram interrelates speed, time and distance. For example, a speed of 80 mph is reached in 23 sec over a distance of 1700 ft from the starting point.

$$T = M_e \xi_{tt} \eta \left(\frac{12}{r} \right) = M_e \xi_t \eta \left(\frac{12}{r} \right) \quad (272)$$

Further steps in the calculation of tractive forces for the truck example are identical with those for the passenger car. Sum of resistance forces is subtracted from the gross tractive force (Equation 272), giving free tractive force T_f . For the industrial vehicle in this example, which usually operates at speeds below 25 mph, air resistance is neglected. In the calculation of rolling resistance, the assumed coefficient $f = 0.02$ is considered as speed-independent for the relatively narrow operating-speed range. Results of such calculations are given in Table 9.

Gradability: Free tractive forces, calculated for both the passenger car and the truck, can be used to obtain values of grade the vehicles can negotiate at constant speed. From Equation 61 (Part 5),

$$G = \frac{100 T_f}{W} \quad (273)$$

The graphical representation of T_f can also be directly transformed into corresponding gradabil-

ity values, since T_f and G are related by the equation

$$T_f = R_g = \frac{WG}{100} \quad (274)$$

Maximum speed obtainable on each particular grade is then graphically determined at the intersections of the grade grid lines with the free tractive force curve, Fig. 75 and 76. Limits set by available friction naturally determine maximum gradability.

Acceleration: To determine acceleration, use is made of the basic equation of vehicle motion

$$am\gamma = T - \Sigma R \quad (275)$$

where γ is the factor expressing the effect of rotating parts, and ΣR is the sum of resistances in constant-speed vehicle motion. Free tractive force is defined as

$$T_f = T - \Sigma R \quad (276)$$

Substituting Equation 276 into Equation 275,

$$a = \frac{T_f}{\gamma m} = \frac{T_f}{m'} \quad (277)$$

Here, m' is the effective mass to be accelerated and $m' = \gamma W/g$.

PASSENGER CAR: Value of the factor γ is obtained from Equation 86 (Part 6), which has acceptable accuracy for all road vehicles:

$$\gamma = 1.04 + 0.0025 \xi^2 \quad (278)$$

The first term expresses the contribution of the vehicle wheels, and the second term the contribution of parts rotating at engine speed, which is related to wheel speed by the reduction ratio ξ . Results obtained when Equation 278 is evaluated for the passenger car are listed in Table 10.

As a final step, free tractive force T_f is divided by values of the effective mass m' , giving acceleration a . Results are plotted in Fig. 77 as functions of vehicle speed. Results of calculations are also given in Table 8.

INDUSTRIAL TRUCK: Corresponding calculations giving acceleration for the torque-converter installation follow basically the same steps as for the passenger car. The one exception is that the reduction-ratio value substituted into Equation 86 for determination of the factor γ is not the speed ratio ξ_t of the transmission. Explanation of this behavior of the torque converter is that vehicle speed is not directly proportional to engine speed. This effect can be clearly observed from the speed-ratio curves in Fig. 74 and 78, where translatory speed-up of the vehicle is accompanied by almost no change in engine speed (curves a and b), especially in the low-speed range. At the same time, the total speed ratio ξ_t is very high.

The ratio value substituted into Equation 86 must express change in engine speed Δn_e in relation to change in vehicle speed ΔV , and therefore

Table 10—Mass Factors

Gear	Total Ratio ξ	Mass Factor γ	Effective Mass	
			m' (lb-sec ² -ft ⁻¹)	
First	9.4	1.26	157	
Second	5.75	1.12	140	
High	3.6	1.07	134	

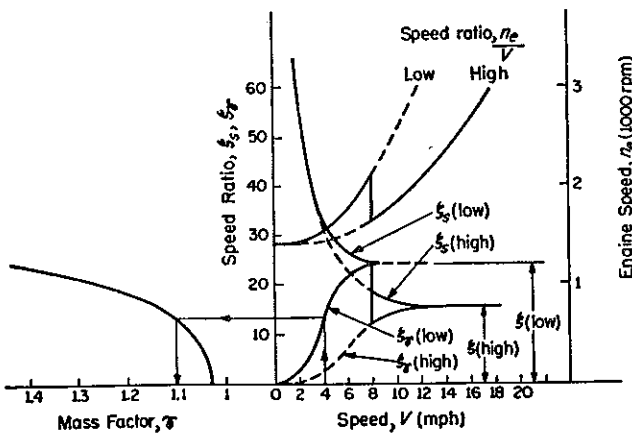


Fig. 78—Determination of inertia mass factor γ for the torque-converter transmission. Overall speed ratio ξ_t decreases from ∞ at converter stall speed ($V=0$) to the mechanical-stage ratios ξ_t (low) and ξ_t (high) when the converter acts as a coupling. The actual relationship between engine speed and vehicle speed is given by the n_e/V curves. Inertia effect of rotating engine parts is proportional to dn_e/dV , which is represented by tangents to the n_e/V curves. The ξ_t curve, constructed by measuring tangent slopes, gives values ranging from zero at $V=0$ to the values ξ_t (low) and ξ_t (high). At the left side of the plot, γ is shown as a function of the ratio ξ_t .

a new ratio is introduced. It is defined as

$$\xi_\gamma = \frac{dn_e}{dV}$$

and is shown graphically in Fig. 78. When the torque converter begins to act as a hydraulic coupling at high speeds, engine and vehicle speeds again become directly proportional, as in the case of the gear-shift transmission. Consequently, $\xi_\gamma = \xi_e$.

For the truck in this example, where an extremely heavy vehicle is powered by a relatively small engine, the constants of Equation 86 must be adjusted. As a rough approximation,

$$\gamma = 1.03 + 0.0006 \xi_\gamma^2 \quad (279)$$

Results of these calculations are shown as functions of ξ_γ in Fig. 78. Values of γ can be taken directly from the plot for any vehicle speed. Finally, acceleration is calculated from Equation 277. Complete results are given in Table 9 and plotted in Fig. 79.

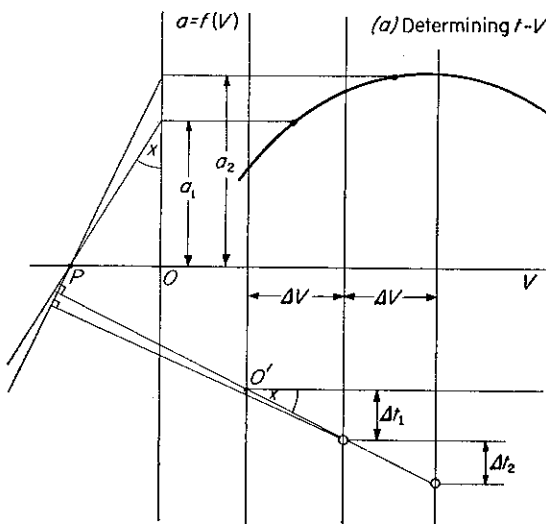
Time-Speed Relationships: In Fig. 77 and 79, calculated values of maximum acceleration for the car and the truck are plotted against vehicle speed. Acceleration, however, is not entirely suitable as a factor for illustrating vehicle performances. Time-speed and time-distance relationships

Table 11—Graphical Integration

Problem: By graphical means, determine the time-speed relationship represented by Equation 281. The technique requires solution of the equation

$$\Delta t = \frac{\Delta V}{f(V)} = \frac{\Delta V}{a}$$

where the curve $f(V)$ vs. V is given.



From similar triangles in a ,

$$\frac{\Delta t_1}{\Delta V} = \frac{OP}{a_1} \text{ or } \Delta t_1 = \frac{(OP)\Delta V}{a_1}$$

$$\frac{\Delta t_2}{\Delta V} = \frac{O'P'}{a_2} \text{ or } \Delta t_2 = \frac{(O'P')\Delta V}{a_2}$$

The graphical construction, illustrated for increments Δt_1 and Δt_2 , is repeated for the velocity range of interest. Then,

$$t = \Sigma \Delta t = \Delta t_1 + \Delta t_2 + \dots + \Delta t_n$$

Solution to Equation 281, which is the time-speed relationship, is obtained by fairing a curve

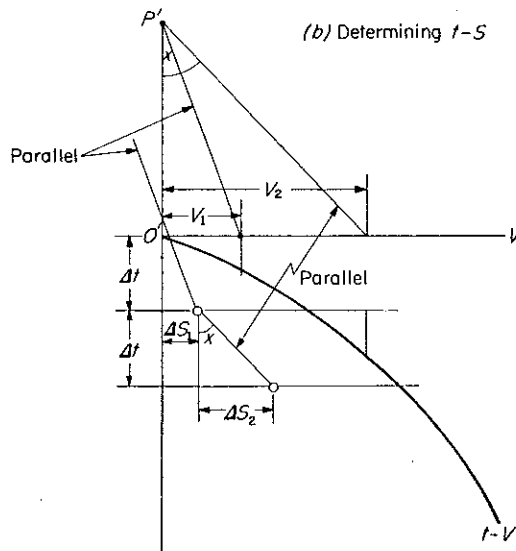
through the graphically determined points.

Problem: Determine the time-distance relationship by graphical integration of the time-speed relationship.

The incremental equation is

$$\Delta S = V \Delta t$$

where the curve of V vs. t is given in b .



From similar triangles,

$$\frac{\Delta S_1}{\Delta t} = \frac{V_1}{O'P'} \text{ or } \Delta S_1 = \frac{V_1 \Delta t}{O'P'}$$

$$\frac{\Delta S_2}{\Delta t} = \frac{V_2}{O'P'} \text{ or } \Delta S_2 = \frac{V_2 \Delta t}{O'P'}$$

Therefore,

$$S = \Sigma \Delta S = \Delta S_1 + \Delta S_2 + \dots + \Delta S_n$$

A line faired through the points represents the required solution.

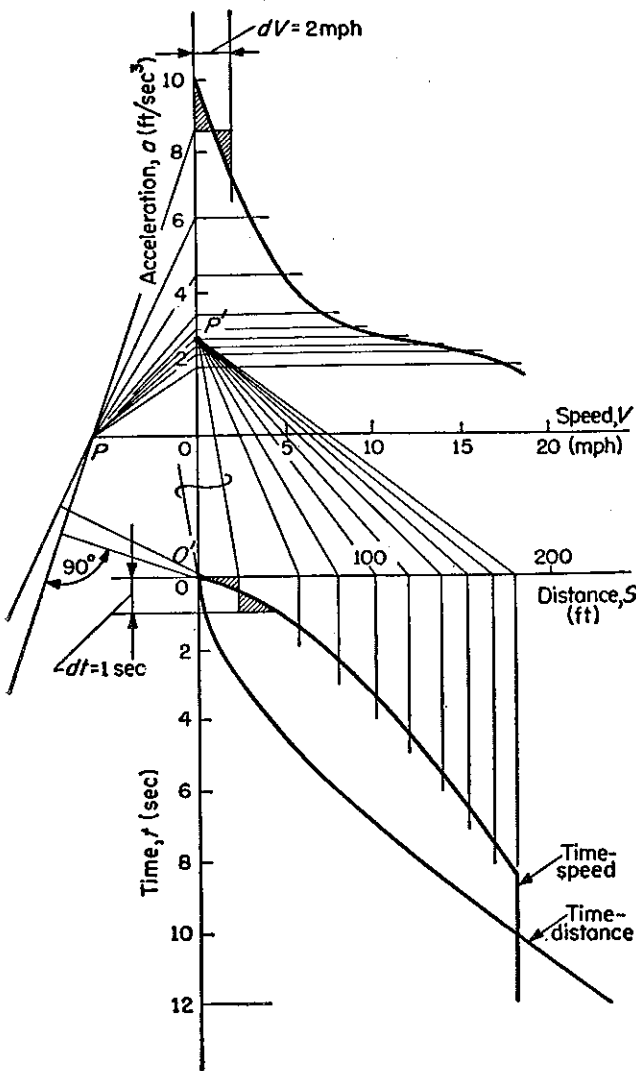


Fig. 79—Construction of time-speed and time-distance curves for the truck example. Techniques are the same as those used in construction of Fig. 77. Acceleration values in this case do not reach zero since maximum engine speed is limited by an engine governor.

offer more information.

Calculations for these relationships are based on the equation for accelerated motion, which in differentiated form is

$$\gamma m \left(\frac{dv}{dt} \right) = T - \Sigma R = T_f \quad (280)$$

Consequently,

$$dt = \frac{\gamma m (dv)}{T_f}$$

Unfortunately, free tractive force T_f is itself a function of V , which makes the equation relating time and speed not integrable by conventional methods. Form of the equation is

$$t = C \int_{v_2}^{v_1} \frac{dv}{[f(V)]} \quad (281)$$

where units of V are mph.

The graphical method of integration offers a solution with sufficient accuracy. Theory of graphical integration is not detailed here.¹⁵ However, techniques are demonstrated for the car and truck examples, using values plotted in Fig. 77 and 79. Graphical basis of the technique is illustrated in Table 11. Outline of procedure is as follows:

1. On the plot representing acceleration as a function of vehicle speed V , the area between the acceleration curve and the speed axis is divided into small sections to represent the differential dV (Fig. 77).

2. A rectangle of width dV is constructed with area equal to that enclosed under the curve proper (shaded areas equal).

3. Height of this rectangle is then projected on the acceleration axis (or a line parallel to it), and the point thus created is connected by a straight line with the integration pole P .

4. From this line, a perpendicular is erected to the speed-time co-ordinate system. The first such perpendicular is drawn through the zero-zero point to intersect the ordinate at 10 mph extended from the upper diagram. This gives a point on the time-speed curve. The second perpendicular, corresponding to the interval from 10 to 20 mph, is drawn through the point just located and extended to meet the 20-mph ordinate. This process is repeated until zero acceleration and maximum speed are reached. The result is a complete graphical representation of the time-speed relation.

5. On the points where gears are changed, the power connection to the engine is interrupted, and the vehicle is decelerated by rolling and air resistances. An accurate determination of the speed-time relation during this part of the vehicle progress was shown in Part 12 of this series. Gearshift time is usually between 1 and 2 seconds.

6. Distance of the pole P from point O is determined by the graphical scales used for the three variables involved. The relationship giving PO in length units is

$$PO = \frac{(\text{speed scale})}{(\text{time scale})(\text{acceleration scale})} \quad (282)$$

where units of length chosen for the construction must be consistent for all scales.

In construction of the time-speed diagram for the passenger car, Fig. 77, $dV = 10$ mph, $dt = 4$ sec, and evaluation of Equation 282 gives

$$PO = \frac{10(1.47)}{4(1)} = 3.68 \text{ (length units)}$$

In this equation, the factor 1.47 converts the speed scale (mph) to the same units as the acceleration scale (ft per sec²).

Similarly, evaluation of Equation 282 for the truck (Fig. 79) gives the result

$$PO = \frac{2(1.47)}{1(1)} = 2.94 \text{ (length units)}$$

Time-Distance Relationships: Graphical integra-

tion of the t - V curve gives the time-distance relationship. Form of the equation for the t - V curve is

$$s = \int_{t_2}^{t_1} V[f(t)]dt \quad (283)$$

The method of integration is as follows:

1. The diagram representing the relation between time t and speed V is considered to be known. The fields under curves in Fig. 77 and 79 are again divided into small sections representing the differential dt .

2. A rectangle of width dt is then constructed with an area equal to that enclosed between the curve and the t axis (shaded areas equal).

3. Height of this rectangle is projected to the distance and speed axis, and the point thus created is connected with integration pole P' .

4. A line parallel to the connecting line determines the time-distance curve for that particular section of dt , since it represents the integral of Equation 283. This process is repeated until the

range of maximum (constant) speed is reached; here the distance progress becomes a straight line.

5. The distance of the integration pole $P'O'$ is found (as for the time-speed calculation) from the scales of the variables. The relationship is

$$P'O' = \frac{(\text{distance scale})}{(\text{speed scale})(\text{time scale})} \quad (284)$$

Evaluation of Equation 284 gives $P'O'$ for the passenger car (Fig. 77) as

$$P'O' = \frac{500}{10(1.47)(4)} = 8.5 \text{ (length units)}$$

Similarly, pole distance for the truck example (Fig. 79) is

$$P'O' = \frac{20}{2(1.47)(1)} = 6.8 \text{ (length units)}$$

Accuracy of graphical integration depends on the size of the differential sections. Acceptable results are reached, however, with fairly large sec-

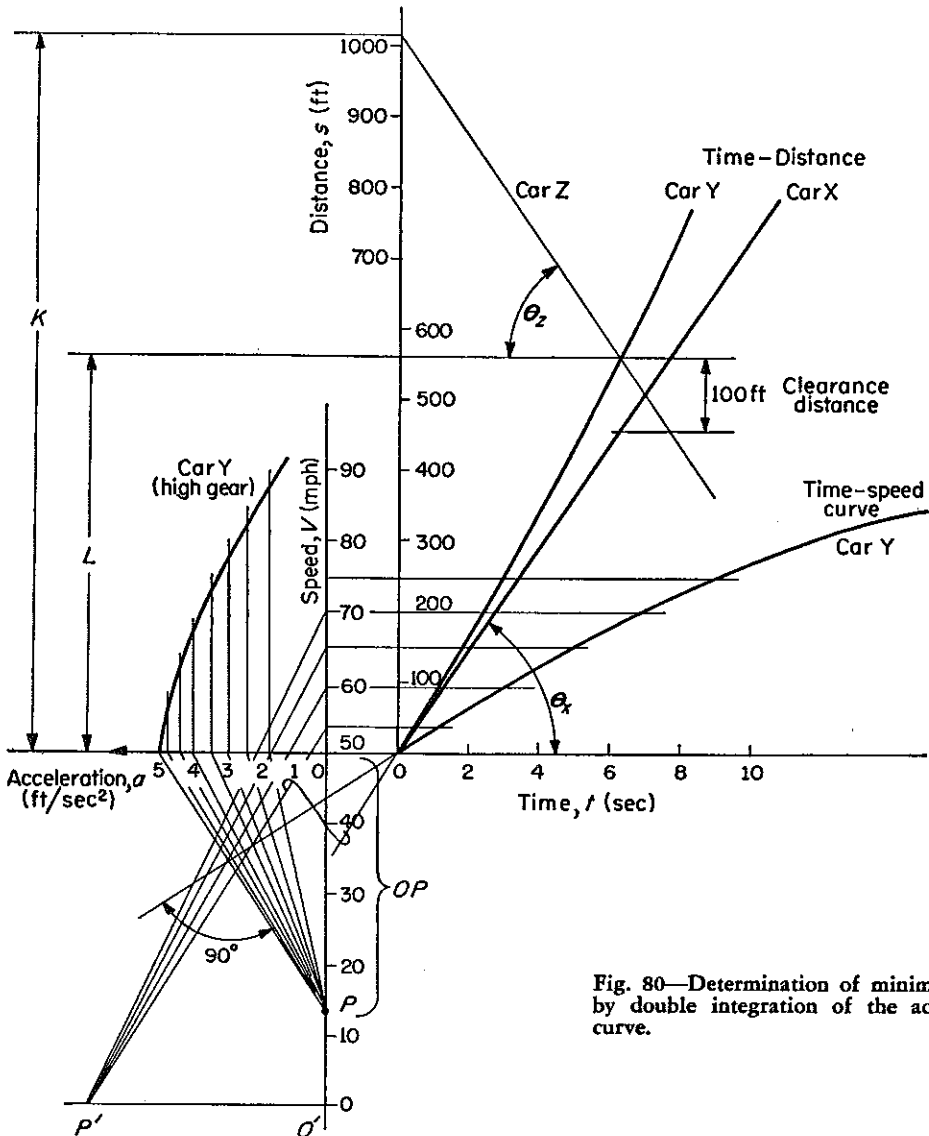


Fig. 80—Determination of minimum passing distance by double integration of the acceleration vs. speed curve.

tions. Curves, which in the first stages of construction are multiple broken lines, are finally faired into smooth curves.

Passing Distance: Time-distance curves can be used for graphical determination of distances required for passing. The technique is shown in Fig. 80, which solves a situation involving three cars:

CAR X: Car X is traveling at constant speed of 50 mph, represented by the line with slope θ_x .

CAR Y: Car Y is the car considered as an example in this article and is traveling in third gear at a constant 50 mph. At time zero, the throttle is suddenly opened wide, and the car begins to accelerate.

CAR Z: The third car is approaching from the opposite direction at a constant speed given by the line under angle θ_z . In this example, speed of Z is also taken as 50 mph.

The acceleration vs. speed characteristic of car Y in high gear is taken from Fig. 77 and is shown in the auxiliary diagram on the left of Fig. 80. Only the part above 50 mph, which is required for this calculation, is shown.

The first graphical integration, based on the principles explained in earlier sections, delivers the auxiliary time-speed curve. The pole distance PO is given by Equation 282 as

$$PO = \frac{5(1.47)}{1(1)} = 7.34 \text{ (length units)}$$

The time-speed curve is again integrated, delivering the time-distance curve of the car Y. The pole distance $P'O'$ of this integration is determined from Equation 284 as

$$P'O' = \frac{50}{5(1.47)(1)} = 6.8 \text{ (length units)}$$

If the minimum clearance distance required be-

fore the car Y can pull back into its own line is 100 ft, minimum free distance for passing is $L = 560$ ft.

In case, however, car Z is approaching from the opposite direction, it can safely pass abreast of car Y at the minimum distance L , that is, after car Y has pulled back into line. The minimum distance K between cars Y and Z at time zero is taken from the diagram as 1020 ft.

The advantage of such a graphical presentation is that it permits the effects of different speeds to be determined without repeated calculations.

REFERENCES

44. Preceding articles in the *Mechanics of Vehicles* series by Jaroslav J. Taborek and the *MACHINE DESIGN* issues in which they appeared were as follows:
 Part 1—"Motion of Wheels" May 30, 1957
 Part 2—"Cornering and Directional Control" June 13, 1957
 Part 3—"Steering Forces and Stability" June 27, 1957
 Part 4—"Stability on a Curve" July 11, 1957
 Part 5—"Motion-Resisting Forces" July 25, 1957
 Part 6—"Resistance Forces" Aug. 8, 1957
 Part 7—"Center of Gravity" Aug. 22, 1957
 Part 8—"Longitudinal Stability" Sept. 5, 1957
 Part 9—"Limits of Vehicle Performance" Sept. 19, 1957
 Part 10—"Performance Limits" Oct. 17, 1957
 Part 11—"Dynamics of Braking" Nov. 14, 1957
 Part 12—"Braking Performance Limits" Nov. 28, 1957
 Part 13—"Powerplant Characteristics" Dec. 12, 1957
45. Hütte—*Mechanics*, Part 1, W. Ernst Verlag, Berlin, 1953.
46. Lavender, Webb—"Acceleration," *Automobile Engineer*, London, 1953.
47. J. L. Koffman—"Performance Prediction," *Automobile Engineer*, London, Sept., 1954.
48. J. L. Koffman—"Vehicle Performance," *Automobile Engineer*, London, Dec., 1955.
49. Symposium—"Where does all the Power Go?," *SAE Transactions*, 1956:
 C. E. Burke, L. H. Nagler—"The Engine, the Power Source."
 E. C. Campbell—"The Accessories, the First Bite."
 W. E. Zierer, H. L. Welch—"Effective Power Transmission."
 T. D. Koster, W. A. McConnell—"What the Customer Gets."

Extra copies of the entire "Mechanics of Vehicles" series, bound as a pamphlet, may be obtained for \$2.00 each from: Reader Service Dept., *MACHINE DESIGN*, Penton Bldg., Cleveland 13, Ohio.